Recycled Glass Beam

The applicability evaluation of recyled-glass beam made of waste float glass

Rong Yu
Graduation Thesis 2019
Delft University of Technology

Author:

Rong Yu
4618319
+31 0614780868
52christina.ryu@gmail.com

University:

Delft University of Technology
Faculty of Civil Engineering and Geosciences
Master Building Engineering, Structural Design track
Faculty of Architecture and the Built Environment

Graduation Committee:

Prof. Ir. Rob Nijsse
Faculty of Civil Engineering and Geosciences
Structural Design and Building Engineering

Ir Telesilla Bristogianni
Faculty of Civil Engineering and Geosciences
Structural Design and Building Engineering

Dr. Ir Fred Veer
Faculty of Architecture and the Built Environment
Architecture Engineering and Technology

PILKINGTON

NSG GROUP

TU Delft Delft University of Technology
Glass & Transparency Research Group

Acknowledgement

This graduation projects accompany with me through my second to third year living in the Netherlands, witnessing my growth not only as an engineer in the society but also as a human in the world. During these 10 months, I experienced happiness, excitement, “gezellig”, joyful and the sense of achievement, in the mean time, the sadness, disappointment, hesitating and frustrate are also closely associated with me. It is interesting that when I look back, both the passive and hopeful moments are cheerful, they made the one who I am by now.

To go through the dilemmas, most of the helps come from my supervisors and colleagues. The first sincerely thanks to my daily supervisor Telesilla Bristogianni, for her selfless help and warm care. She is the one lead me to glass world and taught me everything in the lab, support my ideas and also point out better directions. Also appreciates for the care when I got sick and the encourage when I felt lost, she is the best teacher and also the best friend. Besides, I would like to give my most earnest appreciate to Fred Veer, who give me precious suggestions especially in the chemical and structural aspects. His abundant knowledge and rich experience always guide me to the fastest way, his agreement and humor is definitely a great encourage for me. The most important thanks to Rob Nijsse, the one guide me to the engineering industry and open the door of glass world for me. I will always remember at the very first meeting, he told me to always think about safety, sustainability and economy as an engineer. Also thanks for his kindness and understanding, which helps me and support me devoted myself into this project. There is an ancient Chinese say:” Once a supervisor, forever supervisor”, great great appreciates to all my committees, when I got lost or fall in trouble you all gave me courage to stand up and continue, thank you for everything!

Besides, I would like to thank Clarissa Justino de Lima for her thoughtful care and valuable advice, it is my great pleasure to work with her. Also thanks to Tomasso Venturini, for his friendly help in laboratory work, it is delightful to have him in the lab. A great appreciate for Kouchi Zhang, Kees Baardolf, Albert Bosman and Paul Vermeulen, as well as Ruud Hendrikx for the patience and kind help in experiments. Thanks to TU Delft and Pilkington, especially Martijn Rietveld for the support of my graduation projects. Sincere appreciates to all my friends, thank you for your accompany and support. Special thanks to Liying Feng, Yu Xie, Jiaxing Fang, Yue Zhang, Zidan Wang, Zhiyuan Su, Qiyou zhang, Homer Xie, Xin Chen, Nan Lin, Simo Lu, Fanxiang Xu, and Yuan Chen, thank you for all the support and love, it is my extraordinary fortunate to have all of you in Holland to color and enrich my master life. Still earnest thanks to Yan Li, Yafei Ou, Ting Li, Yipeng Ren, Cedric Zhou and Hao Ge, thanks for the support and care tramping over mountain and sea.

The essential acknowledgement to my family, for both the economical and emotional support. The understanding and love from my family support me to live the life I want. I would give the last but not least special appreciate to my dearest Haiyan Peng and Linhai Yu, thank you for your selfless love and endless support, I love you both until the very end!

Rong Yu

Delft, The Netherlands, Early spring, 2019

To greatest Linhai and Haiyan, who created me and always love me.

献给我的爸爸妈妈，我爱你们。

Abstract

Aiming at maximizing the recyclability of glass and integrating the sustainability with glass structural application, the concept of recycled glass beam has been proposed at the beginning of this project. Based on the investigation of existing glass manufacturing and recycling industry, the resource material has been targeting at float glass from building sector. This thesis present the recycling process in the lab, as well as the selection of experiment method. In the view of structural application, the mechanical property of the recycled float glass has been tested and the results has been discussed in combination with chemical composition analysis. The prediction of the material property for this recycled float glass, especially the structural behavior has been raised on account of the empirical data and the computational analysis. At last, the applicability of the recycled float glass has been proved, following by the data of relative mechanical properties. This thesis is end up with the discussion of the possibility for further development and the conclusion of this recycled float-glass beam project.

Table of contents

Part 0 Introduction

At the very beginning of this thesis, an introduction of the project will be presented, including the problem statement, research objectives, and thesis outline. The problem statement will demonstrate the background and motivation of this project, showing how this thesis started. Next, the targets and methodologies will be roughly illustrated in the objective part. Finally, the outline of this thesis will be given so that the reader can read this paper following by the organized thoughts depending on the outline.

Figure 0.1: The recycled glass samples made by kiln-casting, photo by author.

0.1 Problem statement

As we all know, the glass is regarded as the completely sustainable material owing to its hundred percent recovery rate. In order to investigate the usefulness of the study in glass recycling, a rough research has been carried to the existing glass recycling industry. The study results shows that the glass recycling origins form second world war with continues developments afterwards. By now, there are two main types of recycling including closed loop recycle and open loop recycle. The former is aiming at producing new bottle or containers by the old glass bottle or containers, the application of the glass products are remain the same before and after recycling. Normally, the closed loop recycle are only consists of cleaning and sanitizing without the change of glass status. The other recycling method called open loop recycling is transfer the product purpose into other areas, such as using glass cullets as additives in concrete. This method is usually accompany with the mixing and crushing of the waste, less attempts in the change of glass status. Therefore, a concept of creating a new recycling method of glass has been put forward.

However, what should we do with the glass products after recycling? Observing the wide range of attempts in glass structures, such as the Glass Bridge in Delft and the Apple Store in Hongkong, the structural application of recycled glass produces is taken into consideration. Integrated with the recycling method mentioned before, there are known cast products in the glass structure field, such as glass beams or columns. To take the notice of unexplored field, the casting glass beam is a wise choice. By combining the environmental-friendly glass recycling and the challenging attempts in glass beam, the initial objectives of this thesis has been proposed as recycled glass beam.

Figure 0.2: The Glass Bridge in green village, Delft, photo by author.

0.2 Research objects

Referring to recycled glass beam as the end products, there are many questions occurred. The first two questions raised on the resource selection and recycling method selection, which are simplified in two questions as below:

1) What to recycled?
2) How to recycled?

Before deciding detailed objectives, these two questions have to be answered. When talking about the resource of glass recycling, through the study in the existing glass market, the waste float glass from building industry takes a major part in the waste glass. By now, glass manufacture company has attempts in adding waste glass cullets into the raw material for the next generation of production. But the quality requirement of adopted waste glass is very high, and only limited category of float glass will be selected waiting for recycling. It is not a completely recycling for glass due to the absence of coated float glass. Thus, the float glass from building industry has been selected as the resource material in this project, further option will be discussed in chapter one.

Making mention of the recycling method, three scenarios have been put forward:

1) The creative thinking in stacking methods of recycled glass products through lamination or adhesives;
2) The casting method for glass recycling resourcing from float glass cullets;
3) The fusion technology attempts in glass recycling.

The first scenario has the lowest energy consumption in the recycling process, while the adoption of lamination or adhesives violates the sustainable concept, thus it should be excluded from recycling methods. The third scenario has the second least energy consumption among these scenarios, which aiming at combining waste float glass cullets with common flat glass by fusion technology. The estimated highest temperature will be around 765 degrees, based on the glass fusion artistic. However, the structural application raised high requirement of the material properties. The fusion scenario can hardly reaching a homogeneous distribution which result in difficulties for the prediction of structural behavior. Taking the above-mentioned into consideration, the second scenario which recycling through casting is selected as the recycling method for float glass recycling, even though it has a relatively high energy consumption. But comparing to the factory manufacture of float glass, the energy still has been saved through the recycling process. The diagram of these three scenarios has been simply presented in figure 0.2, the numbers in the figure are not precise enough since they are the estimation deriving from the literature.

According to all above, the end products detailed from “recycled glass beam” to “recycled float-glass beam”. To organize the following arrangement, several objectives have been proposed at the beginning:

1) Introducing all the category of float glass and clarify the final material selections;

2) Clarifying the recycling process from waste float glass to end products;

3) Providing a standard quality of the recycled end product;

4) Check the structural behaviour of recycled float-glass beam.

Through this thesis, all of the objectives will be obtained and the relevant studies and test will be illustrates. The conclusion will be proposed in the last chapter, which will certainly fulfil all the objectives, probably together with added bonus results.

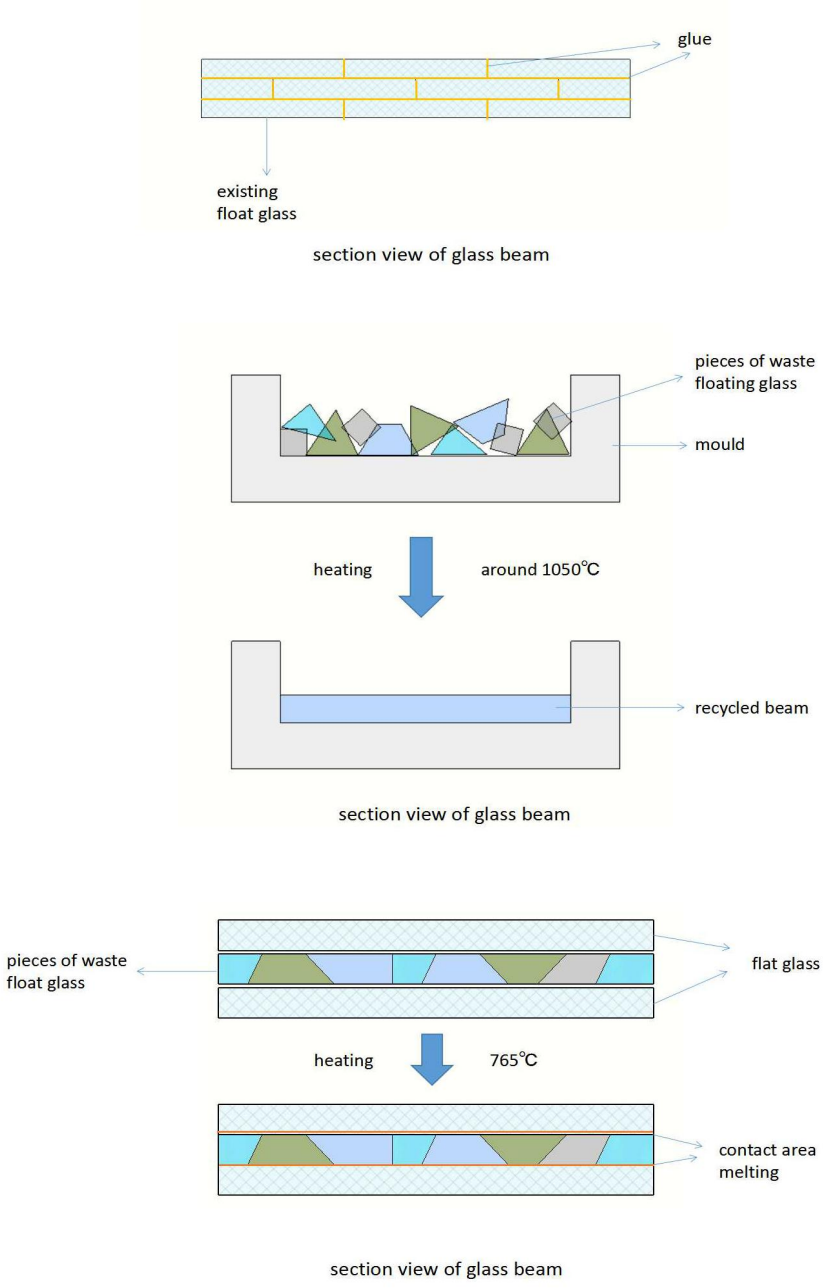

Figure 0.3: Three scenarios proposed at the beginning of this thesis, from scenario one to scenario three corresponding from the top diagram to the bottom diagram.

0.3 Research outline

The following flowchart teasing the thoughts of this thesis, by showing the aims and end products. The demonstration of this thesis will following the organization of this thoughts, with the help of experiments illustration and the result analysis.

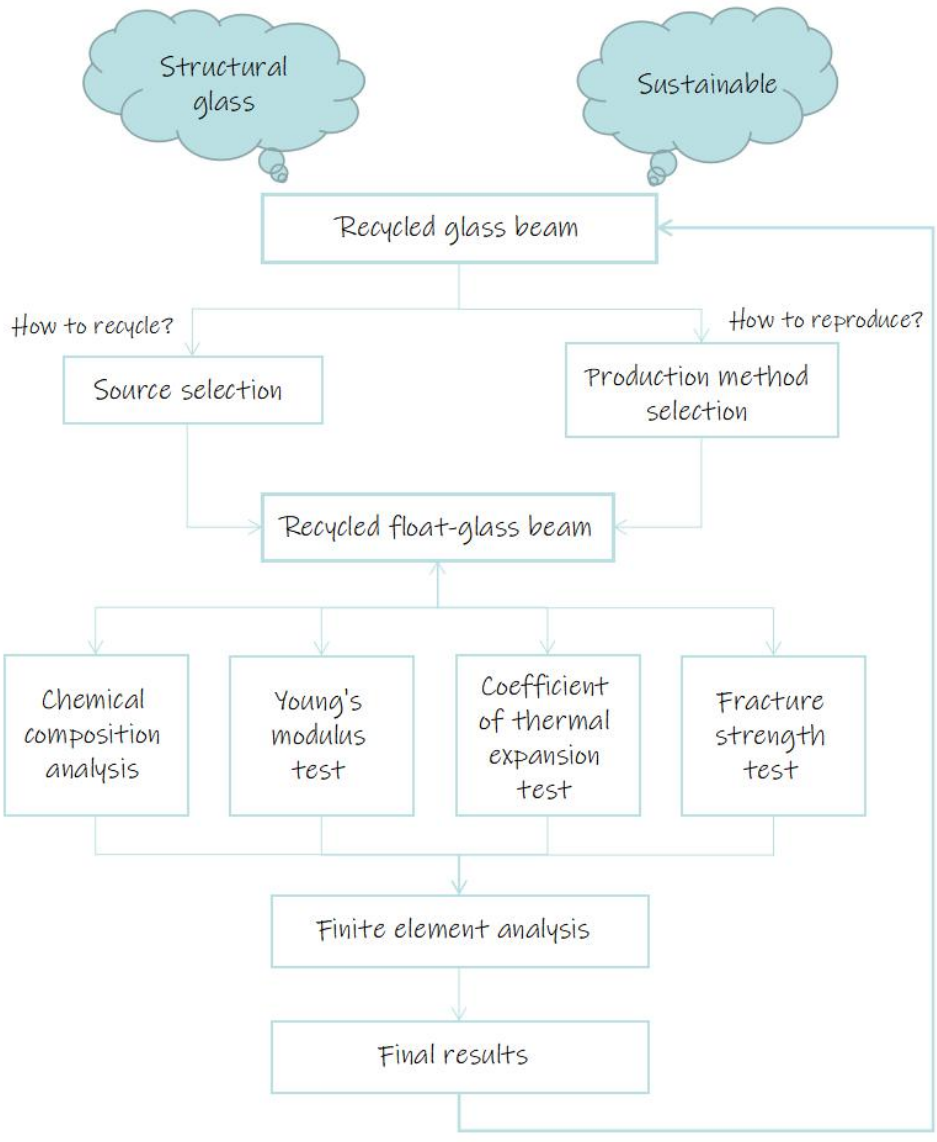

Chart 0.1 The outline of the thesis "Recycled Glass Beam"

Part 1 Glass literature study

At the beginning of the research, substantial basic knowledge is obligatory for the experiment design and result analysis. Hence, this part aiming at introducing relevance background of float glass and glass recycling, combining with the introduction of structural glass, especially glass beam, to present the possibility and meaningfulness of this research. Furthermore, the literature study about the correlative experiments will be presented in this part as well. Through comparisons among different methodology, legitimately illustrating the reason for methodology selection and subsequent influence.

Figure 1.1 The optical glass house in Hiroshima, Japan, by NAP Architects

Chapter 1 Background

This part briefly introduces the background of the development of glass, focusing on the history of float glass. Besides, the current situation of the glass recycling industry will be elaborated in this part. In the meantime, the float glass industry and the application of structural glass are demonstrated as well. In the light of the literature study, the motivation and the rationality of this research can be clarified, the fundamental information for the following study is able to be obtained.

1.1 History of float glass

Initially, the evidence of glass existence was found from volcanic glass obsidian in Mesopotamia back to 5th century BC. In 1500 BC, the manufacturing methodology was very common among ancient Egypt and even spread to the area near east Europe. [1] The ancient flat glass were limited in size and thickness, it was produced by pouring melt glass into a clay mold, following by cooling down and polishing the glass surface. Until 200 BC, the glass-blown method has been invented by Babylon, after when glass products can be manufactured manually. Flat glass patterns made from glass bubbles blown by craftsman. They rotated the iron pipe as fast as they can when they blowing glass bubbles so that the material was able to expended outward to form a flat circular disc. After blowing and rotating, they cut the glass from the iron pipe so that the flat glass plate completed after cooling. As a result, from the 10th century, flat glass as architectural glass which prevents us away from wind and dust appeared in most churches. [2]

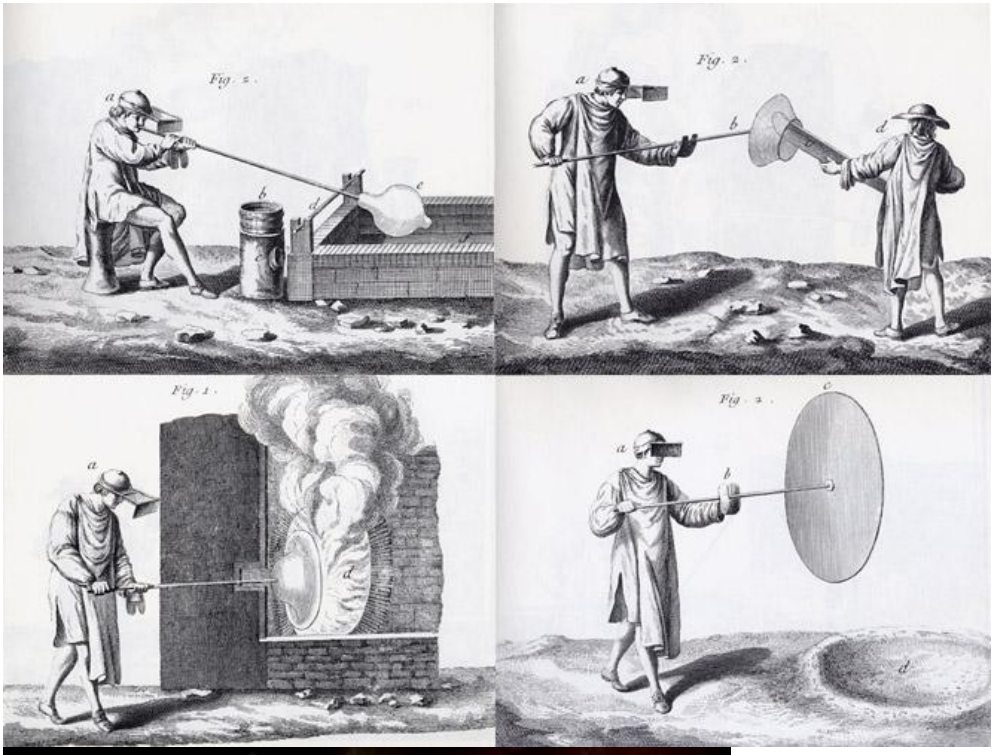

Figure 1.2: The early stage of glass manufacture: blowing skill (top).

Figure 1.3: Crown glass manufacture skill (left).

However the circular glass plate was not easy to be installed, therefore a new method to produce square glass plate appeared. In the eleventh century, Germany improved flat glass manufacture technology: craftsman blew glass bubbles into a cylinder shape, and cut them along the edge when they were still hot, afterwards glass panels can be spread into a flat square plate. Thanks to the flat glass manufacture technology, these religious buildings express their spirit and belief through the gorgeous lattice window. [3]

With the development of industrial society, glass manufacture methodology has a great progress in almost every area. In 1839, Chance improved the cutting and polishing period in the glass production process, which significantly increased production efficiency. [4] As a consequence, Joseph Paxton could offer large quantities of glass panels to built Crystal Palace, shown in figure 1.4.

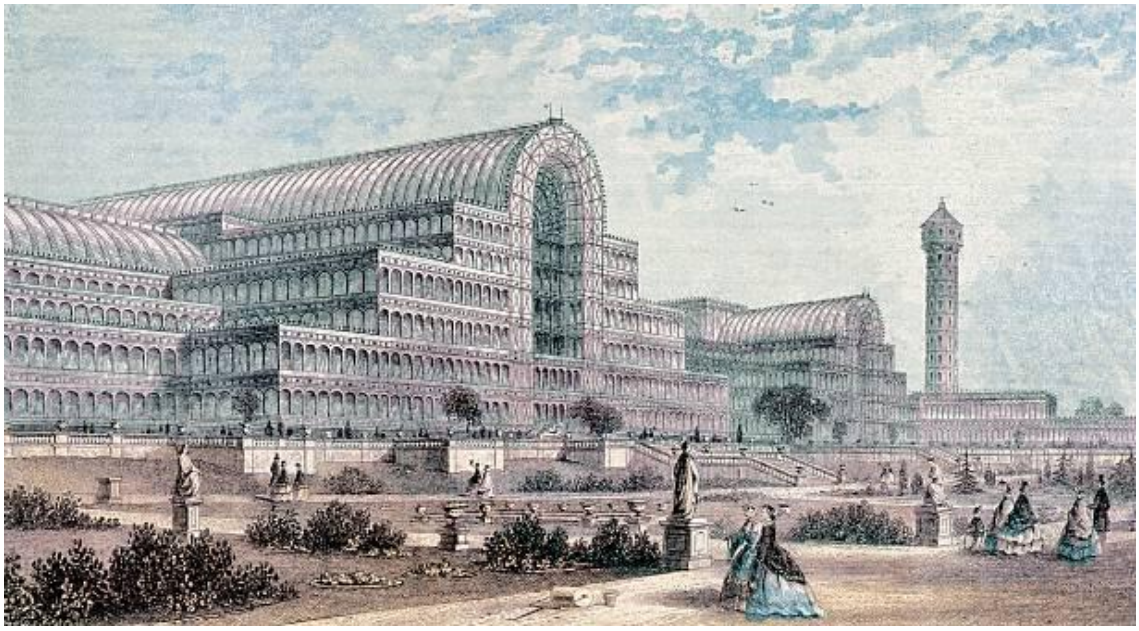

Figure 1.4: Crystal Palace in London, United Kingdom, design by Joseph Paxton, 1854.

By the 20th century, a higher requirement of glass quality was requested, especially the smoothness of glass surface, due to the application in the showcase, auto and mirror. At first, workers pouring molten glass into a glossy conveyor and using a rolling machine to press them into a flat plate. However, this kind of pressing methodology has a significant smoothness requirement of the conveyor and rolling machine, which indicates more labour and more costs. In the 1950s, Alastair Pilkington (1920-1995), a British engineer and businessman came up with the idea to create a perfect surface by keeping molten glass floating above some special liquid with a smooth surface. After years of effort, he invented and developed a methodology to produce a perfectly flat glass plate, which was called the float glass process. [5] This process maintained its lifeblood since then, meanwhile, because of the increasing kinds of glass application, it has been improved as well for different purposes.

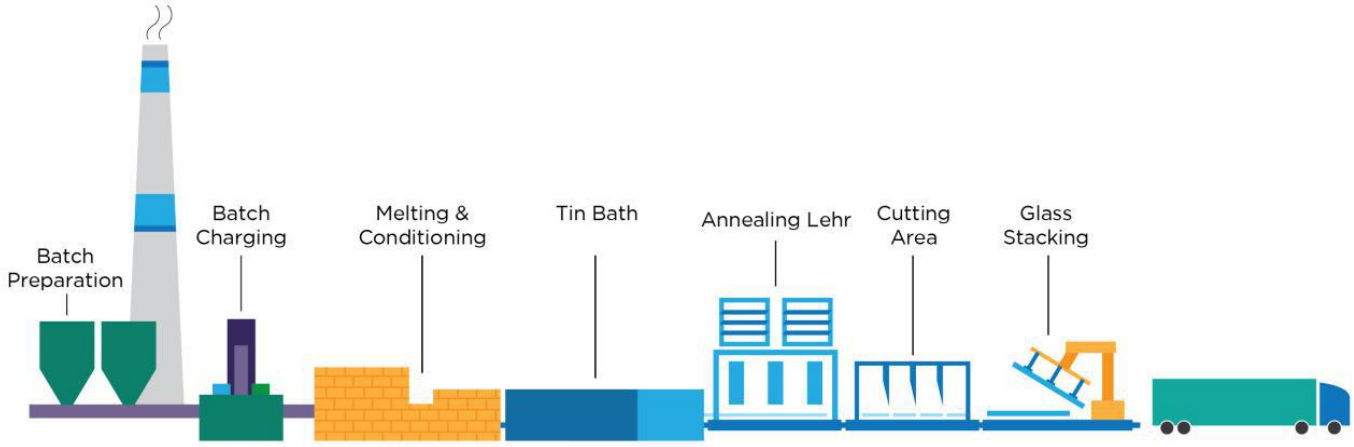

Figure 1.5: Manufacture process of float glass in industrial level.

Nowadays, the float glass industrial production process can be described as six steps: firstly, pouring ingredients into furnace then melting them at around 1500 degrees, after several hours, depends on the different composition of ingredients, the molten glass is able to be used unless no bubbles exist. Next, the float bath, which means molten glass flows gently and continuously to the surface of molten tin, at the same time, the temperature will drop from 1100 degrees to 600 degrees. After the float bath, molten glass turns into a solid state, a preliminary flat glass is produced since this step. In the following step, coatings can be added in order to qualify flat glass special optical properties, a detailed description will be given in the following paragraphs. Considering the residual stress grows when ribbon glass goes through high temperature to air temperature, the annealing of glass is an essential anchor. The ribbon glass should go through a lehr, in where the temperature can be controlled well, as well as stresses. Before cutting into pieces, the quality inspection takes place, which mainly to ensure bubbles are removed, no sand grain exist and no ripples on the surface. Finally, the ribbon glass will be cut into normative size, usually in water jet cutting which ensures a smooth edge, then packaged to on sale products. [6]

1.2 Development of glass recycling

Glass recycling is widely known as transform waste glass into newly available products by the public. The history of glass recycling could be traced back to the second world war, due to the shortage of resources and materials. During war times, Americans made a great effort to recycling and reuse of glass products, especially in the years of economic recovery, mainly personal effort. Like other material, glass manufacture also cost energy according to heating and transportation, which indicated the consumption of energy and raw material, as well as the emission of carbon dioxide. Growing with the greenhouse effect, the awareness of glass recycling by public increasing. [7]

Until the 1970's, companies who produced the beverage with glass containers recognized the importance of re-utilization, started to encourage consumers to return glass bottles and containers through introducing deposit receiving. Following by rewash, refill and resold, the beverage company could reuse them successfully. [8] However, this kind of glass recycling stream limited to glass containers, and to be more precise, it is more likely a reuse behaviour rather than recycling. In fact, the glass recycling could be realized by not only mixing glass cullet with other materials for different purposes but also remelting and reformed into new products. It is well known that glass is a hundred per cent recyclable material, benefit from its structure which will not deteriorate during reproducing. By now, a mature glass recycling industry has been established, especially to the source of glass containers and bottles. According to some statistics, [9] each new glass bottles for food and beverage contains 33 per cent recycled glass on average.

Figure 1.6: Glass recycling spot in Amsterdam.

Generally, there are two methodologies of glass recycling, the closed loop and the open loop. The former technology indicates remelting glass wastes, sometimes mixing with raw materials, then transform them into new products without deficiency of performance comparing to initial products. On account of the closed loop, there are five steps in the glass recycling process. At first, glass waste will be gathering together from every drop off bin, then transported to the factory field. After collection and delivery, all glass waste will be separated manually from other waste such as plastic or ceramics. The visually selected glass wastes will be transmitted to the next station, where the wastes are going to be broken by huge hammers. In the next step, preliminary glass waste will go through a trommel, where paper labels and cork caps can be distinguished through weight difference. Besides, the trommel has a revolving screen which can sort glass particles into different sizes. Third, glass wastes passed through the magnet area, where metal element is able to be separated. By now, the rough glass waste particles are almost ready, unless washed by water and dried in low temperature, in order to get rid of sugars and bacteria. After successful selection, dried and cleaned glass particles transferred to the first rotary screen to provide proper dimensions which fit pulverizer in the next station. All glass cullets are under endless circulation until they fit the required dimension to next step. At last, end glass cullets with satisfactory dimensions are able to be produced after final classification by the secondary rotary screen. The specified size of glass cullets is on the basis of different purposes and markets, especially considering closed-loop application or open loop application. For instance, if the glass cullets are used as glass fibre in concrete, a smaller diameter of glass cullet is required. It is easier for the reuse of glass waste after its transformation from waste into pure glass cullets. In a closed loop consideration, glass cullet will remelt into liquid and manufacturing into new products such as glass containers. Sometimes extra raw material can be added, as well as special manufacture technology, so that final product with new functions can be obtained, such as heat resisting laboratory glassware. [10]

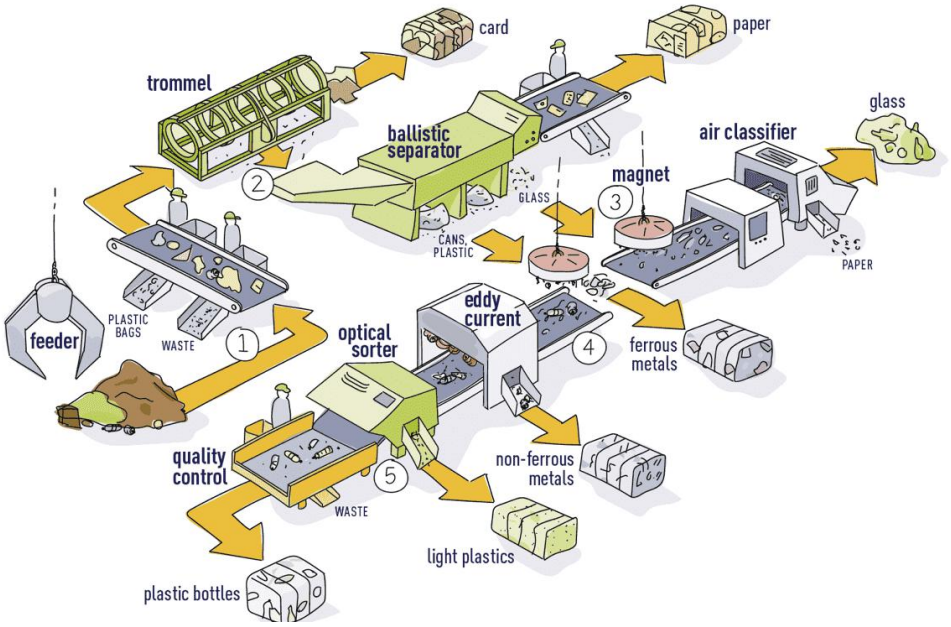

Figure 1.7: Glass recycling process in industrial level.

While considering open loop, after recycling and transferring glass waste into glass cullet, the end meshing cullets will be put into concrete or bricks without change of physical state. Normally, with the help of glass cullet, the strength of concrete and bricks can be enhanced significantly. More particularly, some glass cullet also used in highway project to produce a reflection of the road during the night. Nowadays, the most existing glass recycling industry has a complete production line, shown in figure 1.7.

However, the resource of recyclable glass is only limited to glass bottles and containers, which are belonging to the light industry field. It is obvious that the glass industry is more than bottles and containers, the rest diverse glass products such as architectural glass, laboratory glass and even glass screens of electronic products, are waiting to be explored. Based on research, [11], the laboratory glass requires a higher temperature to melt, which is energy consumption, and the quantity of wastes electronic screens may not enough for structural products manufacture. Synthesizes relevancy, economic efficiency and feasibility, this project choose waste float glass as source material.

Figure 1.8: Different types of waste glass, by Bristogianni.

There is evidence that glass recycling makes sense considering different aspects. First of all, it is obvious that glass recycling devotes to a better environment, through saving energy and material consumption, also waste emission. It is said that in the US, 1 ton of carbon dioxide is reduced for every 6 tons of recycled container glass used in manufacturing (glass packaging institute). A relative 10% increase in glass recycling reduces 8% particulates, 4% nitrogen oxide and 10% sulfur oxide at the same time. Besides, glass recycling formed a new industry field which offers plenty of working opportunities.[8]

1.3 Background of structural glass

There are thousands of history for glass utilization, although the development is not very fast. For centuries, the glass becoming more and more essential in science and technology, as well as daily life for ordinary people. It is widely used in optical equipment, light industry and especially the architectural field. With the development of modern technology and the progress of glass manufacture process, architectural glass is not only used for daylighting but also claimed for lighting and temperature adjustment, thermal insulation, safety guarantee and artistic decorations etc. Nowadays, architectural glass has developed to lamination glass, strengthened glass, solar glass and so on. In pace with the blossom of the glass industry, it becomes the third largest material served in the building industry, behind concrete and steel.

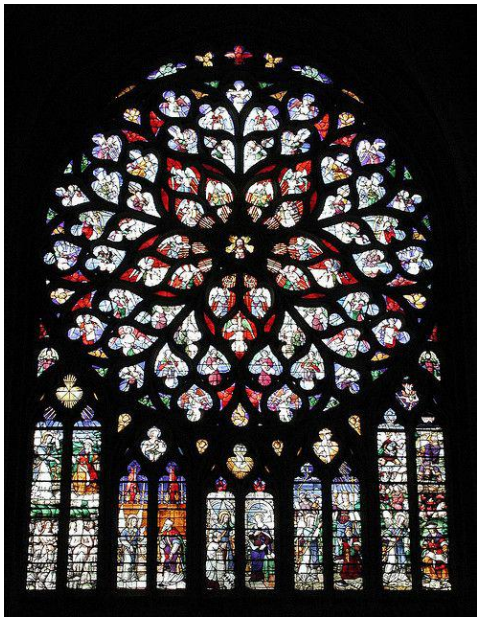

Figure 1.9: Lattice window in Milan Cathedral

The first architectural glass period appears in medieval ages teeming with the Gothic architectures. This cloud-kissing spire along with colourful lattice window to show their religion and culture. Glass bridged architecture with religious belief, introduced mystical holy light into the church, helps people get closer to heaven. Then comes to the Baroque period, which focuses on the extension of space. It is realized by big windows and commodious openings. These roomy space asked for a better interaction between inside and outer environment, meanwhile, the requirement for glass as the main material to realize open architecture was increasing heavily.

From late 16th century to mid 19th century, green house played a main role in the architecture area. In that period, green house was only made of iron frame and glass. Except for normal iron frame and windowpane, we could hardly found any beam to support the roof, thus before glass installation, a light breeze would cause sway of the whole structure. Fabulously, once the glass panels installed in the iron frame, all building has been solidified to withstand external force. From that period, fragile glass began partly bearing loads as a structural component, which strengthened overall stiffness and stability of the building. [12]

Figure 1.10: Royal Botanic Gardens,Kew, located in United Kingdom. It is a typical green garden architecture, which used curved glass directly connected to steel frames. It expressed the uniqueness of glass that combined both practical and decorative.

After green house, shopping galleria gained popularity in many big cities. Most of them used extended-in-all direction corridors, which usually covered by steel arch and glass panels, to connected adjacent buildings. For example, the Vittorio Emanuele 2 designed by Giuseppe Mengoni in 1861, located in Milan, shown in figure1.10. Benefit from transparent glass, people could hang around under natural light but without the attack from wind and rain.

Below: Figure 1.11: Vittorio Emanuele, Milan, Italy.

Figure 1.12: Oriel Chambers, the first glass curtain wall.

In the early 20th century, inspired by “less is more” from Ludwig Mies Van der Rohe(1886-1969), architects are passionate for the simple but elegant building which can present a brief framework and full of modern sense. Such as Oriel Chambers located in Liverpool which is the first glass curtain wall project in the world, created by architect Mies and engineer Peter Ellis(1805-1884) in 1865, shown in figure 1.12. Blending with the domino system concept raised by Le Corbusier (1887-1965), who introduce glass curtain wall instead of the traditional solid wall into column structure, so that the self-weight of the building is obviously decreased. [13] It benefits buildings for losing weights to grow higher, and it is the right beginning for “invisible city” with glass facade skyscrapers rising from the ground.

As time goes by, architects and designers have growing propensity to maximize the transparency of building, along with maximizing the interaction between environment and human activity. Under this circumstances, glass is subtly used as structural material to realize fully transparent building. Unlike formerly, at when the glass is used as window or facade decoration which only considering wind load and self-weight, glass tactfully transit vertical load as a structural component. In the late 20th century, Dutch engineers proved that glass could work as load-bearing structure component through a house design in Almere, shows in figure 1.13. The living room of that house is enclosed by sandwich glass panels as load bearing walls in three directions, working together with glass fins as support for the roof. Since then, glass structural has been widely promoted to infrastructures, commercial buildings and private residence. Apart from glass fins and glass columns, all glass structure draw great attention from all over the world. Regard as one of the first all-glass architecture, the entrance pavilion of Broadfield House Glass Museum was completed in 1994 by Design Antenna, shown in figure 1.14. It is supported by glass columns, with a height of 3.5 meters, and glass beams consist of three-layers lamination glass. Due to the mortise and tenon joint connection, adding with adhesives, there are no visible metal supporters or connections exist in the structure.

Bottom left: Figure 1.13: House in Almere, The Netherlands.

Bottom right: Figure 1.14: Night view and day view of entrance pavilion of Broadfield House Glass Museum.

Till now, lots of spectacular glass structure can be found around the world, such as Glass bridge in Rotterdam, Crystal House in Amsterdam, Yurakucho Subway Station in Tokyo and so on. The potential of the glass structure is being discovered by engineers and architects, as well as technicians who have a deep attachment to glass.

Figure 1.15: Night view (left) and day view (right) of crystal house, Amsterdam, The Netherlands.

1.4 Background of glass beam

Unlike the glass column and glass fins, the application and development of glass beam are comparatively late. One of the earliest application of glass beam can be found in the workshop of Musee de Louvre in Paris. It was made of four-layer lamination glass, each layer was 15 mm thick. They were supporting the roof, which was consist of four-layer toughened glass laminated together. Nevertheless, the glass beam in Louvre was carried by a solid wall, thus the connection between glass beam and wall are metal supporters. A similar situation happened in Rotterdam, the first glass bridge ever built in The Netherlands. The enclosed bridge connected two adjacent buildings made of wood and brick respectively, creating an elegant outlook without causing any visible influence to original buildings. The link spans to 4 meters, and all the enclosure were glass including glass roof and floor, glass side wall and glass beam. Adhesives and metal connections were applied in details. [14]

Glass beam progressing with the development of glass structure, as we mentioned before, the first all-glass structure in London shows the one-way glass beam to column system. It spans 1.1 meters and the beam heights 300 mm, furthermore, it directly located in the glass column through mortise and tenon joint which inspired from wooden connections, no metal connection was used in this construction.

After several years, with the accomplishment of Glass Cube Reading Room in Arab Urban Development Institute, designed by Nabil Fanous Architects, a two-way structure with glass beam and columns are created, shown in figure 1.17. An 8m X 8m X 8m grid was formed by portal frames, which consists of glass beams and columns through a friction grip connection. [15] Going through optimization and improvement, the two-way glass structure was applied to lots of unforgettable projects such as the famous Apple Cube on Fifth Avenue in New York (figure 1.18).

Figure 1.16: the glass bridge in Rotterdam, design by ABT, The Netherlands.

Above left: Figure 1.17: The Glass Cube Reading Room in Arab Urban Development Institute, Riyadh, Saudi Arabia.
Above right: Figure 1.18: The apple cube in 5th avenue, New York City, The United States.

Biologically, human beings object to seemingly vulnerable structure, such as brittle glass structure. The invisible support is not able to give resident enough feeling of safety. Why we still keep exploring in this field? Considering rebuilt or add an additional connection between existing buildings, this transparent material is the peerless choice. It hardly affects the primary construction or blocks the view from residents of original buildings. What's more, in the reconstruction of historical buildings, it plays an irreplaceable place that preserves the historical outlook and produces untouched sense of history. Beside the pursuance of aesthetics by artists and architectures, glass structure does have physical evidence that it wins out among construction materials. The most decisive reason that glass can be used as a structural material is the high compressive strength, which is almost two times than that of steel. It builds up the cornerstone of glass structure development, together with the high strength to density ratio. Compare to concrete and steel, the strength to density ratio is relatively high, which indicates glass can bearing more stress under the same self-weight level. The high compressive strength and comparatively low tensile strength give the glass a similar property of concrete, meanwhile, the Young's modulus of glass is much more than that of concrete, approximately two times. To some extent, glass has better performance than concrete as a compression resistance component. Also because of the durability of glass is excellent that nearly no chemical reagent can ruin it. In addition to all above, thanks to the transparency and sustainability, glass shows significant benefits in the environmental area. More transparency the building is, more natural ventilation and sunlight the inhabitant has. At the same time, the life cycle of glass suggests glass production cost less energy and produce less waste than other material. Broadly speaking, all these benefits drive us to discover the possibilities of structural glass and create smart and environmental friendly architectures.

Chapter 2 Introduction of methodology

Extracting from this chapter, four experiment technology has been explained in detail, including the available methods, the production material and also the correlation factors. In cast technology section, two types of casting method known as kiln-casting and hot pour casting are introduced. A similar elaboration appears in mould technology section, showing the similarities and differences among sand mould, lost wax mould and permanent mould. In Young's modulus test section and CTE test section, three methods in each section has been illustrated, but there is a more exhaustive elaboration for the introduction of CTE.

2.1 Casting technology

Unlike the practical float glass production industry, to make a component completely made of recycled glass, a casting process will be adopted in this experiment. Generally, there are two types of glass casting laboratory approach, [16] hot-forming and kiln-casting, which are distinguished by different required equipment.

The hot-forming casting comes from an ancient technique, it is also a melt-quenching casting technology outside of the oven, which requires crucibles and steel moulds. During hot-forming casting, the glass will be molten in a crucible in the furnace, and pouring the molten glass in the steel mould through heat resistance equipment, following by preheating in another furnace. The temperature ranging from more than 1250℃ (first melting in the furnace) to 500℃ (preheating in the second furnace) before annealing to atmospheric temperature.

Figure 1.19: Hot forming casting, right from the Youtube, left from Bristogianni's paper.

In contrast, kiln-casting only requires one furnace to achieve whole melting and annealing process. The starting material is put in the mould, or in the terracotta flower pot which lies above the mould, before placed into kiln. The melting stage (with a heating rate at 50℃/hr) and annealing stage (usually from 1250℃ down to ambient temperature) can be completed mechanically, except for the rapid cooling stage. Since manual open and closing the furnace saves time and makes the operation easier. This sharp temperature decrease also exists in the hot-forming approach when molten glass pouring into cold mental mould. It is essential because it avoids the appearance of crystal molecular, which introduce weak point under structural consideration.

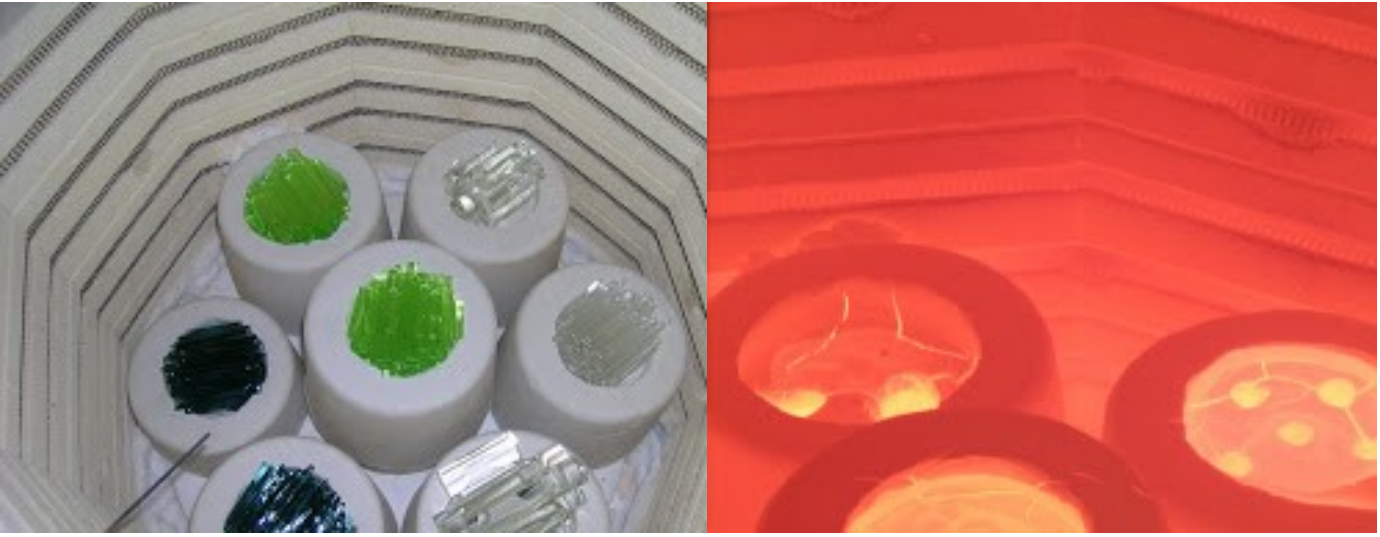

Figure 1.20: The kiln-casting with free placement of glass pieces; the left figure shows the mould with glass before casting; the right figure shows the mould with molten glass during casting; both of the figures comes from the Washington glass school.

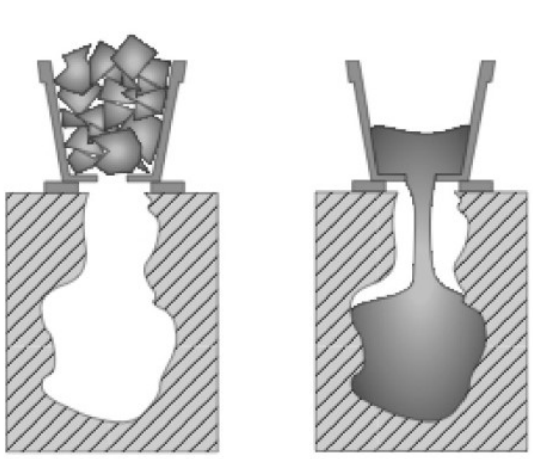

Figure 1.21: The kiln-casting with flower pot, placed on top of the mould, as a container for glass cullets; the left figure shows the glass melting process during casting; the right figure present the situation before casting.

With regard to the glass samples from Pilkington, the estimated melting temperature ranging from 900℃ to 1250℃. It is based on former experiments of float glass recycling, on which the normal float glass is not completely molten but fused in 900 degrees. [11] Integrating with safety and operation convenience, the kiln-casting is employed in this experiment, one kiln with a dimension of 44cm by 68cm is adapted. Because the flowability of melting glass is unknown, glass pieces will be free-placed directly in the mould. The detailed casting process and mould fabrication will be discussed in chapter three.

Figure 1.22: the float glass recycling through kiln-casting method, in 900 degrees (left) and 1250 degrees (right).

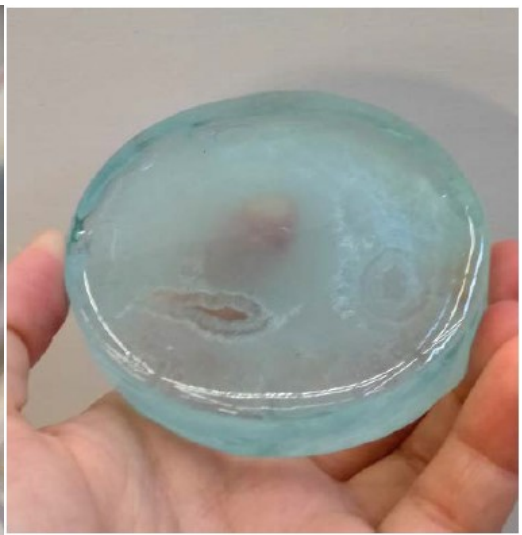

2.2 Mould technology

As mentioning in the former section, a mould manufacture is required no matter which casting method is adopted. Depend on different operation situation, different purpose and different casting method, there are various moulds await to be selected. In general, there are three main aspects waiting for considering in mould selection, including the recyclability of mould, the concavity and convexity of the mould and at last but not the least, the casting temperature. In the following paragraph, several common mould types will be introduced on account of these three aspects.

Sand mould

Figure 1.23: The sand mould for hot pouring casting.

It is widely known that sand casting method is a usual casting process for metal casting process. The name of sand casting stems from the mould material, which is consists of sand as a dominate composition adding by clay as a bonding material, during the casting process. Benefit from the figurability of moistened sand-clay mixture, a negative mould can be derived through pressing positive model into the mixture.

A flask is applied to support the negative mould generation and prevent the mixture deformation. If there is less requirement for surface performance, dimension accuracy and cast amount, it is not only used for metal casting but also suitable for glass casting. This method has a great advantage in costs and time consumption, as well as the recyclability. [17]

Lost wax

Figure 1.24: The lost wax mould.

With a view of model diversity, a versatile method has been developed to be appropriated for different shapes. This method is called as “lost wax” method, incorporating with harmless property and easy transfer between liquid and solid state. In the advantage of removable property, lost wax method creating a cavity for glass products in the refractory mould, through simple steaming process.

In laboratory experiment, the refractory material for the mould is usually chosen as silica or concrete, the specific option will be decided by different casting temperature. The lost wax method have advantage in cost and easy operation, but spend more time in cooling and steaming process of wax. In particularly, to creating the wax model, an extra steps to form a stretchable mould with a cavity of original model is required, as shown in figure 1.24. Furthermore, although the stretchable mould and the wax itself is recyclable, the wax model has to be reshaped when more amount of glass products are demanded. Identically, the refractory mould is disposable due to the damage from fetch out the glass products. [17][18]

Figure 1.25: The steel permanent mould for hot pouring casting.

Permanent mould

In contrast to the disposable mould, a permanent mould exists for reutilization in glass casting. In comprehensive consideration of casting temperature and the material durability, the stainless steel, cast iron and graphite are commonly used as the permanent mould material. Profit from the smooth surface of these material, the permanent mould is able to provide the most smooth surface to the glass product, compared with sand casting mould and lost wax mould.

For specific requirements, the permanent mould can be formed by several parts, which can be connected firmly together before glass casting. However, the stainless steel and graphite are expansive. Besides, it can only be produced special technician under specific conditions, which make it harder to acquire. In addition to this, a nickel coating should be applied before glass pouring, to easier the product release.[16] [17]

2.3 Young's modulus test

Generally speaking, there are three methods to extracting the elastic modulus of a solid material: load displacement, ultrosonic wave velocity, beam vibration.

Load-displacement method

Basically, Young's modulus can be described theoretically through the measurement of stress-strain curve slope, depending on the Hooke's Law. This derivative process is regarded as the foundation of the static method. It is common to adapt three bending test for this static method. According to the International Standards Organization, the samples are restricted in a specific dimension of 25 mm in length, 2 mm in width and 2 mm in depth, with allowable 1 mm deviation in length and 0.1 mm deviation in width and depth. [19] Besides, the testing equipment is also stipulated by ISO, with a fixed distance of 11 $\pm$ 0.1 mm between two supports, which located in parallel position, and a compression load applied in the middle of two supports. In practice, the dimension of the sample specimen is less restricted, but still corresponding to different experimental apparatus. From figure 1.26, is a practical three-point bending test for Young's modulus.

On basis of the flexural test, the applied load and the deflection within the elastic range of the specimen can be collected, coupled with the measured dimension of specimen, [19] Young's modulus can be calculated according to the basic equation of:

$$E = \frac{Fl^3}{4\lambda a h^3}$$ (Equation 1.1)

E: Young's modulus

F: Downward force in the middle position

l: Effective length of the component

λ: Deflection in middle position

a: Thickness of the component

h: Height of the component

Figure 1.26: The three point bending test for Young's Modulus capture.

The complexity of this experiment located in the control of loading direction, which should be restrained along one axis. Besides, since the test is manually operated, the loading situation might have deviation for each test, indicating errors in measurement. In that case, at least five parallel experiment for one category are required, to guarantee the reliability of results. Despite of the complexity of experiment apparatus and the consumption of sample specimens, the dimension of samples have limitations to fit the apparatus as well.

Beam vibration method

As the complexity in experiment settings and the limitation in loading rate of static methods, a simper but efficient methodology has been developed, which is called beam vibration method. This method is rooted in the elementary Euler-Bernoulli beam theory with fixed-free boundary conditions. For a free end cantilever beam, the vibration frequency, when applying a bending at the free end, can be described through the material properties and specimen dimensions. [20] The relevance is presented in the equation below:

$$f_0 = \frac{3.516}{2\pi l^2}\sqrt{\frac{EI}{\rho S}} \qquad \text{(Equation 1.2)}$$

3.516: Dimensionless factor, a modal eigenvalue
L: The length of vibration area
E: The Young's modulus of beam material
I: The second moment of cross section
ρ *: The density of beam material*
S: The area of cross section

This equation works under the assumption that the ratio of vibration length to lateral dimension is larger than 10. To withdraw Young's modulus from this relationship, the equation 1.2 can be rewrite as below:

$$E = 3.1935 f_0^{\,2} \rho S l^4 / I \qquad \text{(Equation 1.3)}$$

Aiming at gaining the results of vibration frequency, most of the dynamic experiment demanded the equipment for excitation and detection. Nonetheless, this vibration experiment does not require additional equipment, presenting in figure 1.27 is the experimental setup from Rafael's test[]. One side of testing sample is placed in a platform, connecting with a force sensor, while the other side is placed freely without any support. Meanwhile, the force sensor is supported by an alternative device. In Rafael's test, an extra thermocouple is settled so that the change of Young's modulus over temperature range can be collected. Through the restoring force data, detected by a force sensor, together with the Fast Fourier Transform software, the flexural resonance frequency will be determined.

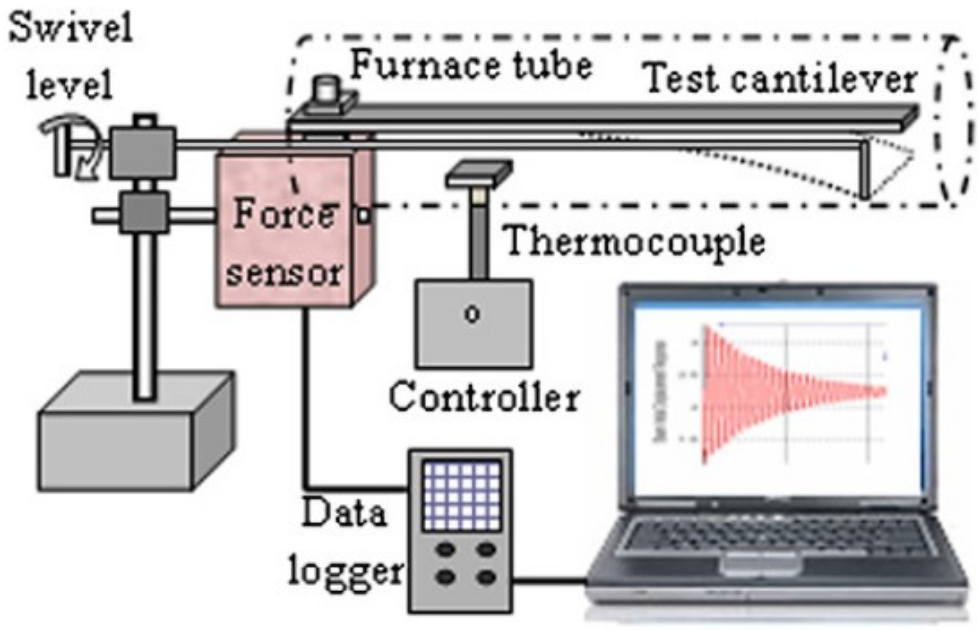

Figure 1.27: The experimental diagram of beam vibration test; on the screen shows the frequency of beam vibration.

This cheap and simple flexural vibration experiment can derive the Young's modulus straightly, in the premise of accuracy assurance. Rely on this method, the amount of testing samples is minimized due to the repeatability, and it is easily operated even for the Young's modulus test under thermal cycle. However, the dimension of sample is restricted by the assumption of Euler-Bernoulli theory. [19][20]

Ultrasonic wave velocity method

Referring to simplified Young's modulus testing method, the representative approach is ultrasonic testing methodology. As we all know, sound travels with different speeds in different media and different materials, resulting from the vibration or oscillatory motions of particles of the material. Nevertheless the particles are decided by mass and spring constants of the material, which indicating the relevance between material properties and the sound wave propagation through the material. Unlike the propagation in air, the solid material provide normal and shear stress with the sound wave, result in longitudinal sound wave and shear sound wave. [21] The former wave shares same direction with solid particle motions while the later one propagates perpendicular to the particle movement direction, shown in figure 1.28.

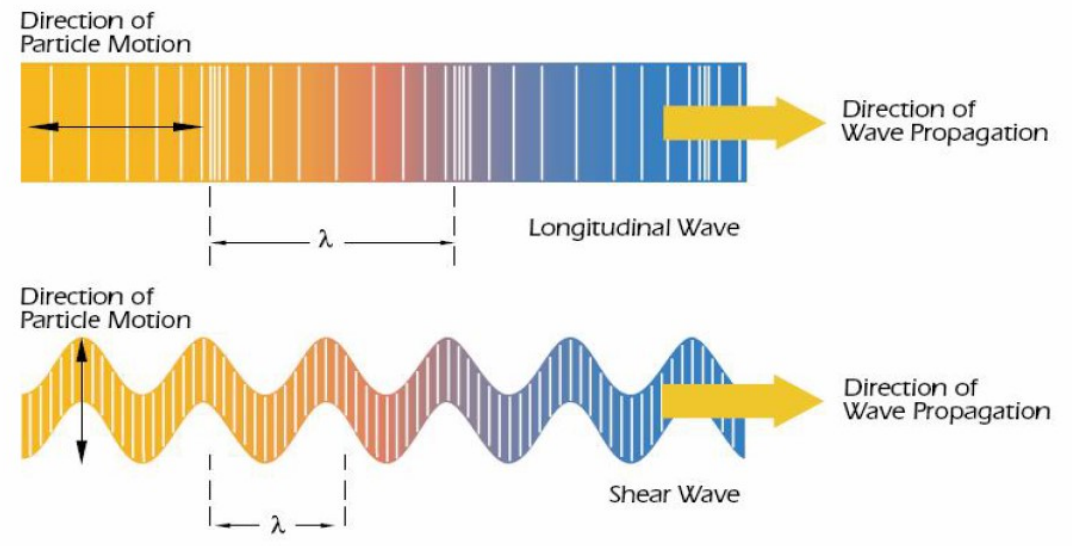

Figure 1.28: The direction of wave propagation and particle motion.

Benefit from different waves, the Young's modulus and shear modulus can be related to the sound propagation in different directions. To only considering Young's modulus, based on the Newton's Second Law and Hooke's Law the sound velocity can be calculated as

$$v = \sqrt{\frac{E}{\rho}}$$

(Equation 1.4)

E: Young's modulus
V: Sound velocity
ρ : Density of the material

The sound velocity can be acquired by the length of the specimen in longitudinal direction divided by the time of flight of longitudinal sound waves, which is detected by ultrasonic transducer and ultrasonic pulse receiver. Therefore, the equation can be rewrote as:

$$E = v^2 \times \rho$$

(Equation 1.5)

Figure 1.29 schemes the ultrasonic measurement experiments, with transducer and pulse receiver on each side of the sample in longitudinal direction. The digital signal on the screen shows the sound wave propagation through the specimen.

Figure 1.29: Ultrasonic velocity measurements in geological samples from Olympus company.

This sound velocity approach will not damage the sample, which favoured for the limited sample amounts. Besides,profit from the simplified operation and digital data processing, it saves lots of time and human labour, as well as saving laboratory space. Meanwhile, there are researches show that the ultrasonic measurement test is the most reliable method among Young's modulus test for isotropic solid material [22].

2.4 Coefficient of thermal expansion test

Introduction of CTE

Generally, a solid material will have a dimensional change along with the temperature variation. In order to define this expansion or shrinkage behavior, the coefficient of thermal expansion (CTE) has been introduced. To better describe the scale change of material, there are two types of the coefficient, which are coefficient of linear thermal expansion and coefficient of cubic expansion. Literally comprehension, the former coefficient present dimensional change of material through the linear distance change between two point of this material, expressed by the equation 1.6 below. Similarly, the coefficient of cubic expansion represents scale variant through the ratio of changed volume and original volume after the temperature change, shown in the equation 1.7. It is worth mentioning that both the linear and cubic CTE are not a fixed value for the same material, they are relative variations of length or volume when the temperature increase or decrease. The value differs corresponding to different temperature range. In the practical test, the average value within the assigned temperature interval is adapted to represent the thermal expansion behavior.

$$\alpha_L = \frac{dL}{L \cdot dT} \quad \text{(Equation 1.6)}$$

$$\alpha_V = \frac{dV}{V \cdot dT} \quad \text{(Equation 1.7)}$$

α_L: Coefficient of linear thermal expansion
α_v: Coefficient of cubic thermal expansion
L: The length of tested material at temperature T
V: The volume of tested material at temperature T
T: The testing temperature

Specially, for isotropic material, there is relationship between linear and cubic CTE as following:

$$\alpha_V \cong 3\alpha_L$$

In contrast, the anisotropic material usually has different CTE in different directions. Generally, a higher value of CTE exists in the direction of lower elastic modulus, and vice versa.

Influence factor

Obviously, the CTE is affected by temperature increase or decrease. In the atomic level, the dimensional change under temperature variation result from the change of an average distance among material points. It is a macroscopical reflection of material particle movement. In another word,

the value of CTE can be defined not only by temperature variation but also decided by the material itself. First of all, chemical composition plays the main role among all influence factors. The different chemical composition indicates a different strength of chemical bonding. A higher chemical bonding strength restraint the material particle movement when temperature growing, as a result, this material is less easy to expand, which means a smaller CTE. Apart from the chemical composition, the crystal structure is another important aspect. Broadly speaking, a material with compact crystal structure has higher CTE compared with the material with loosely crystal structure. Such as two-dimensional silicates, which has an infinite sheet structure. As we know, silicates are consists of four oxygen atoms and one silicone, forming an tetrahedron structure. On the sheet structure, three corners from one tetrahedron are connected with another tetrahedron, as a consequence, a looser crystal structure with lower density is developed. Hence the crystal silicates often have lower CTE than other material.

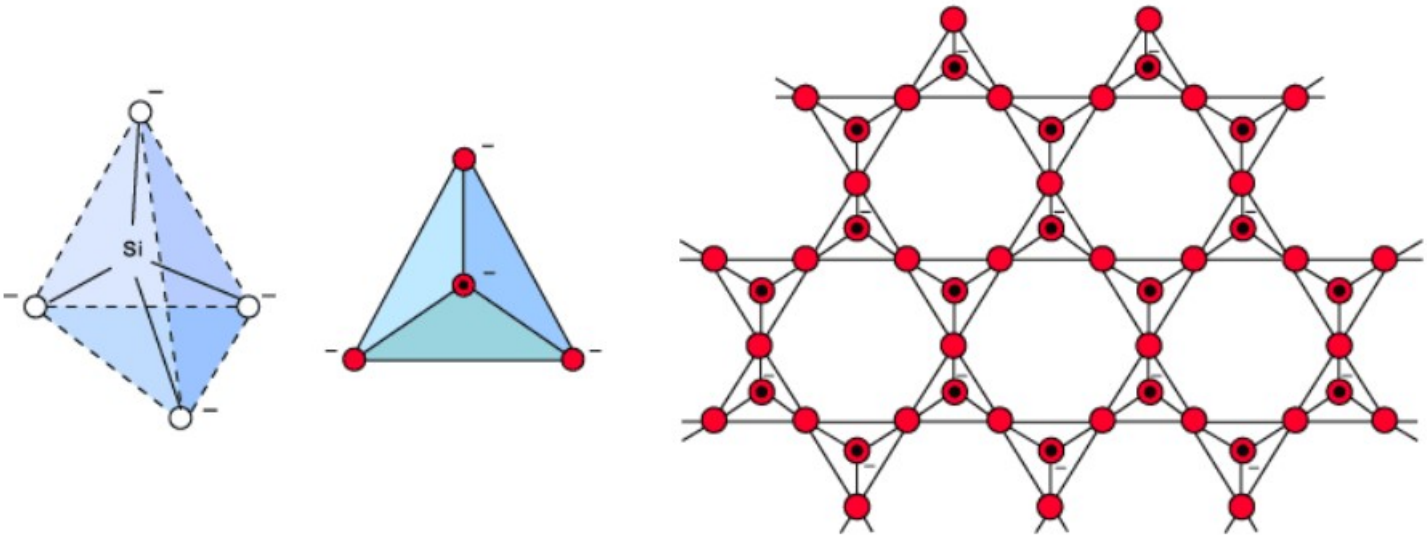

Figure 1.30: Left: The silicate tetrahedron and the top view of simplified silicate tetrahedral; Right: the silicate sheet structure.

Besides, ferro-magnetism of metal or alloy element, the internal flaw or cracks as well as the crystal defects can also affect the material performance when temperature changes, whereupon the value of CTE differs.

Correlation properties

Since the essence of thermal expansion can be concluded as the enhancing lattice vibration after heating, following by the volume expansion of the material, the energy of thermal motion of the lattice will increased at the same time. Correspondingly, heat capacity, which describes the energy increasing ability of a material, is connected with CTE. The correlation is represented by Gruneisen

relation, illustrating that after heating, the change of the volume and the change of the thermal energy has the same tendency. [on Gruneisen's equation for thermal expansion] the common equation shown below, introducing Gruneisen parameter, which is a physical quantity express the nonlinear vibration of crystal lattice.

$$\alpha_V = \frac{\gamma}{KV} C_V \qquad \text{(Equation 1.8)}$$

γ : *Gruneisen parameter*

K: The elastic modulus of tested material

V: The volume of tested material

Gruneisen has also proposed a limit equation of thermal expansion of solid body, shown in equation 1.9. It demonstrates for common metal, the ratio of volume expansion is approximately 6% from zero degree to melting point.

$$b = \frac{\Delta V}{V_0} = \frac{V_{TM} - V_0}{V_0} \approx 0.06 \qquad \text{(Equation 1.9)}$$

V_{TM}: the volume of tested material at melting point

V_0: the volume of tested material at zero degree

According to the above equation, the solid body will have a higher CTE with a lower melting point, since the ratio of volume expansion is a fixed constant value. Nonetheless, not all metal has a 6% expansion limit, it differs from various atom combination and lattice structure. The relationship between linear CTE and melting point can be presented by an empirical formula below:

$$\alpha_L T_M = b \qquad \text{(Equation 1.10)}$$

α_L*: Linear coefficient of thermal expansion*

T_M: Melting point of the metal material

Optical method

The testing method of CTE is first developed by applying optical apparatus in displacement measurement. With temperature rising in the sample area, the laser as a light resource is going to determine the elongation of samples. It requires manual recording by laboratory technician for the primary setting.

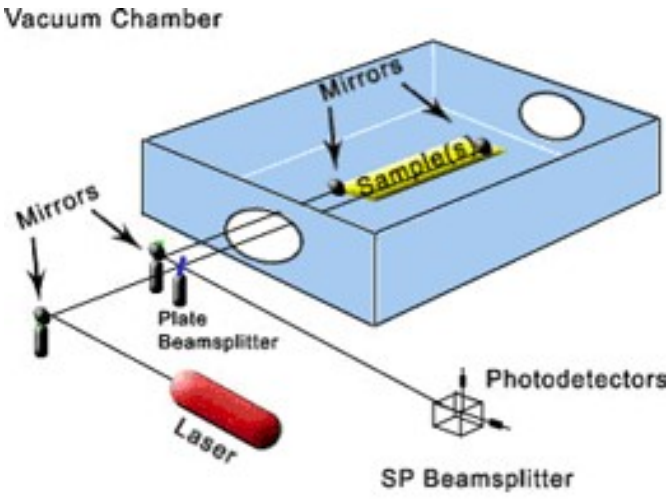

Figure 1.31: The simplified diagram of optical lever methodology from Precisions Measurements and Instruments Corporation Laboratory in

As time goes by, there are photo detector helps recording the measurement, and interpolation techniques to precise the length unit into nanometer. Meanwhile, there are limitations for optical lever method, such as the fixed shape and dimension of specimen awaits for testing. Considering the test instruments placement, there are also minimum distance requirement between mirrors and samples.[23]

Dilatometry test method

The Dilatometry test method is a common way to measure this fundamental material property. As presented in figure 1.32, the equipment mainly consists of three parts, including heating area, connecting area and measuring area. The sample material and reference material will be placed in a holder, covered by a furnace. Both the sample and reference specimen are attached with a push rod, which connects them with detectors. When the furnace starts heating, the expansion of material will push the rob to the receiving area, with the help of the displacement sensor, the linear elongation is able to be recorded. To minimizing the deviation, the push rob and material holder are often made of temperature-insensitive material, such as quartz glass whose CTE value towards zero. Separating from various position of sample (horizontal or vertical position) and different measuring sensor, the dilatometry equipment are divided into different types.

Figure 1.32: The simplified diagram of Dilatometry from Department of Physics of Material in Univerzita Karlova; (top middle); the horizontal dilatometry equipment; (bottom left) the vertical dilatometry equipment (bottom right)

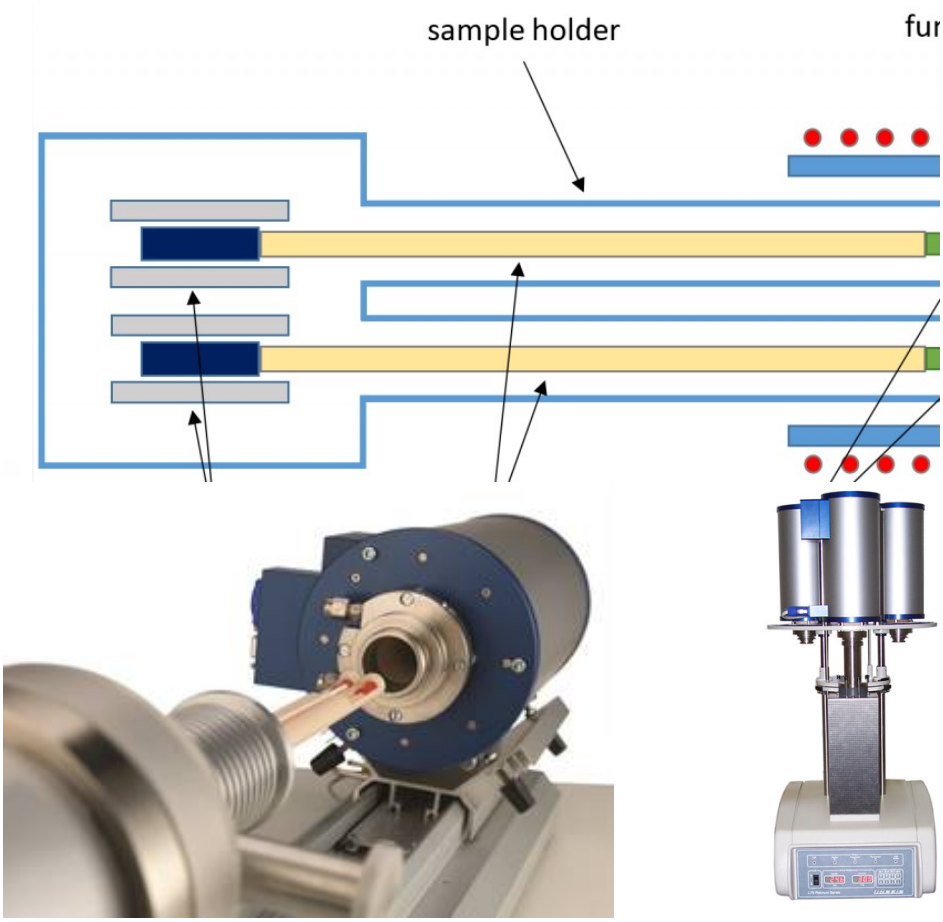

Although the dilatometry methodology is widely applied in practice, it is bond to has restrictions. The main drawback is born from the temperature variation along the length of push rob and sample holder. Even though the CTE of quartz glass rob and sample holder are very low, the different temperature on the top of specimen and on the bottom of specimen still cause different elongation, which will affect the results, thus a correction of the measured results is required. Besides, the specimen has to be produced in fixed dimension which limited the flexibility of CTE test. [24]

Strain gauge method

Basically, the measurement of CTE is the deformation measurement of the target material over the temperature range. When it comes to deformation measurement, the strain gauges are one of the most popular instruments. Applying strain gauges on the smooth surface of samples, the linear expansion within temperature interval can be determined through electronic indicator. When temperature altered, the sample has a deformation on the surface, along with the deformation of attached foil, resulting the change of electrical resistance of strain gauge. Mostly, the electrical resistance is detected through a Wheatstone bridge. In other words, the strain gauge method transform physical deformation into electrical information, so that the results are more precise and reliable. At the same time, a temperature sensor will collect the data of temperature change. [25]

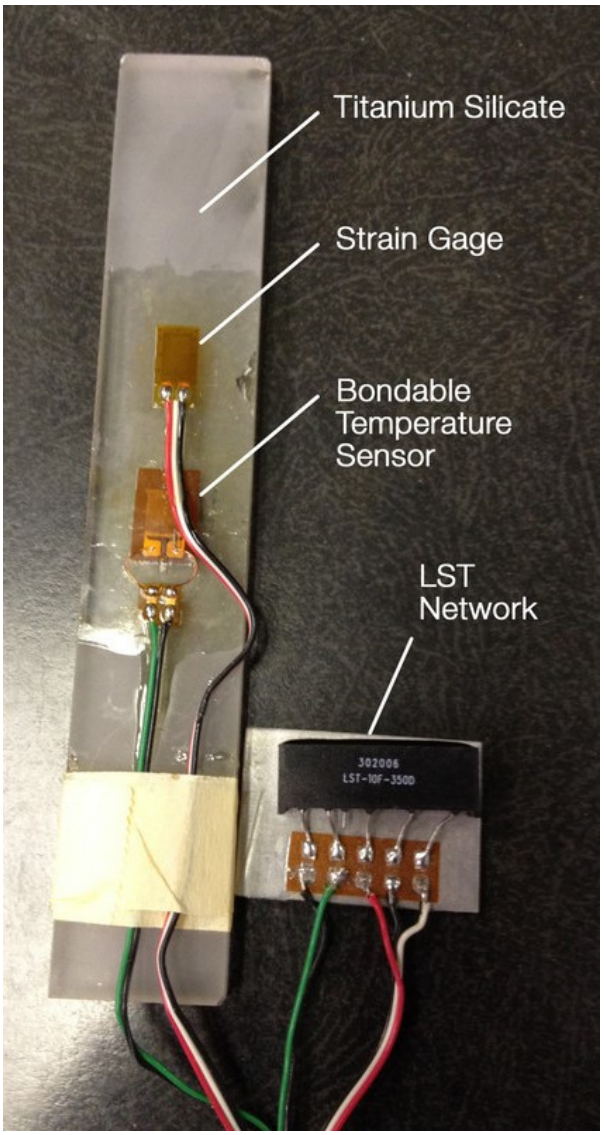

Figure 1.33: The test figure for strain gauge method.

Compare to other methods, the strain gauge methods have less restriction, except for a smooth surface. In addition to this, the selection of strain gauge and corresponding glue varies from different temperature range.[measurement of thermal expansion coefficient using strain gauges] Since the strain gauge is attached to the surface, which is more favourable for linear CTE testing, it is not suitable in the cubic CTE test.

Part 2 Experimental research

Generally speaking, aiming at structural application of the recycled glass, four material property should be tested, which are Young's modulus, thermal coefficient, Poisson's ratio and fracture strength. Exceptionally, glass as a specific material usually has extreme low Poisson's ratio and similar characteristic compared to concrete, which indicates a good performance under compression. Therefore the author pays more attention on Young's modulus and fracture strength. Referring to the literature study, the chemical composition and the basic bonding strength among atoms of a specific material is one of the dominate dependence of material property. In order to obtain the material property, the production and chemical analysis of sample glasses, recycled from source material, is necessary.

Figure 2.1 The first batch of recycled glass samples after kiln-casting, photo by author.

Chapter 3 Experiment design

Aiming at the recyclability of coated glass in structural level, the recycled samples are required to be manufactured. There are two batches in this experiment, the first batch including recycled samples from different coated glass independently, while the other batch is the mixture of three kinds of coated glass. The former batch is provided to material property test including Young's modulus test, coefficient of thermal expansion test and chemical composition analysis. While the later batch is produced especially for the fracture strength test, thus precise dimension is required. Apart from the manufacture procedure, the source material selection, the data collected by XRF test and the corresponding analysis will also be illustrates in following sections.

3.1 Source material selection

As mentioned in the last chapter, the float glass used as architecture glass are used in this experiment. According to [11], the float glass has similar composition compared with drinking glasses based on Panalytical Axios Max WD-XRF spectrometer analysis. Which especially shown in approximately 74% silicon dioxide and 12% sodium oxide, by comparing clear Coca cola bottle (73.529% silicon dioxide and 12.008% sodium oxide) and PPG clear glass (74.214% silicon dioxide and 12.438% sodium oxide). On the basis of similar chemical composition and clear appearance, why Coca Cola glass bottles are able to be recycled while float glass can not? On the one hand, because of the functional requirement, the glass bottle recycling are physical process which without chemical reaction of glass. On the other hand, float glass contains numerous categories, examples provided in table 2.1 (data from Pilkington), which has chemical composition diversity. Furthermore, in order to embedded in the frame float glass used as architecture glass always has bond material along the edge, indicates a difficult separation between adhesives and waste glass.

Solar control	Pilkington Arctic Blue	- blue body-tinted - surface coating - possible specified as toughened or laminated	
Thermal insulation	Pilkington K Glass	- hard coated - pyrolytic low-emissivity coated - inner pane of an energy-efficient IGU	
Fire protection	Pilkington Pyroshield	- monolithic wired glass - safety clear - wire mesh between two glass panels	
Noise control	Pilkington Optilam Phon	-laminated glass with PVB interlayer in between - possible to be incorporated with thermal insulation	
Self-cleaning	Pilkington Activ	- single coated glass - possible to incorporated with tints and laminations	
Decoration	Pilkington Optimirror	- reflective silver layer - greater resistance to natural corrosion	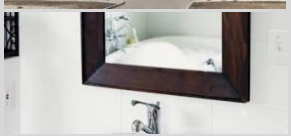

Table 2.1: Example glass in different categories from Pilkington.

This report eliminates the mirror glass, which is normally applied in skyscrapers as building glass, thus silvering will not be considered in following content. Accordingly, adhesives, inter layers between laminated glass, glass tints and glass coatings are generally concluded as four main difficulties during float glass recycling. Luckily, several recycling companies has been at the forefront of the float glass recycling such as Maltha glassrecycling company. Under the information from Maltha, the adhesives on the glass edge can be removed artificially so that the binding material will not join in the recycling process. Meanwhile, the inter layers existed in laminated glass will be dislodged before recycling as well. Through bringing out of plane external force, the glass panel will peeled off from the inter layers, afterwards glass cullets and inter layers will step in next phase separately. Because of the structural purpose, tints are less considerable compared to coatings, since color and transparency is not necessary for structural components. Therefore, the coated glass is the most important role in the experiment.

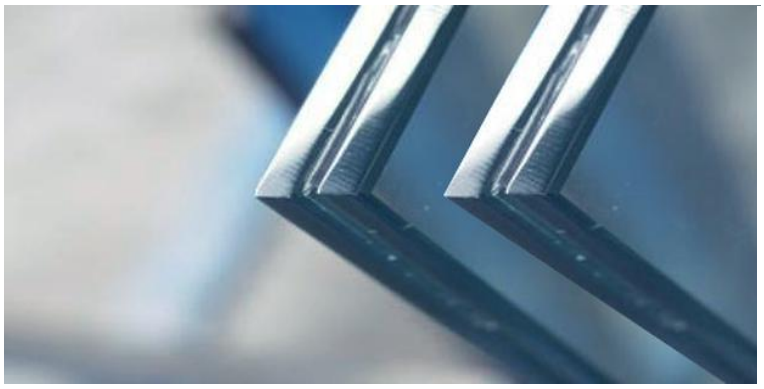

Figure 2.2: Laminated glass. Laminated glass is normally fabricated with PVB layer or EVA layer in between. Used for safety function or insulation functions, with the help of interlayers.

Figure 2.3: Tinted glass. Tinted glass is also called as colored glass, which usually produced to sort light transmission. Nowadays, glass tints are normally combined with other glass technologies such as coatings and laminations.

Figure 2.4: Glass adhesives. Glass adhesives are special binders which make strong connections among glass components or between glass member and other substrates, such as metal frame, plastic frame or connectors.

Figure 2.5: Coated glass. Glass coating mainly aiming at affect the transmission of glass, assisted in improve the glass appearance and surface condition. The coated glass is widely used as thermal control glass as well as self-cleaning glass.

Referring to Pilkington coating technology, there are three approaches to apply coatings on float glass. The simplest way called Plasma Vapour Deposition (PVD), in which a gas plasma is sputtered into the target surface. This vacuum process can be controlled by magnetic field. With the development of magnetrons, coatings are able to be sputtered in various directions with higher rates, thus the time consumption of coating process can be shrunk significantly. Benefit from this technology, multi-layer coatings without influence of transparency is able to be realized. In basic PVD or Magnetron Sputtering process, coatings only attached to the target surface without any chemical reaction so that these two approaches are known as "soft coatings". On the contrary, "hard coating" also exists. A coating process contains chemical bond rupture and formation is called Chemical Vapour Deposition (CVD), in which the gaseous mixture will be introduced to the target float glass, under a high temperature ranging from 482℃ to 732℃. This hard coating is the outcome of pyrolytic reaction, which indicates strong chemical bond connection, thus it is hardly to be removed from the glass surface. [26]

Figure 2.6: The hard coating process (above) and soft coating process (bottom), origins from ShenZhen King Glass.

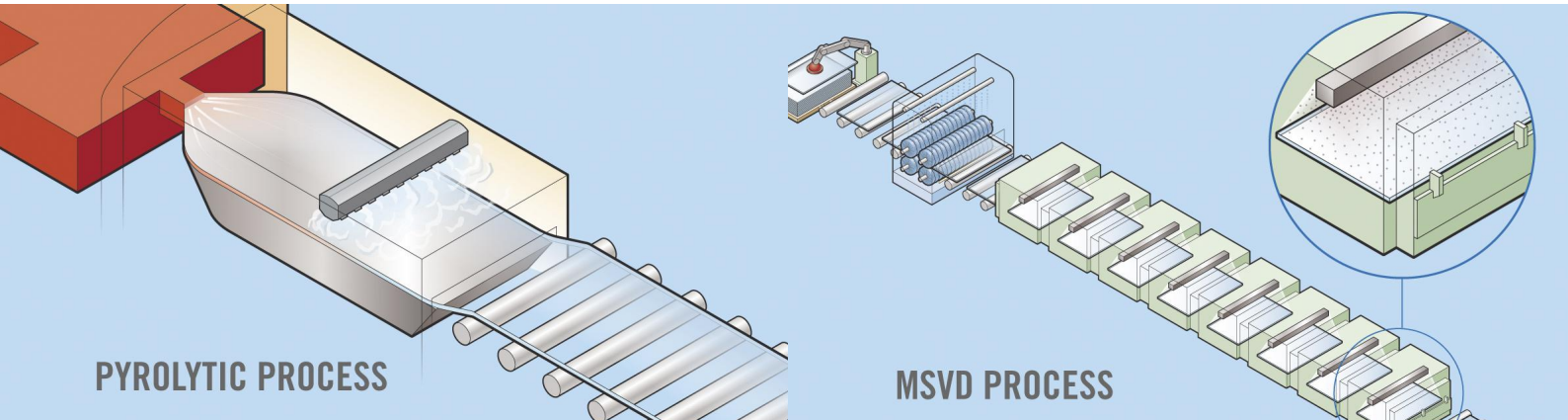

During this experiment, coated glass are simply divided into two categories which are soft coating and hard coating. Thanks to the support form Pilkington glass company, four kind of glass samples are provided, shown in figure 2.7, including normal float glass, soft coating glass 1 with dark green tints, soft coating glass 2 with light green tints and hard coating glass. All glass samples are coated only on one side. Based on the manufacture process of float glass, there will be a tin bath side in the float glass as well. Not only the coated side should be recognized but also the tin bath side and bare side should be distinguished, a detailed differentiation will be obtained through XRF test.

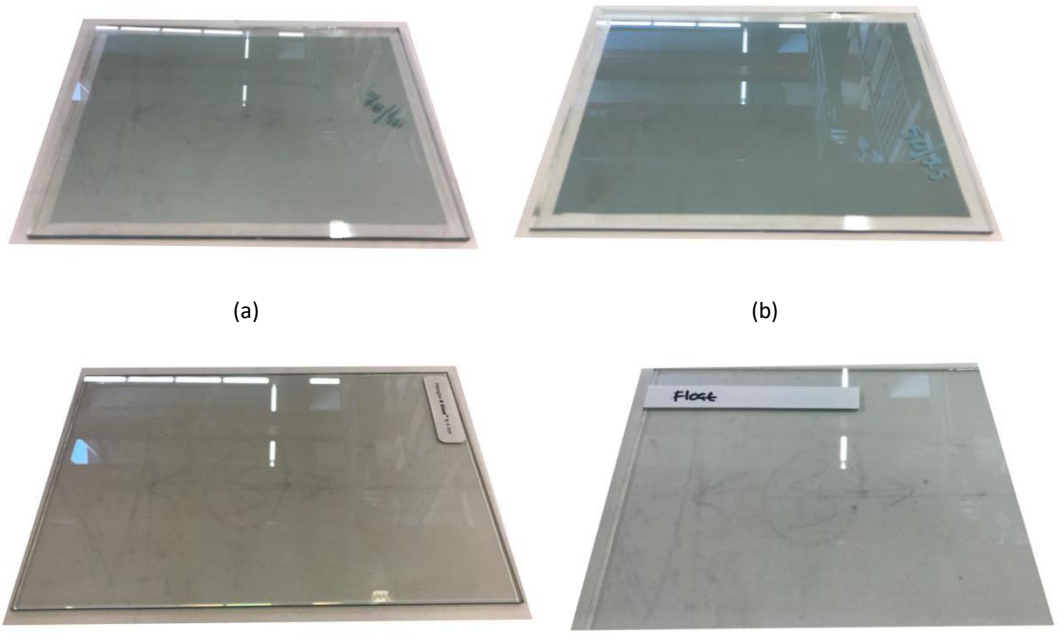

Figure 2.7: Float glass samples from Pilkington. (a) is the soft coating glass with type 70/40, in light green tints; (b) is the soft coating glass with type 50/25, in dark green tints; (c) is hard coating glass; (d) is normal float glass.

3.2 Cast procedure

Mould preparation

Considering the previous experiment experience and existing test condition, two types of mould are taken into consideration. When kiln-casting held below 1000 degrees, a crystal-cast mould will be used. Nevertheless, when firing above 1000 degrees, a heat-resistant concrete protective coat is required. The crystal-cast mould made of powder named Crystalcast M248, which contains cristobalite, quartz and gypsum.

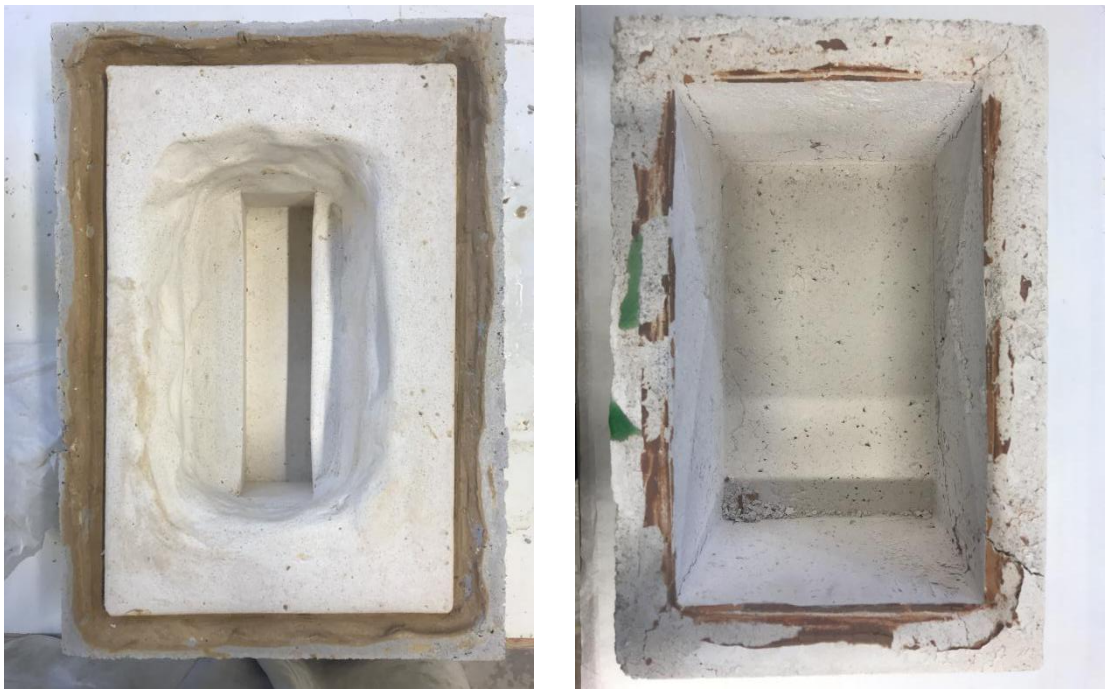

Figure 2.8: Moulds for glass casting. On the left is crystal-cast mould with a 1cm-thick concrete cover, while on the right side is a bare heat-resistance concrete mould.

As discussed before, the lost-wax method is selected for mould preparation, which starting with a beam-shape original models. There are four steps to produce the crystal-cast mould, presenting in the following:

1) Preparation of original model

At first, a original model, usually made of wood, bamboo, metal or plastic, which have a stable shape and enough ability to withstand the pressure from liquid plaster, with desired shape of final product is required. In this material testing experiment, a plastic cuboid box is employed as original model, which is fixed by clay on the operating platform to avoid moving and restrain deformation. Since there are no strict requirements for the dimension of finished product in material testing, the plastic box is

roughly measures as 15.5cm in length 4.5cm in height and 3.5cm in thickness.

2) Produce rubber mould

Based on the original model, a flexible mould will be produced in the second step. In general, this flexible mould is fabricated by polyurenthane rubber. After fixing original model, the mould boundary should be clarified through wooden panels. Similarly settled by fixer, together with clay applying so that the liquid, which is used to form the rubber mould, will not leaking. The rubber mould is made of plaster, which in a ratio of 1.75 to 1 with water. The solidification period of plaster mixture will be last for at least 24 hours.

Figure 2.9: The production process of rubber mould. The left sub-figure shows rubber mould while curdling, with wooden panel and clay as fixer. On the right side is the finished rubber mould, which are well-placed before making wax mould.

3) Produce wax model

After rubber mould is finished, the original model will be taken out from the mould, before filling in the empty space with hot wax. During the cooling period of wax, which normally lasts for around 3 hours, the side face of rubber mould should be supported to restrain the deformation. The time consumption of cooling period is related to the environment temperature as well as the volume and dimension of the specimen. The solid wax model shown below is the finished positive mould for the final product in material property test.

Figure 2.10: Wax model. Two finished wax models with corresponding rubber moulds shows in left sub-figure, while the right sub-figure presents the fixed wax model above a plastic base before crystal-cast mould fabricating.

4) Produce crystal-cast mould

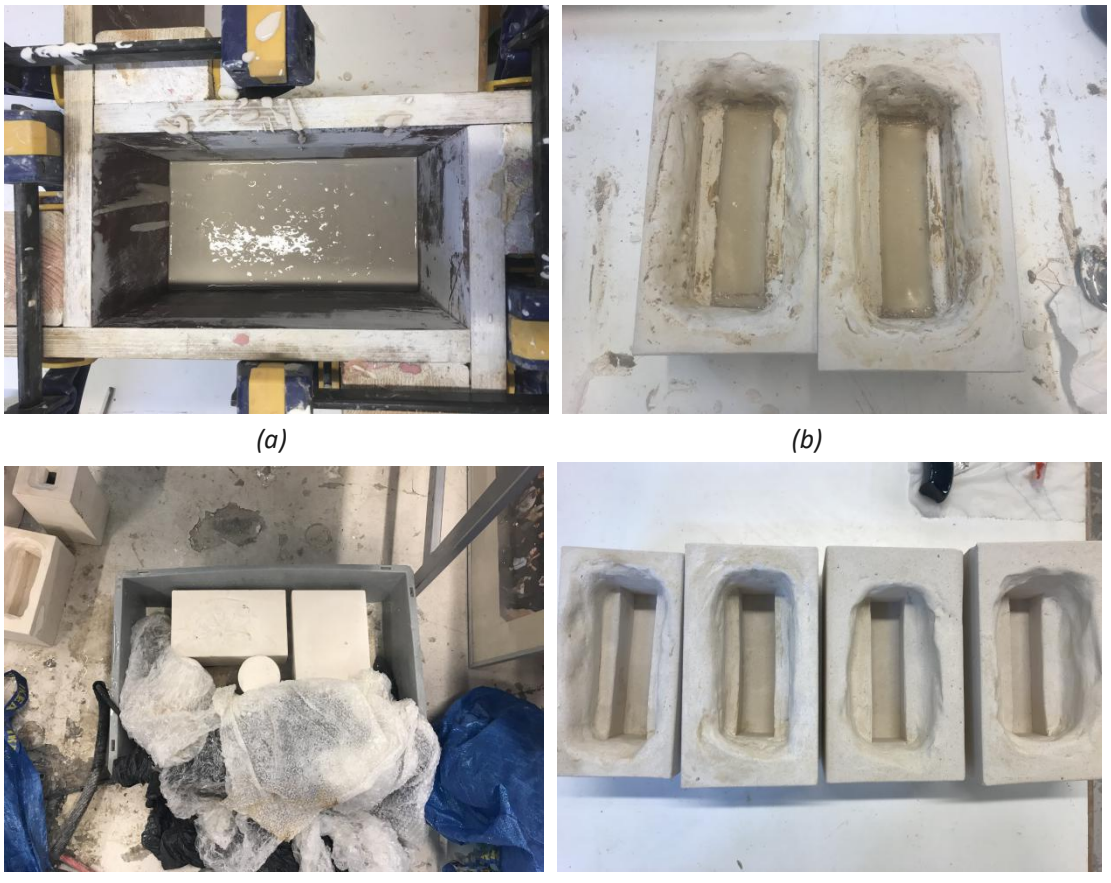

(a) *(b)*

(c) *(d)*

Figure 2.11: The process of crystal-cast mould production. (a) shows the liquid crystal-cast silica mixture, pouring on top of the wax model, with boundary setting by wooden panels and fixers; on figure (b) is the solidified crystal-cast mould, with wax model in side; the solidified crystal-cast moulds are placed up side down in figure (c) inside a steamer, after several hours steaming, wax will come out of the mould; after cleaning and smoothing, the finished crystal-cast moulds are presented in figure (d).

To fabricate the final mould, the wax model will be placed in the operation platform with a solid box on below. This solid box produces an extra room for glass during casting. Similarly, the model and solid box will be fixed by clay. 2 centimeters away from the model, wooden panels and fixer will setting the boundary and deciding the thickness of final mould. Before pulling refractory mixture, in order to easier the process of separating wax and crystal-cast mould, a small amount of soap water will be sprayed onto the surface of model and clay base. Consisting of crystal-cast silica, the final mould will be generated under a powder to water ratio at 2,8 :1. With a at least 2-hours cooling period, the crystalline silica mixture will be solidified, and wooden panels can be taken away as well as clay and solid base. After smoothing the edges, the whole mould along with the wax inside will be placed upside down in a steamer. Through at least one and half hours, the wax turns into liquid and flow out from the mould due to gravity. At last, smooth and clean the surface of mould, especially the touching area of glass, remove remaining clay and wax.

In general, the fabrication of heat-resistance concrete mould is similar to crystal-cast mould production. While the consist of mixture is different, which is a concrete powder to water ratio at 3:1, curing for at least one day in room temperature.

Glass casting

Before putting into the furnace, on basis of free-set placement, glass will be carefully cleaned by propanol, following by being broken into pieces and placed orderly inside the mould, which should be cleaned by air pressure in advance. Exact weight and category should be recorded accurately, as well as the position in the furnace.

Figure 2.12: The prepared glass samples before kiln-casting.

time	Temperature (℃)	Temperature ramp (℃/hour)	Dwell (hour)	Total time consumption (hour)
	25		0	0
1	150	50	2.5	2.5
	150		2	4.5
2	700	50	11	15.5
	700		2.5	18
3	1120	50	8.4	26.4
	1120		8	34.4
Opening the kiln				
4	760	-360	0	34.4
5	560	-160	6	35.65
	560		12.5	45.65
6	550	-2	5	50.65
	550		7.5	56.65
7	525	-2	5	69.15
	525		7.5	74.15
8	510	-2	1	81.65
	510		18.5	86.65
9	480	-4	13.8	94.15
	480			95.15
10	370	-6		113.48
	370			113.48
11	25	-25		127.28
4	25			127.28

Table 2.2: The record of temperature along with time passing during the kiln-casting process.

As mentioned before, the float glass will not remelting completely at around 900℃, obvious lumps are fused together in the recycled sample. Thus the estimated melting temperature for float glass is between 900℃ and 1200℃. Suggested by Telesilla Bristogianni, the author set an aim temperature at 1100℃, the planned testing temperature arrangement shown in table 2.2. Shown in the casting plan above, in the first stage, the temperature growth is set as 50 degrees per hour, and when temperature arrives at 150℃ and 700℃, the kiln will hold the temperature for 2 hours and 2.5 hours respectively. When temperature reaches 1100℃, the kiln will be opened manually so that the temperature will sharply decrease, this stage called quenching stage which presented in figure 2.13. The quenching behavior will be carried until the kiln temperature lower than 660 degrees the kiln will be closed again to continue annealing process. This operation resulting from preventing crystallization zone from 780 degrees to 660 degrees.[43]

Figure 2.13: The manual quenching process during kiln casting.

Restricted by the resource delivery, the hard coating samples are recycled separately. The kiln-casting firing schedule is slightly different from the schedule above, but they are sharing the same highest temperature. The figure 2.14 shows the hard coating glass before recycled, and the firing schedule for hard coating will be demonstrated in the appendix, which is automatically programmed by the kiln itself, without manually quenching. The highest temperature and quenching time is similar to the manual-quenching kiln casting process.

Figure 2.14: The hard coating glass before kiln casting.

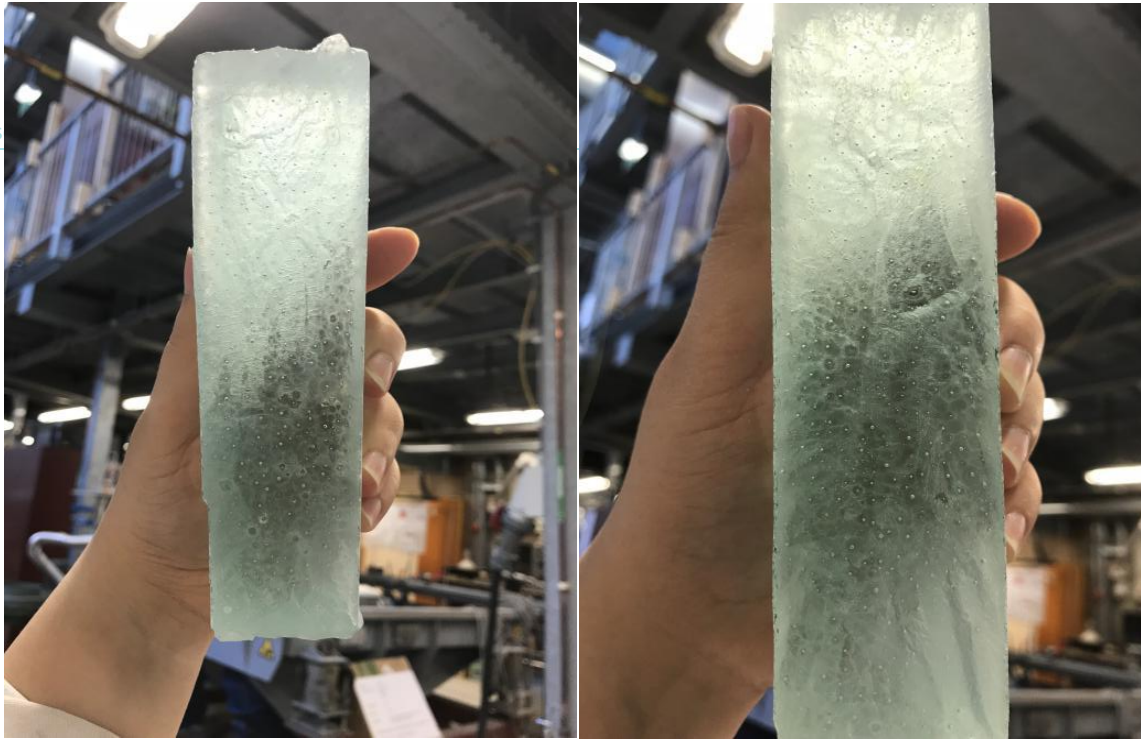

Figure 2.15: The finished recycled glass samples made of normal float glass.

Fetched from the kiln, glass samples can be easily taken out of the crystal-cast mould. As emerged in figure 2.15, some lovely cell-shape trail shown in the top surface, which exposure to air, of the sample. None crystallization from the mould-touching surface is observed, because of the rapid cooling from 780 ℃ to 660 ℃, which is the danger zone where crystallization forms. [27] The avoidance of the crystallization benefit for the structural performance under loading conditions.

Afterwards, the finished glass samples will be adjusted by grinder and cutting machine, to present a more regular shape with smoother edge and surface. Through adjustment, the samples are ready for the further testing. From the figure 2.16, the color of the final products are similar to each other. It is not easy to distinguish dark tints from light tints, which may indicate the not apparent influence in float glass recycling from tints.

Figure 2.16: The recycled glass samples after kiln-casting. On the left are three glass samples taken out of the kiln, covered by the mould; the middle sub-figure shows glass samples without mould in correspond to their category, the right sub-figure shows the recycled hard coating samples.

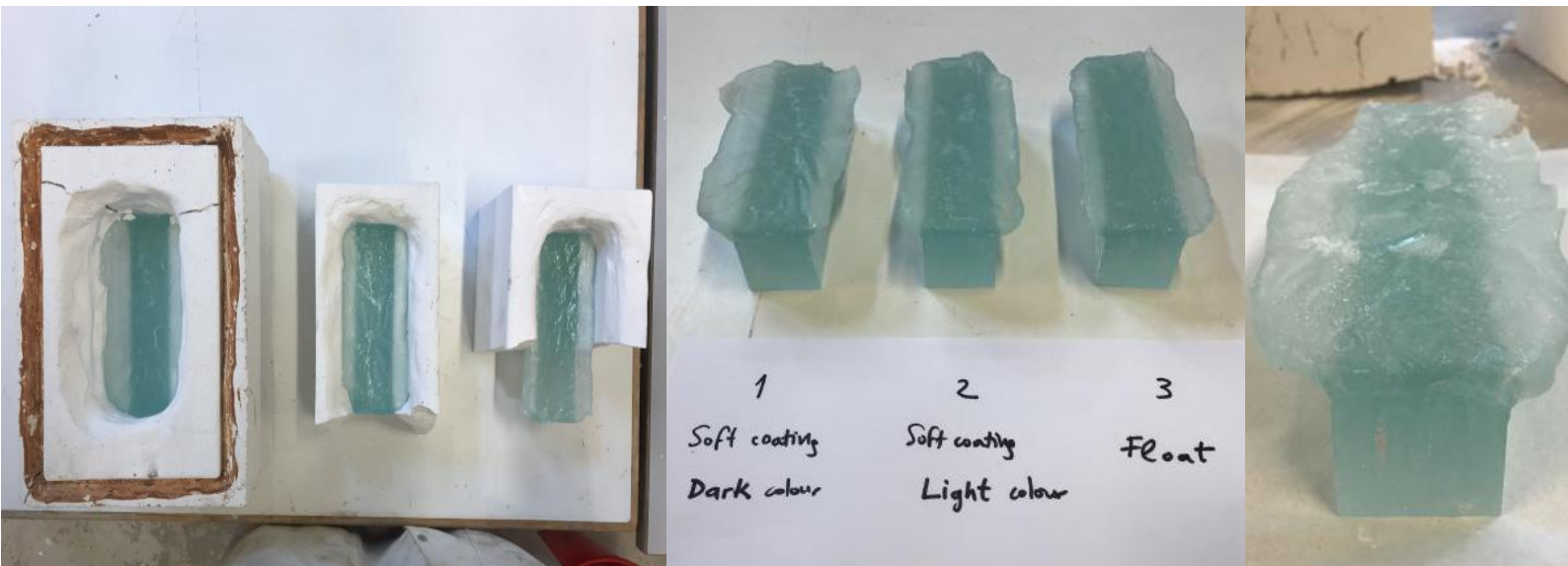

3.3 Data collection through XRF test

In order to processing further analysis and comparison, the chemical composition of original glass sample should be comprehend beforehand. Consequently, the X-ray fluorenscence process is introducing for chemical analysis. This XRF test defined different chemical composition by different energy release, which is determined by characteristic of specific element. Conclude from the XRF test result by Ruud Hendrikx, the chemical composition for the four glass samples on both sides are presented in the following table:

	Normal float glass		Soft coating (light)		Soft coating (dark)		hard coating	
	a	b	a	b	a	b	a	b
		tin bath	coated	tin bath	coated	tin bath	coated and tin bath	
SiO2	74.432	73.212	64.96	73.301	64.665	72.882	49.967	73.412
Na2O	12.524	12.453	4.765	12.483	4.736	12.714	0.577	12.086
SnO2		1.175	2.67	1.076	2.732	1.236	32.384	
CaO	8.23	8.397	8.969	8.406	9.253	8.45	14.241	9.063
MgO	3.884	3.797	2.318	3.778	2.273	3.83	1.153	4.262
Al2O3	0.55	0.577	0.506	0.571	0.549	0.52	0.317	0.561
K2O	0.145	0.135	0.16	0.139	0.16	0.134	0.453	0.295
SO3	0.113	0.14	0.097	0.125	0.171	0.112	0.237	0.144
Fe2O3	0.057	0.051	0.079	0.056	0.094	0.065	0.35	0.11
TiO2	0.029	0.028	0.294	0.025	0.364	0.022	0.154	
SrO	0.009	0.01	0.024	0.01	0.024	0.009		
P2O5	0.009	0.011	0.011		0.009	0.01	0.009	0.022
ZrO2	0.009	0.008	0.03	0.012		0.006	0.055	0.015
MnO	0.006	0.005	0.016	0.008	0.009	0.008		
ZnO	0.002	0.002	15.064		14.703	0.002	0.02	
Ag2O			0.03		0.04			
Au			0.007					
NiO					0.033			
Cr2O3					0.021			
Rb2O							0.013	
Cl							0.069	0.03

Table 2.3: The chemical composition content of original float glass.

Depending on the content of tin, the original glass panels can be easily separate from the tin bath side, which has approximately 1% content, and the side without a tin bath. Referring to the coating side, it is also obvious to distinguish due to the relevance with tin content as well, comparing with normal float glass without coatings. As shown in the table above, the normal float glass has the maximum content of silicate dioxide compared with the other three types. While the the hard coating glass has great advantage in stannum content in the coated side. For soft coating glass, the tin bath surface are separate from the coating surface, which is different from hard coating glass, as a result of different

manufacturing techniques as mentioned in former sections. Through comparing the chemical constitution of tinted glass (light soft coating and dark soft coating) with the transparent glass (normal float glass and hard coating glass), the iron content is higher in former glass than later, corresponding to the green color given by ferric oxide. Besides, in comparison within the tinted glass, the dark soft coating has extra chromium oxide, which provide extra green for the dark tints.

Except for the XRF analysis for original float glass, the recycled glass has also taken for XRF test. At first, the sample surface part has taken to the XRF test, in the side which exposure to the air without touching the mould. The results shown in the table below, from the highest silica dioxide content for recycled dark soft coating glass to recycled normal float glass with lowest silica dioxide content. While the differences between four samples in silica dioxide are not distinct. The chemical compositions, such as ferric oxide, which result in tints for the original glass have nearly equal amount after recycling, apart from chromium oxide existing in original dark soft coating which is unmeasurable after recycling. The amount of the chemical composition result in tints are so small that it can hardly apparently affect the mechanical properties of the recycled glass.

	SiO2	CaO	Na2O	MgO	Al2O3	SO3	K2O	Fe2O3	TiO2	Cl	MnO	SrO	ZnO	P2O5	ZrO2	Rb2O
Recycled dark soft coating	90.895	5.404	2.148	0.873	0.3	0.11	0.099	0.089	0.031	0.022	0.013	0.008	0.007			
Recycled light soft coating	90.765	5.84	1.907	0.88	0.293	0.129	0.073	0.105				0.007				
Recycled normal float	89.973	6.354	2.115	0.94	0.3	0.118	0.075	0.117				0.009				
Recycled hard coating	90.002	6.299	1.934	1.133	0.284		0.157	0.143		0.008		0.005		0.019	0.015	0.002

Table 2.4: The chemical composition content of surface of recycled glass samples

However, the silicate dioxide content are extreme high for all of the samples, which might indicating a movement and exchange of the chemical content during casting process. As the result, a further XRF analysis has been applied into the top, middle and bottom area in height direction of the samples. Restricted by the cost and time consumption, only recycled normal float glass and recycled hard coating glass are setting as the target samples.

In table 2.5 and table 2.6, not only the chemical composition of recycled samples are exhibited, but also a chemical content for the corresponding original samples are presented as a comparison. Based on the XRF test results, the silicate dioxide content turns to the common value in the body material, hence, the XRF test for the middle area can be regard as reliable resource for following material property analysis.

Normal float glass						
	Normal float glass		Recycled normal float glass			
	Bare side	Tin side	Surface	Top	Middle	Bottom
SiO2	74.432	73.212	89.973	71.882	72.341	71.855
Na2O	12.524	12.453	2.115	12.883	12.545	13.052
CaO	8.23	8.397	6.354	9.93	9.861	9.74
MgO	3.884	3.797	0.94	4.051	3.959	4.069
SnO2		1.175				
Al2O3	0.55	0.577	0.3	0.593	0.558	0.649
SO3	0.113	0.14	0.118	0.295	0.374	0.344
K2O	0.145	0.135	0.075	0.166	0.169	0.171
Fe2O3	0.057	0.051	0.117	0.075	0.1	0.068
TiO2	0.029	0.028		0.036		
P2O5	0.009	0.011		0.016	0.018	0.009
SrO	0.009	0.01	0.009	0.011	0.009	0.01
ZrO2	0.009	0.008				
MnO	0.006	0.005				
ZnO	0.002	0.002			0.009	0.006
Cl				0.046	0.048	0.027
CuO				0.016	0.009	

Table 2.5: The chemical composition content of recycled normal float glass, different layers in vertical direction.

Hard coating						
	Hard coating		Recycled hard coating			
	Tin and coated side	Bare side	Surface	Top	Middle	Bottom
SiO2	49.967	73.412	90.002	73.011	73.167	73.405
Na2O	0.577	12.086	1.934	11.64	11.799	11.714
CaO	14.241	9.063	6.299	9.268	9.057	9.047
MgO	1.153	4.262	1.133	4.923	4.802	4.814
SnO2	32.384			0.024	0.054	
Al2O3	0.317	0.561	0.284	0.518	0.524	0.523
SO3	0.237	0.144		0.002		
K2O	0.453	0.295	0.157	0.364	0.394	0.331
Fe2O3	0.35	0.11	0.143	0.145	0.142	0.109
TiO2	0.154			0.03		
P2O5	0.009	0.022	0.019	0.029	0.021	0.021
SrO			0.005	0.003	0.003	0.004
ZrO2	0.055	0.015	0.015	0.016	0.016	0.015
ZnO	0.02			0.008		
Cl	0.069	0.03	0.008	0.018	0.007	0.018
Rb20	0. 013		0. 002			

Table 2.6: The chemical composition content of recycled hard coating glass, different layers in vertical direction

3.4 Discussion of XRF test

In order to gain a better understanding of difference before and after recycling, a series of comparison has shown in following tables. Begin with the comparison within the normal float glass recycling, the chart 2.1 transfer chemical composition content from figure to bars, to visualize the movement of chemical compositions. As shown in the bar chart, the silicate dioxide has move to the surface during recycling, along with the deposit of alkali, illustrating by the table 2.7. Meanwhile, although the original glass panels has experiencing tin bath, the tin content is not measurable after recycling.

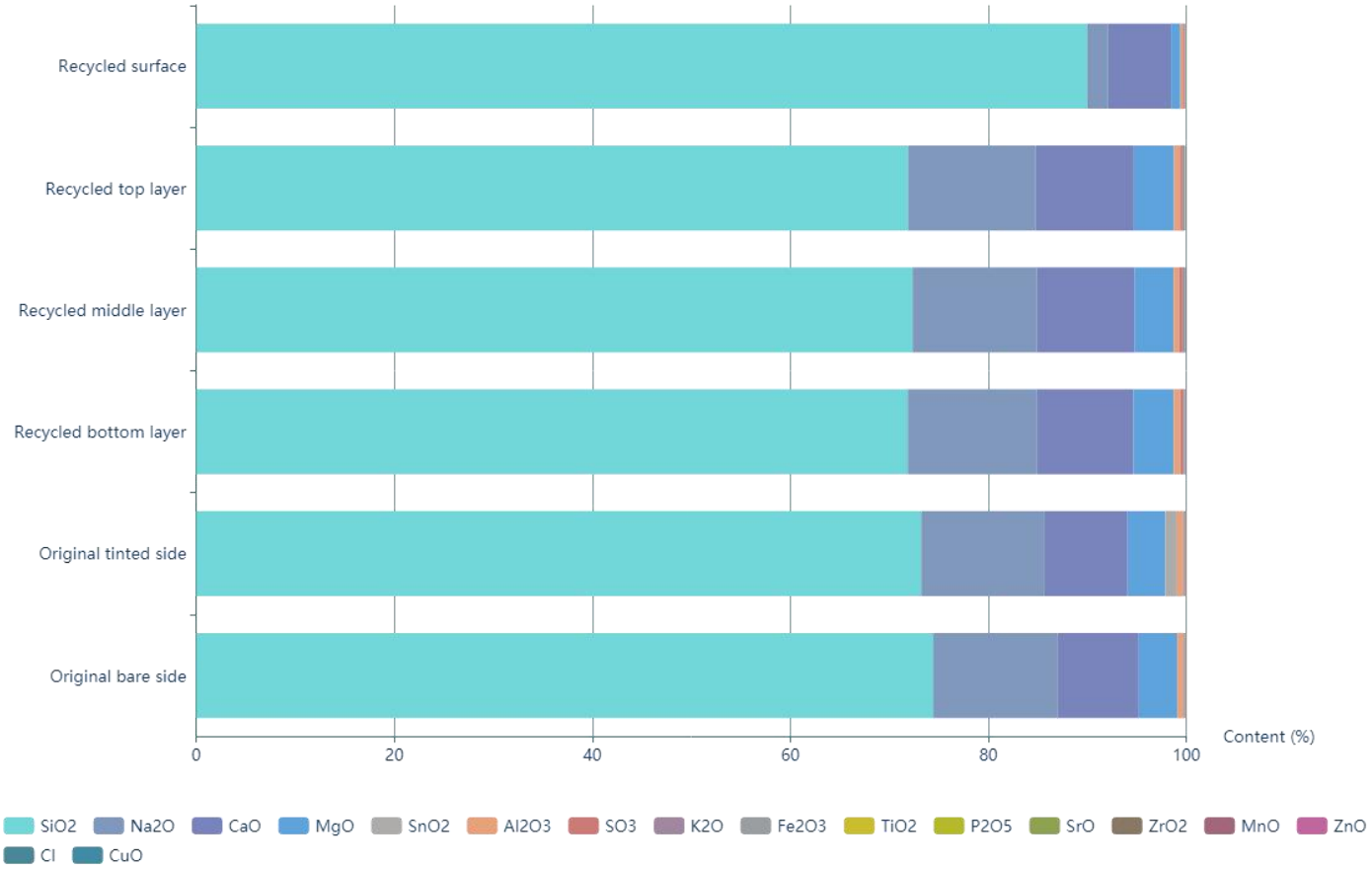

Chart 2.1: Visualization of chemical composition content of recycled normal float glass.

	surface	top	middle	bottom
SiO2	15.541	-2.55	-2.091	-2.577
Na2O	-10.409	0.359	0.021	0.528
CaO	-1.876	1.7	1.631	1.51
MgO	-2.944	0.167	0.075	0.185

Table 2.7: The differentials of dominate chemical compositions between recycled normal float glass and the bare side of original normal float glass.

Similarly, the comparison has been done also for hard coating glass, shown in chart 2.2. Obviously, there are a great difference in the tin content in contrast to the normal float glass. Not only the original hard coating glass has a large amount of content in the surface, which experienced coating and tin bath, but also the recycled hard coating glass has tin remaining, even though it is a very low proportion. This tin residue might become the most unfavorable chemical composition during the following recycling. The movement of silicate dioxide is the same with normal float glass recycling, the recycled surface takes up maximum percentage. While the alkali deposition is not very clear in the recycling of hard coating glass, instead, the alkali content is more well-proportioned after casting.

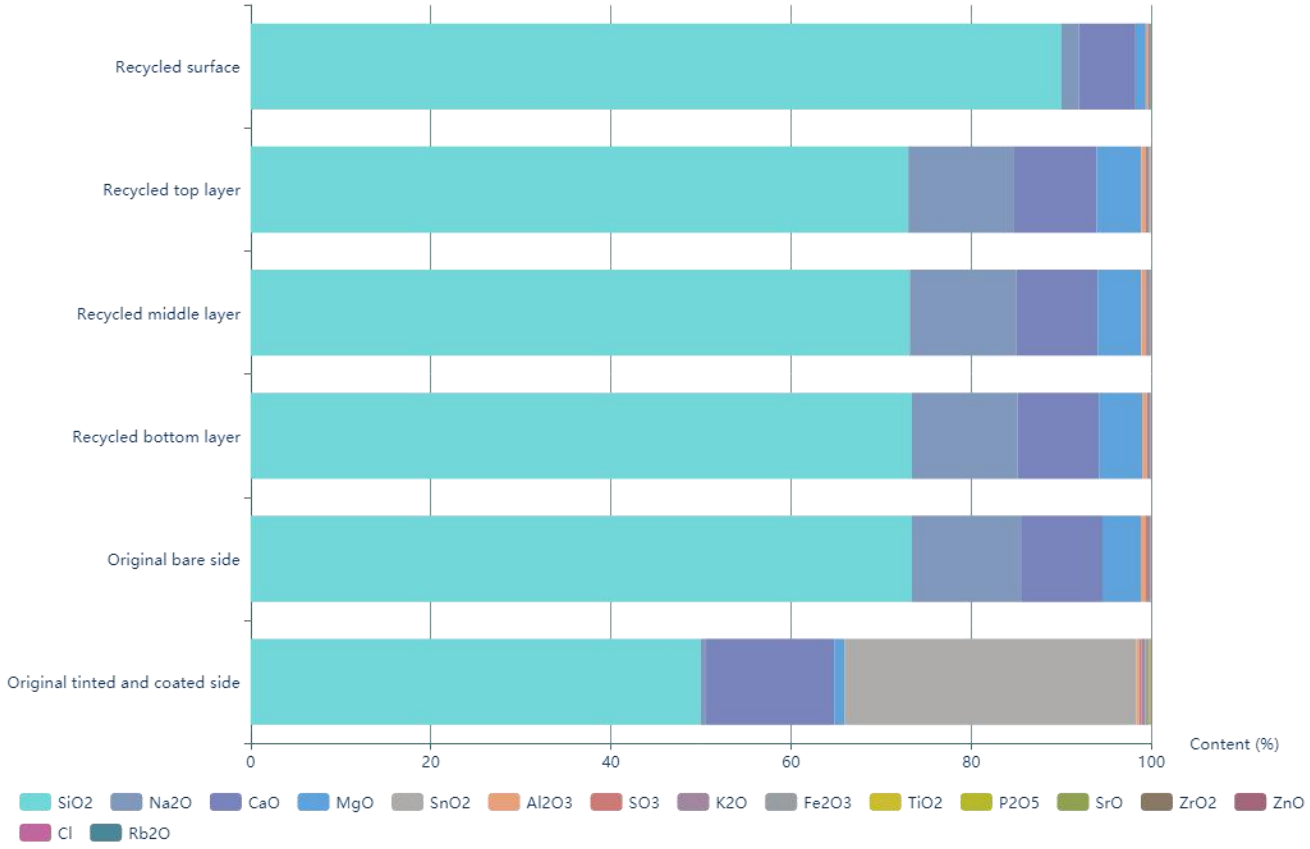

Chart 2.2: Visualization of chemical composition content of recycled hard coating glass.

	surface	top	middle	bottom
SiO2	16.59	-0.401	-0.245	-0.007
Na2O	-10.152	-0.446	-0.287	-0.372
CaO	-2.764	0.205	-0.006	-0.016
MgO	-3.129	0.661	0.54	0.552

Table 2.8: The differentials of dominate chemical compositions between recycled hard coating glass and the bare side of original hard coating glass.

3.5 Polarized observation

Due to the uneven distribution of temperature at the same time in the kiln-casting procedure of glass recycling, the temporary and residual stresses will appear, mostly developed in the annealing stage. After manufacture, the products requires quantitatively inspection on the residual stresses. As the result, integrating with the special transparent and birefringent properties of glass, an optical method based on photoelasticity has been introduced. In the result of stress variation in the material, the refraction index of one specimen will vary in the different position of this specimen. When a polarized light passes through the photo-elastic material, the light will be disintegrated into different light beams due to the different indexes of refractive. Through these variations, integrating with stress-optic laws, the residual stress inside this specimen is able to be quantified.

There are two polarizers, including plane polarizer and circular polarizer. The arrangement of plane polarizer is shown in figure 2.17, filtering by the first polarizer, the monochromatic light will be constrained into the same orientation, following by the specimen. With another polarizer, worked as an analyzer, the fringes corresponding to principal stress and difference between in-plane principal stresses, known as isoclinic and isochromatic respectively. The isoclinic lines are formed by all the points with the same principal direction in the specimen, observing as black fringes. These fringes will change depending on the polarizing axis of the analyzer, therefore it will influence the stress observation to some extent. [43][46]

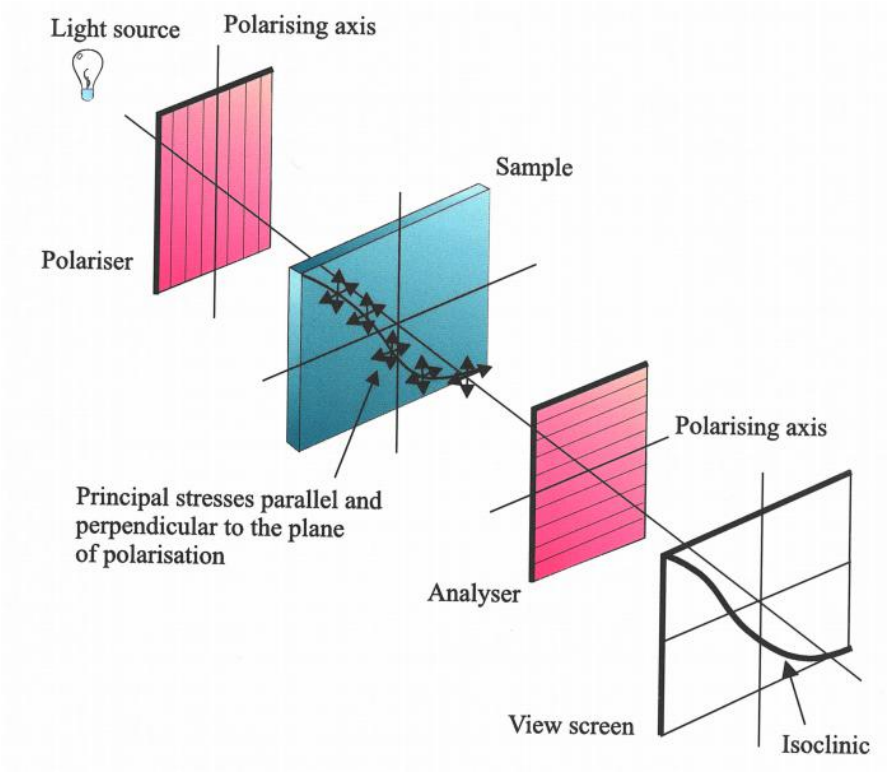

Figure 2.17: The arrangement of plane polariscope and the formation of isoclinc line.[46]

Whilst the isochromatic lines are usually shown as colored fringes, they are the integration of the points with the same difference of principal stresses in the specimen. The isochromatic lines are independent with the polarizing axis, and the exact appearance is corresponding to the light source. With the plane polarize settlement, both fringe patterns will be shown in the view screen. In order to avoid the shade from isoclinic patterns, the circular polarize settlement is introduced as figure 2.18. Benefit from this arrangement, the masking due to the isoclinic line can be prevented.

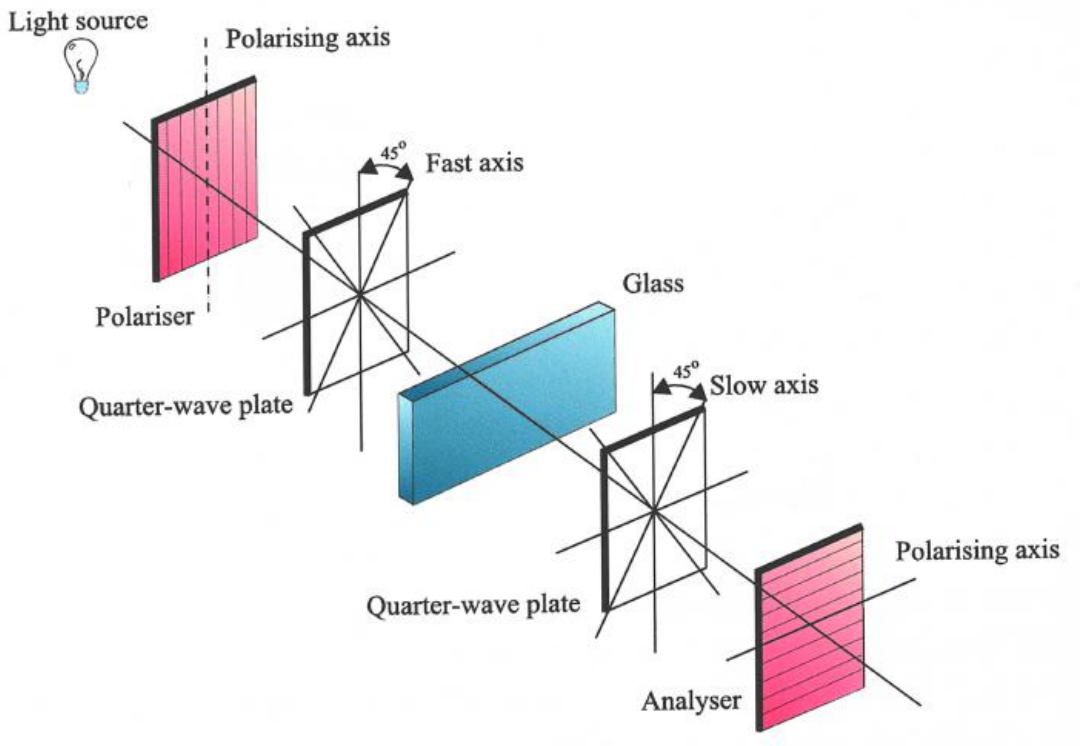

Figure 2.18: The arrangement of circular polariscope.[46]

For the recycled glass samples, fabricated by kiln casting, there are possibilities of the existence for the residual stress because of the considerable thickness. As the result, both plane polariscope and circular polariscope test are arranged. Figure 2.19 and figure 2.20 elaborating the patterns from plane polariscope test, in which the computer screen is chosen as a polarized light resource. Along the edges through the height of the specimen, the patterns shown the trace of stress causing in the annealing period. It is formed by the varying temperature from surface to the central area of the specimen during annealing. However, as we discussed before, the results are the combination of isoclinic patterns and isochromatic patterns. To clarify the isochromatic lines and quantify the relationship between observation and stresses, the circular polariscope test has been introduced.

Thanks to the help of Ilis, a strain scope which can measure and image the mechanical stress of photo-elastic material expediently has been adopted. Limited by the time and expenditure, only one polished recycled glass samples are carried in this test, results shown in figure 2.21 and figure 2.22. The specimen is measured in the side surface, with the top surface in the upper edge. This specimen is half of the original specimen with a cutting surface in left edge, all the surfaces are polished except for the top surface.

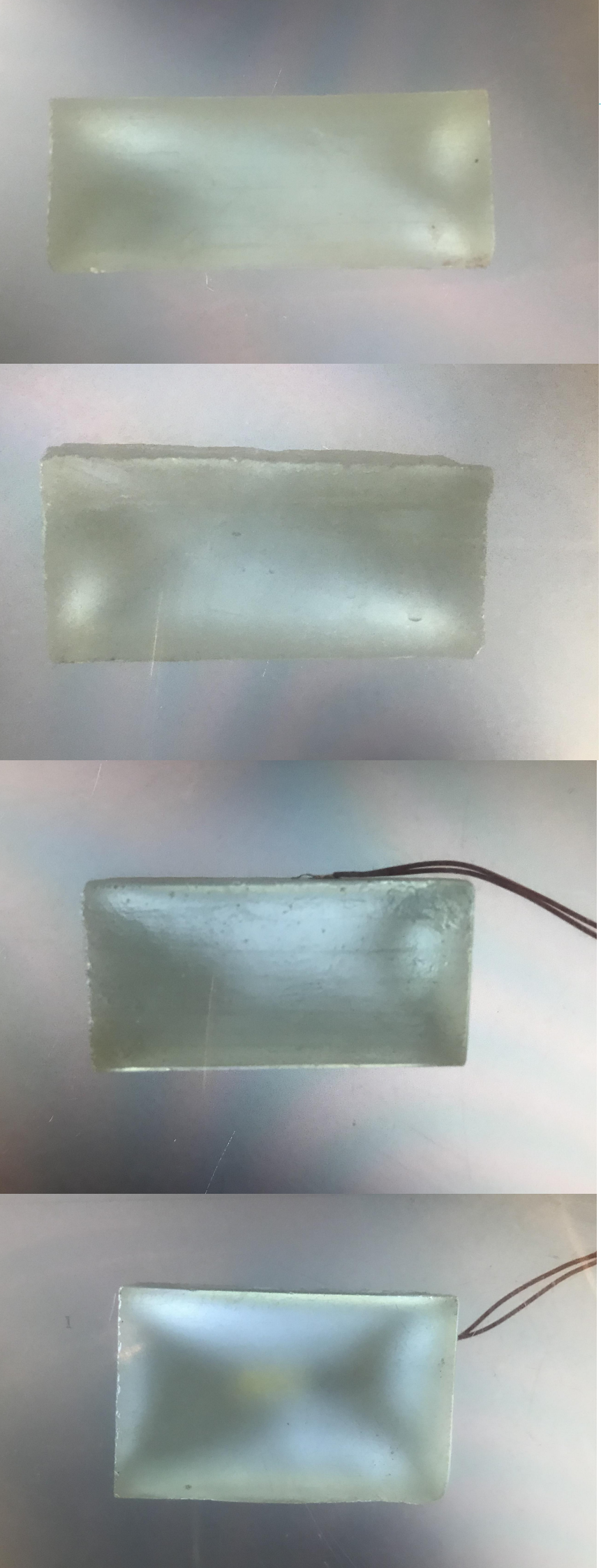

Figure 2.19: The polarised picture of recycled hard coating samples and recycled normal float samples, from top to bottom is the top and side view of recycled hard coating glass, and the top and side view of normal float glass. Among them, only the side surface of normal float glass has been polished.

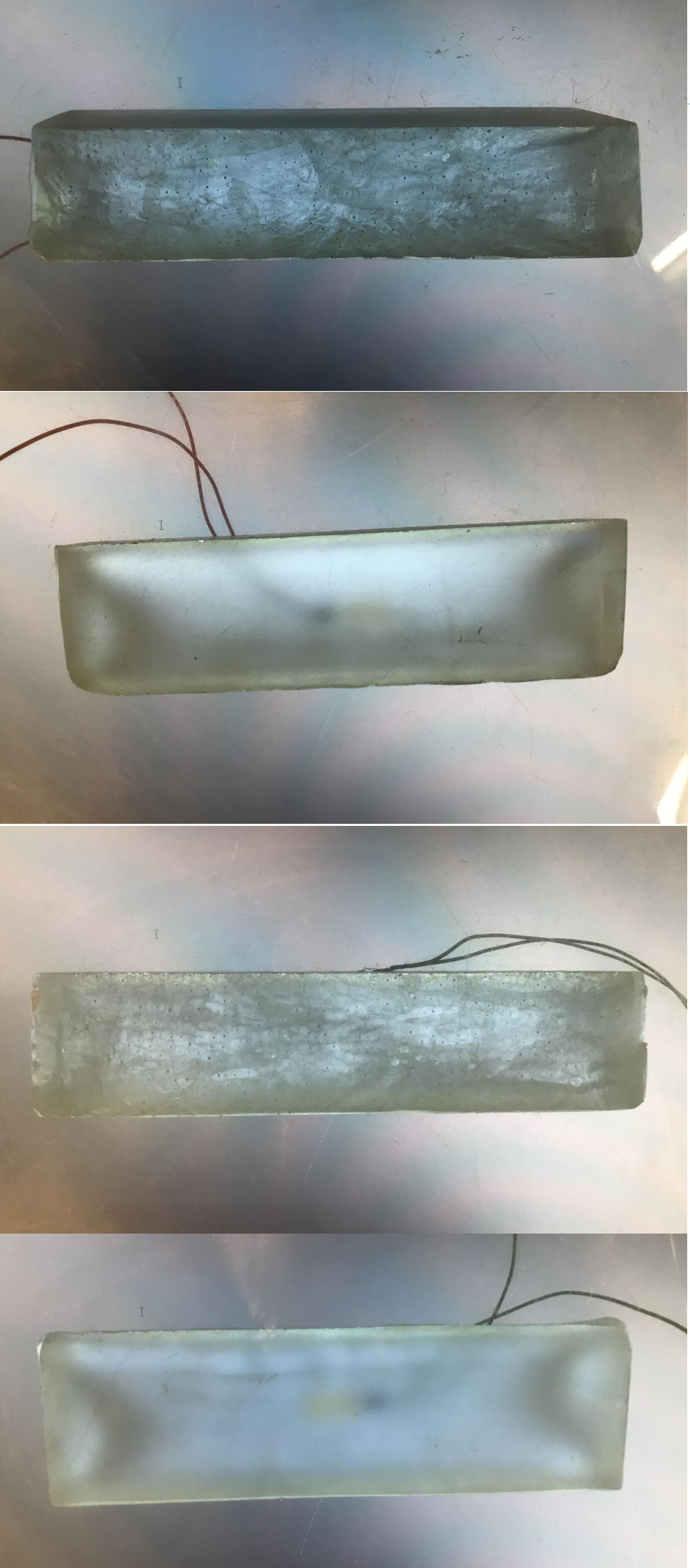

Figure 2.20: The polarised picture of recycled dark soft coating samples and recycled light soft coating samples, from top to bottom is the top and side view of recycled dark soft coating glass, following by the top and side view of recycled light soft coating glass, both of the side face has been polished.

In the figure below, the direction of principal stress is drawn by the dash lines, and the blue area represented area without residual stress. Through the sub-figure (a), the direction of principal stress is perpendicular to the cutting surface, which can be regarded as the original orientation of principal stress along the length of this specimen before cutting. The comparison is shown in the sub-figure (c), exhibiting a rainbow shape against the right edge, which is the surface attach to the mould. This curved shape perfectly performing the formation of the internal stress during annealing. Meanwhile, the green area in the middle part of the specimen expressed the movement of different ingredients during annealing. Link to the chemical composition analysis as we mentioned before, there are alkali depositions which indicating upward movement of other compositions.

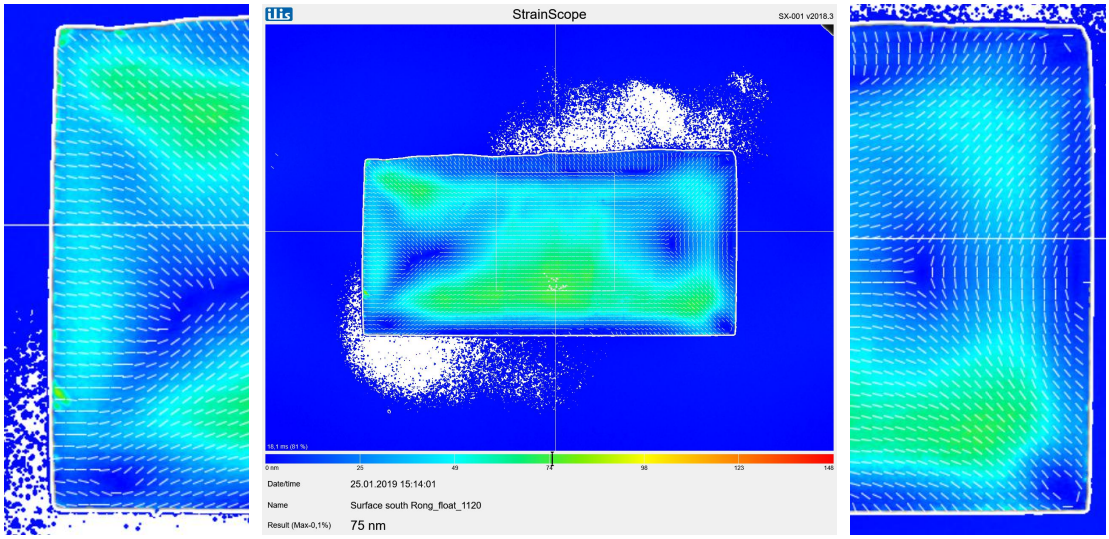

Figure 2.21: (a) The left part of the specimen; (b)The observation output of circular polariscope test by Ilis; (c) The right part of the specimen.

Applying the thickness of 40mm and the photoelastic coefficient of 2.7Tpa^{-1}, the maximum residual stress is calculated as 0.69MPa, which is relatively low as these stress are distributed along the thickness. By observing and calculating, the recycled float glass samples can be regarded as well-annealing and homogenous, based on the photo-elastic results.

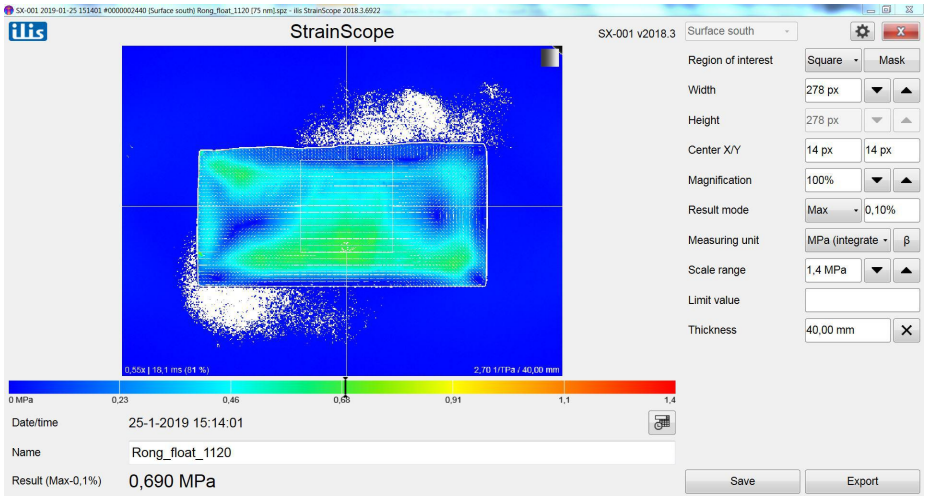

Figure 2.22: The stress calculation through circular polariscope test by Ilis.

3.6 Glass beam casting

Apart from the recycled glass samples for material property test, the recycled glass in a beam shape is required for the four point bending test, to withdraw the fracture strength of recycled material. Limited by the resource amount, the recycled glass beams has to be made of the mixture from hard coating float glass, light soft coating float glass and dark soft coating float glass. On the basis of previous test, the property of this mixture recycling can be simply predicted by average the results of recycled hard coating, recycled light soft coating and recycled dark soft coating, as well as the casting temperature. Synthesizes the amount of glass resource, the kiln dimension as well as the apparatus for bending test, the beam dimension is designed as 360mm in length, 36mm in height and 12mm in thickness. The manufacture procedure is similar to the former process, therefore it will be simply described in the following paragraph.

Step 1 wax model production

As demonstrated beforehand, the final product will present as a slender beam shape with 360mm in length, 36mm in height and 12mm in thickness. In order to make a concave mould for glass, a convex wax model is required. Correspondingly, a stretchy counter mould for a wax model and an original model are necessary. To refining the dimension, a wooden panel with the precise objective dimension is selected as an original model. Fixing with clay following by surrounding through the wooden panels, the raw material for wax mould is silicone instead of plasters. After setting, take the original model out and remove the extra part of the plaster mould along the edges and corners, then the silicon mould is produced and the following wax production can be realized as the same procedure as before.

Figure 2.23: Wax model manufacture process for recycled glass beam.

Step 2 mould preparation

Since the different batch of kiln casting may affect the product quality, to minimize the variation among glass beam products a plan is required for the arrangement of the mould. Depending on the dimensions of kiln and products, as well as the minimum mould thickness between two specimen, which is at least 2 centimeters, two moulds will be prepared. Each of the moulds contains three pieces of the specimen, with a an outer layer of 2 centimeters thick. The length of the specimen will be placed parallel to the length of the oven.

The mould fabrication starting from a foundation, which is a wooden panel with a thickness of approximately 2 centimeters, it will play a role as a glass container before and during casting. Three wax models are placed on the wooden foundation, fixed with clay at a distance of 2 centimeters. On account of the same maximum casting temperature with former glass samples, the raw material for the glass beam mould is also Crystalcast M248, consists of Cristobalite, Quartz and Gypsum.

Unfortunately, because of the limitation of the oven and the thick outer layer of crystal-cast mould, the heat-resistance concrete mould in impossible to apply in this experiment. Nevertheless, the thick outer layer is likely to prevent the mould from cracking during high-temperature casting.

Figure 2.24: Mould preparation process for recycled glass beam.

Step 3 Material preparation

It is more practical to recycle the float glass as a mixture of different types, instead of recycling by different tints or coatings, as the consideration of the industrial applications. Besides, supported by the XRF analysis, the chemical composition contents are very similar within recycled soft coatings, and only small difference existing between recycled soft coating glass and hard coating glass.it is well founded to the inference that the recycling of the mixture is also workable.

Figure 2.25: Mould with prepared glass mixtures before kiln-casting.

In consequence, the glass beam products for fracture testing is planned to consists of a mixture of three coated float glass, including dark soft coating glass, light soft coating glass and hard coating glass. With a view of existing material, the proportion of dark soft coating glass, light soft coating glass and hard coating glass are 3:3:2 respectively, the total glass weight for one mould is approximately 2400g.

Step 4 Casting procedure

Similar to the automatic programming casting and annealing procedure of hard coating glass recycling, the glass beam recycling is also programmed by software, without the manual quenching process. To better illustrates the firing schedule, the temperature change while casting is shown in the function of total time consumption in chart 2.3. From the line chart, it is easily recognized that the first batch casting which has the sharpest decrease in quenching period due to avoidance of crystallization dangerous zone (from 760 degrees to 660 degrees). The detailed casting periods have been clarified in chart 2.4, using casting for recycled glass in first batch as an example.

Step 5 Finalizing

Being trapped by the mould interlayers between two glass beams, it is not easy to remove the crystal-cast mould. A detailed but heavy work with hammer and chisel to remove the remaining mould material is obligatory before next step. Once the glass beams are escaped from the mould, the

cutting and polishing can proceed. Due to the cutting process, some small cracks appear along the edge, which might become the weak point while loading. The elaborate grinding is compulsory to minimize the influence of material stiffness during the bending test. In addition to the cracks, the surface of the glass beams is also covered by exquisite scratches. It is unfavourable for the polarized visualization as well as the air-bubble entrapment.[43]

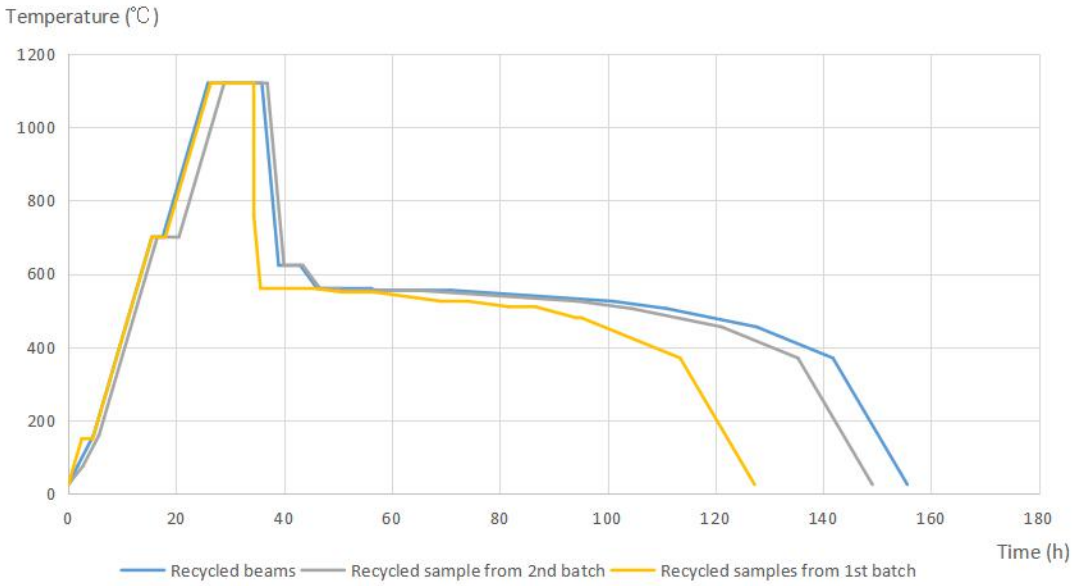

Chart 2.3: The firing schedule for three kiln-casting.

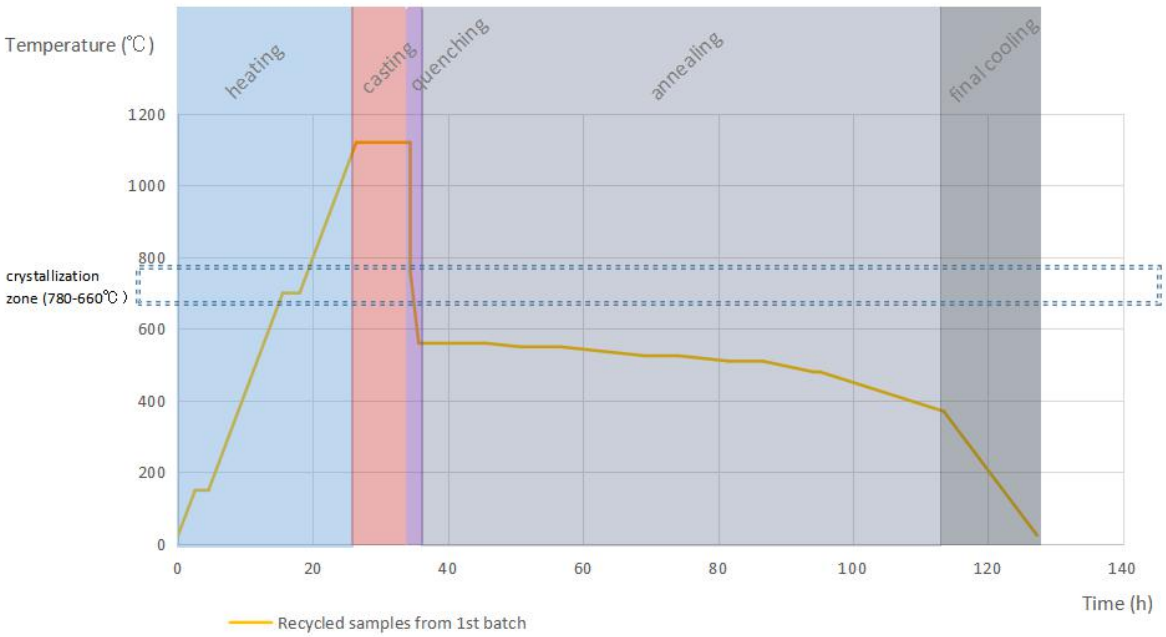

Chart 2.4: The firing schedule and casting periods of first batch kiln casting.

Chapter 4 Young's modulus test

Young's modulus, also called tensile modulus, which demonstrates the resistant ability for deflection of solid material under stretching or compressing. Within the elastic limit, Young's modulus can be defined as the ratio of linear stress along an axis to linear strain along the same axis, described as formula below.

$$E = \frac{\sigma}{\varepsilon} \qquad \text{(Equation 2.1)}$$

E: Young's modulus
σ: Stress of the material
$\mathcal{E}$: Strain of the material in corresponding direction

Referring to common mechanical material, there are several essential properties in mechanical behavior, such as elastic modulus, strength and toughness, which are influence the deflection, load bearing capacity and crack propagation of the material respectively. The deflection of the material is the main concern in this chapter, hence, elastic modulus, which include Young's modulus, shear modulus and sometimes bulk modulus as well as Poisson's ratio, will be discussed. Considering the comparability between glass and concrete, the glass works better in resisting compression than tension, which indicates a greater importance of Young's modulus against shear modulus. In order to predict the elongation or compression of the recycled float glass, it is obligatory to test the Young's modulus of this new material. As we discussed beforehand, there are three different methods to test Young's modulus. In this chapter, the most opportune method will be chosen, the corresponding testing procedure and sub-test will be exhibited, and the final result of Young's modulus will be demonstrated and discussed as well.

4.1 Methodology

Because of the limitation of furnace space, the author only prepared one sample for each category in advance, which makes the load-displacement method and vibration method impossible. Thus choosing ultrasonic testing methodology to test the Young' s modulus for each recycled category is unescapable.

On basis of the theory demonstrated in chapter 2, not only a sound velocity detective is required, but also the length of testing sample, which is the distance of sound propagation, should be prescribed to at least 12.5mm. Meanwhile, the touching surface of samples that the detective will contact with, should be as smooth as possible. Before applying the sensing unit to the side surface of the glass sample, some vaseline will be smeared to the connected area in order to decrease the gap between detector and sample material, so that a better attachment can be provided. The ultrasonic testing process is presented in figure 2.26. On the equipment screen showing the time of sound travel through the lengthwise of the specimen, the same process will be carried to other four specimens as well.

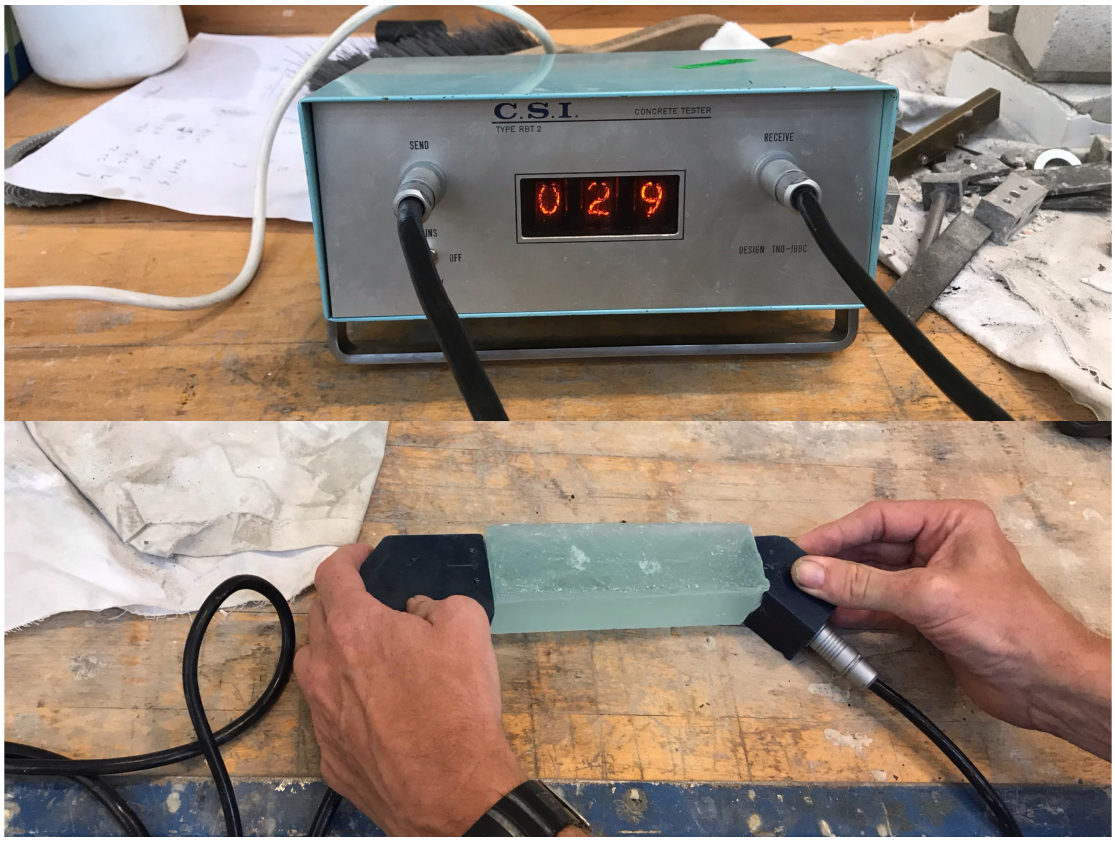

Figure 2.26: The ultrasonic method for Young's modulus testing, photo by author.

4.2 Data collection

Based on the experiment, the time of ultrasonic propagation through the specimen are directly recorded in table 2.9. Despite of the time of flight from the ultrasonic devices, the dimension of four recycled glass specimens are also required, as well as the volume and weight in order to derive the density, on account of equation 1.5. Except for simply measurement of dimensions and weight, the volume will be measured with the drainage method. The dimension data shows in table 2.10.

	Recycled normal float glass	Recycled dark soft coating glass	Recycled light soft coating glass	Recycled hard coating glass
Time of flight (s)	0.000029	0.0000295	0.000031	0.000029

Table 2.9: Collected time consumption of ultrasonic method.

	Recycled normal float glass	Recycled dark soft coating glass	Recycled light soft coating glass	Recycled hard coating glass
Length (m)	0.155	0.157	0.155	0.154
Height (m)	0.044	0.045	0.045	0.047
Width (m)	0.035	0.035	0.035	0.039
Weight (kg)	0.61193	0.60162	0.62539	0.647
Volume (m^3)	0.00025	0.00025	0.00025	0.00026

Table 2.10: Collected time consumption of ultrasonic method.

Since the volume measurement of recycled glass samples are very roughly, which might introduce errors. To decrease the deviation, the drainage volume will be corrected with the calculated volume, which is the product of length, height and width. The corrected result equals to the average of drainage volume and calculated volume, and it will be used in the following calculation . The value of sound velocity is equals to the ratio of length in longitudinal direction to the time of flight. And the density is equals to weight divided by corresponding corrected volume. Depends on the equation 1.5 in chapter 2, the Young's modulus of recycled glass samples are calculated in table 2.11.

	Recycled normal float	Recycled dark soft coating	Recycled light soft coating	Recycled hard coating
Sound velocity (m/s)	5344.83	5322.03	5000	5293.10
Density (kg/m3)	2504.32	2419.67	2531.30	2399.28
Young's modulus (GPa)	71.54	68.53	63.28	67.22

Table 2.11: Young's modulus calculation through ultrasonic method.

4.3 Analysis and discussion

Abstracting from A. Winkelmann and O.Schott's glass modeling, the glass property can be calculated by the chemical composition integrated with corresponding coefficient. Through analysis the relationship between glass properties and specific chemical compositions, a prediction of glass behavior is able to be realized. Therefore, it is worthy to compare and analysis the correlation between Young's modulus and composition of recycled float glass.

In view of the glass database, theoretically, the relevancy of Young's modulus and chemical constitution can be conclude as:

a) The alumina plays the most important role in depending elasticity of glass, it improving Young's modulus by increasing the content;

b) Silica also improve the Young's modulus with a comparatively high coefficient;

c) The content of metal oxide is in proportion to the value of Young's modulus;

d) The alkali oxide will negatively affects glass elasticity;

e) The content of alkali earth oxide is favor of modulus, while when the magnesia oxide takes the dominant place, the Young's modulus will be decreased.

The a) and b) are derived from Eberhard Zschimmer's book[28], it gives the influence coefficient for alumina and silica of 130 to 180 and 70 respectively. The aluminium ion can fill the space in silica oxide structure, which give the glass structure more density, so that the glass can perform better in elasticity. Meanwhile, the silica oxide give a strong bond in the structure, leading to a higher modulus. Besides, the conclusion c), d) and e) are obtained from Varshneya's book [29] and Kiline & Hand's paper [30]. In general, the weaker the bond strength, the lower the Young's modulus. Correspondingly, the alkali will ruin the silica bond, which the alkali earth can worked as the modifiers to improve the bond strength. Depending on the theoretical database, the comparison existing in recycled float glass between Young's modulus and influential chemical compositions are presented in the chart 2.5.

Because the ultrasonic test were applied to the side surface of the specimen and the sound were transfer in lengthwise. Thus only the chemical compositions in the middle area of recycled hard coating glass and recycled normal float glass are taken to analysis. Referring to the chart above, although the recycled normal float glass has lower content in silica oxide, the higher aluminum oxide helps to fill the gap in the structure to increase the bond. In combination with the value of influential coefficient, the recycled normal float glass has a higher modulus. Also, the higher metal oxide content in recycled normal float glass corresponding to the higher Young's modulus. Considering the alkali earth element, the calcium oxide takes the dominant position in recycled normal float glass, which is nicely in consistence with the theory above.

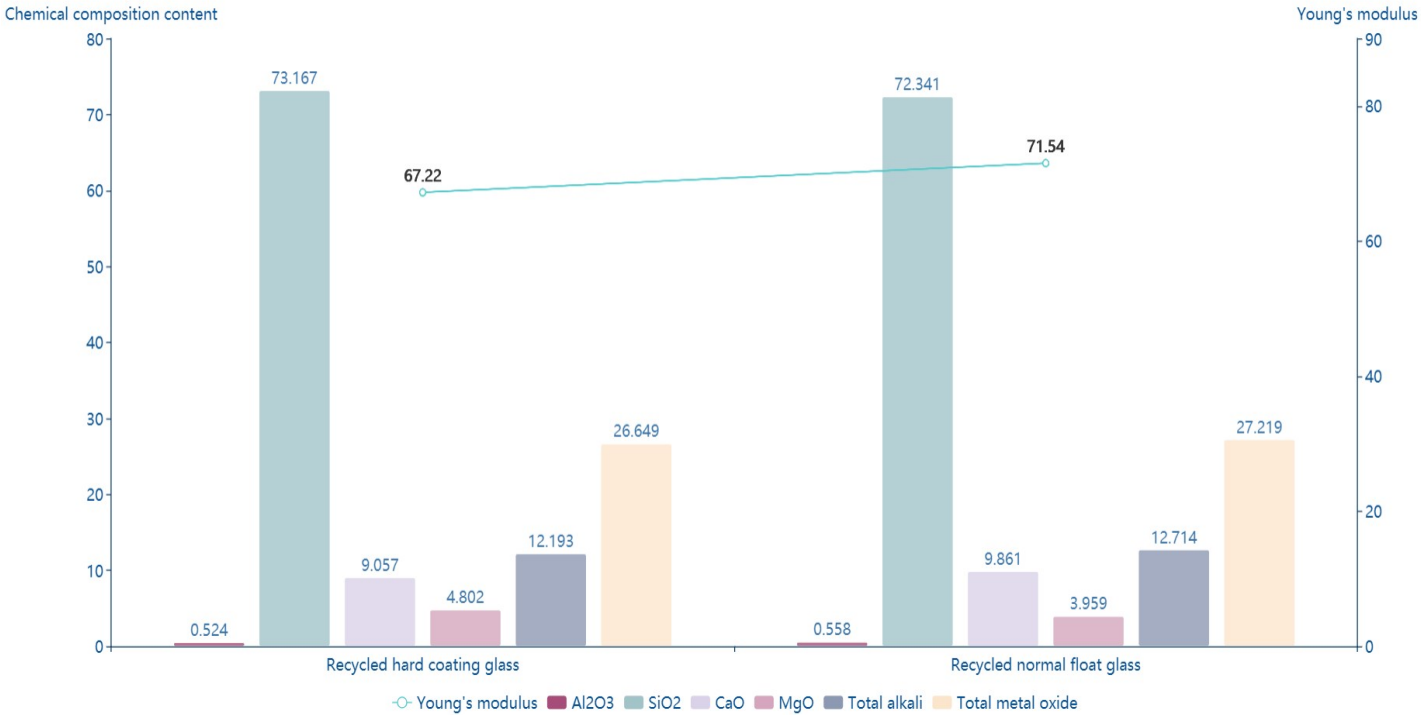

Chart 2.5: The comparison in influential content of Young's modulus, between recycled normal float glass and recycled hard coating glass.

However, the recycled hard coating glass has less alkali content than recycled normal float glass, which indicates less harm to the bond strength, but it has a lower Young's modulus. On the one hand, the disagreement may result from the various distribution of chemical composition along the height of the specimen, as well as the probably density variant in the specimen. On the other hand, this discrepancy can be a certification that the elasticity of glass can not be decided by one category of influential chemical composition. It is possibly to conclude that it is difficult to predict Young's modulus based on one composition, since it depends on complex compositions integration with corresponding coefficients.[47]

Chapter 5 Coefficient of thermal expansion

Coefficient of thermal expansion of glasses, as it evaluates the thermostability and somehow affects other properties of glass itself, it can be regard as one of the essential physical quantity. Used in structural application, the connection with other material is inevitable, where the stress is probably appear due to the altered body dimension. Although it is clear that the value of CTE for normal glass has been defined, the CTE is often extremely influential of particular glass composition. Therefore, with regard to the recycled float glass, which has different chemical compositions compared with resourcing float glass, he define of CTE is an essential anchor for further research.

5.1 Methodology

In consideration of time consumption, laboratory condition and existing samples, the strain gauge method is selected. Briefly, there are three phases of connection before CTE test. First of all, before connecting strain gauges with samples, at least one surface of the cuboid-shape specimen should be polished as smooth as possible, following by deep cleaning by acetone. The more clear surface it has, the more accurate results can be received. After polishing and cleaning, simply mark the attaching area, especially the position and direction of strain gauge.

In view of practical work of recycled float glass, the temperature range of structural application should not exceed nature temperature. Hence, in this test, the temperature interval is set as ambient temperature to 80 degrees (176℉). Correspondingly, a specific strain gauge is selected, together with a relevant glue which works properly from 25℃ to 80℃, shown in figure 2.27 . Moisten the foil side of strain gauge through glue, carefully attach them to the marked position, pressing with polethylene sheet in one direction and hold for a while. Thanks to the property of CN adhesives, it drys within two minutes under room temperature. In order to easier the connection between strain gauges and electronic indicator, the lead wire of strain gauge is soldering with extra wires.

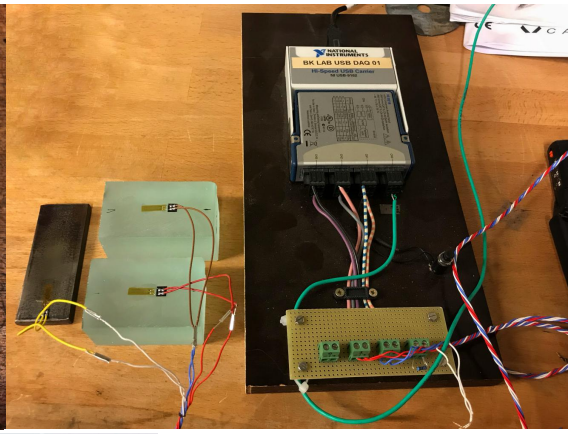

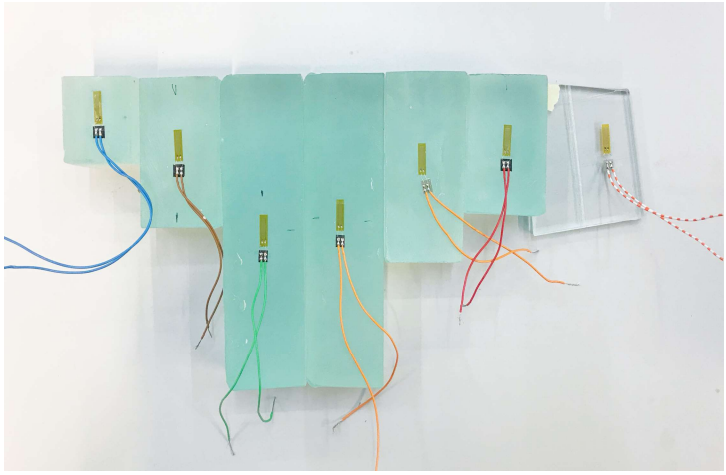

Figure 2.27: The strain gauge and relative glue for CTE test (left);

Figure 2.28: The connection between specimen and DAQ devices (right);

Figure 2.29: The specimens after applying strain gauges (bottom).

The last step before heating is the connection from strain gauge to DAQ receiver and computer. As shown in figure 2.29, the DAQ detector is connected with three specimen and one temperature detector through wires in different colors, which makes the recognition of different specimen more convenient. Among three specimens, stainless steel appears as a reference material while the others are recycled float glass awaited to be test. On the other side, the DAQ instrument is linked with computer with USB cable, the detailed introduction of the software will be illustrates in following section.

After finishing all preparation, lock the door of oven and programming the heating schedule. All these test share the same heating schedule: heating up to 80 degrees by a heating ramp of 200 degrees per hour, and cooling down to the ambient temperature naturally. As presented in figure 2.30 the metal cable on the top part is the temperature sensor which connected with DAQ devices through coarse green cable. And obviously two cuboid-shape glass samples are placed, as well as a stainless steel specimen as reference material. Because of the combination of high value of CTE and bad performance in thermal conductivity for stainless steel, it is widely used as reference material in CTE test, with a known CTE value of 12 µm/m℃.

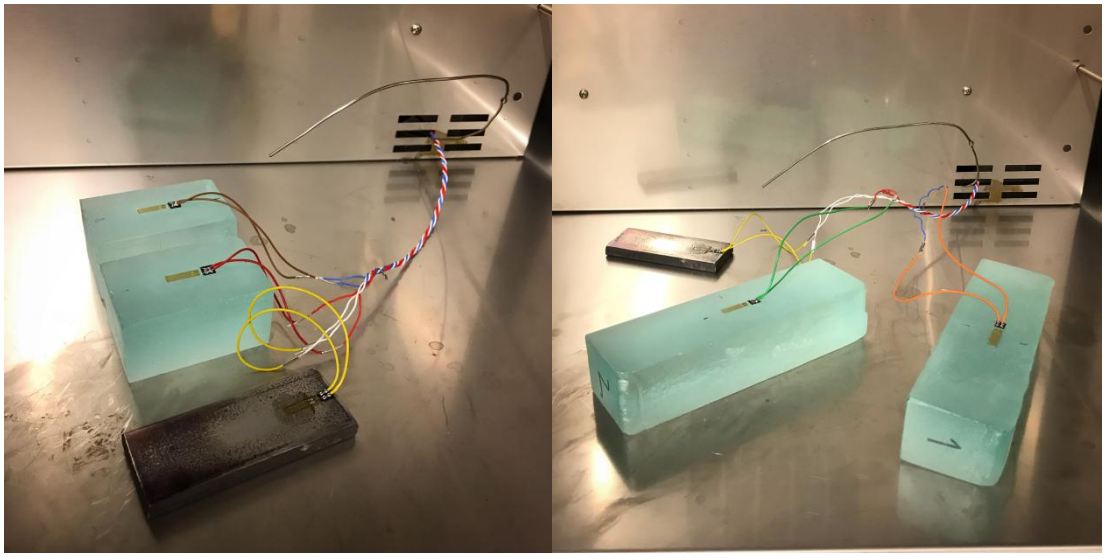

(a) *(b)*

Figure 2.30: (a)Photograph for the first CTE test, both sample material are recycled normal float glass; (b) Photograph for the fourth CTE test, the left sample is recycled dark soft coating glass and the right sample is recycled light soft coating glass.

5.2 Data collection

As alluded above, for each test, the receiver will collect four series of different information: the temperature change, the strain of two sample materials and the strain of reference material. Through the graph on the computer, all the data change over time. On the screenshot of the working interface of the software, the left area shows the information of on-time data for temperature, the strain of reference specimen (connecting with DAQ through white wire) and the strain of sample material (connecting with DAQ through blue wire and red wire respectively), in a sequence of top to bottom. On the right area are two charts, with temperature curve over time on top and three strain curves for specimen below. From the top chart in the screenshot, the temperature will remain in constant at the highest temperature for a period, and the strain of glass samples are continue increasing negatively. Since the specimen has a considerable thickness, it requires some time to adapt the heat. The period of constant temperature gives it time to stable itself.

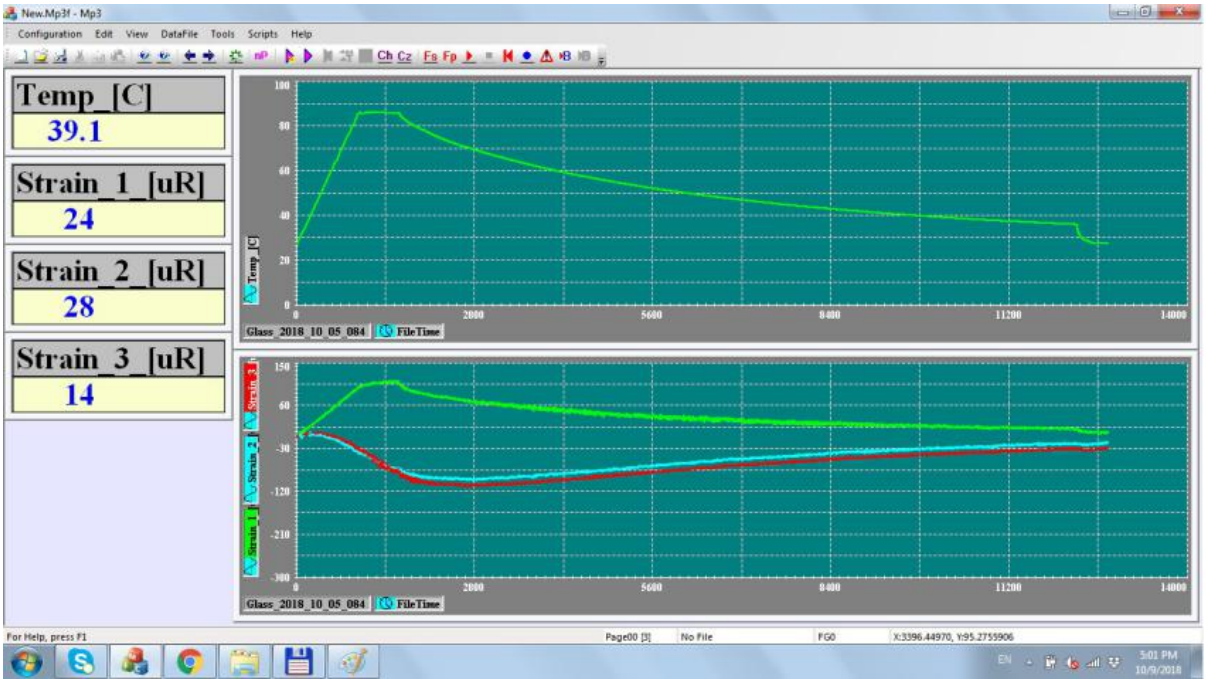

Figure 2.31: The screen shoot of recycled normal float glass CTE test.

In total, seven tests has been finished, shown in the CTE test schedule below. In order to withdraw a more authentic result, the material of recycled normal float glass has been tested for five times, meanwhile the recycled hard coating glass and original float glass specimens have been tested for three times. In the following analysis, the average result for each of these three categories will be selected for final calculation. In addition to this, the dimension of the specimen are different, the

volume of specimen made of recycled normal float glass and recycled hard coating glass specimen is approximately the half of the specimen of recycled soft coating glass. What's more, for the original float glass, the specimen is just cut from a normal float glass panel. However, since the strain gauge covered area are the same for all specimens, it is not likely that the dimension would influence the results. For the recycled specimen, the strain gauge are mostly attached in the polished side face of the specimen, apart form the recycled hard coating specimen in test two. It has the strain gauge connecting in the top surface of the specimen, shown in figure 2.30.

Date	Test number	Strain 1	Strain 2	Strain 3
Friday, 5th October 2018	Test 1	Stainless steel	Recycled normal float glass	Recycled normal float glass
	Test 2	Stainless steel	Recycled normal float glass	Recycled hard coating glass
Monday, 8th October 2018	Test 3	Stainless steel	Recycled normal float glass	Recycled normal float glass
	Test 4	Stainless steel	Recycled dark soft coating glass	Recycled light soft coating glass
Friday, 2nd November, 2018	Test 5	Stainless steel	Recycled hard coating glass	Original normal float glass
Monday, 5th November, 2018	Test 6	Stainless steel	Recycled hard coating glass	Original normal float glass
	Test 7	Stainless steel	Recycled hard coating glass	Original normal float glass

Table 2.12: The CTE test record.

5.3 Analysis and discussion

Strain analysis

As explained before, there are five series of information for recycled normal float glass, to display more clearly, a scatter line plot is introduced. Taken an average results of stainless steel of test 1, test 2 and test 3 as the resource, on which the sample specimens are made of recycled normal float glass. Comparing with five series results of recycled normal float glass. As a matter of fact, the software record strain and temperature each second, to reducing unnecessary work, the strain data is selected at the temperature of 30℃, 35℃, 40℃, 45℃, 50℃, 55℃, 60℃, 65℃, 70℃, 75℃, 80℃ and the initial temperature at around 28℃ as well as the top temperature at around 86℃. Refer to chart 2.6, the strain of stainless steel has an obvious positive growing over the temperature rising. Most of the recycled normal float glass strain curve gradually growing negatively until the top temperature. Except for the recycled normal float glass 3 in the chart, which derived from the data in test 2, it has a increasing tendency over 28℃ to 40℃, then decreasing with a similar trend with other four curves.

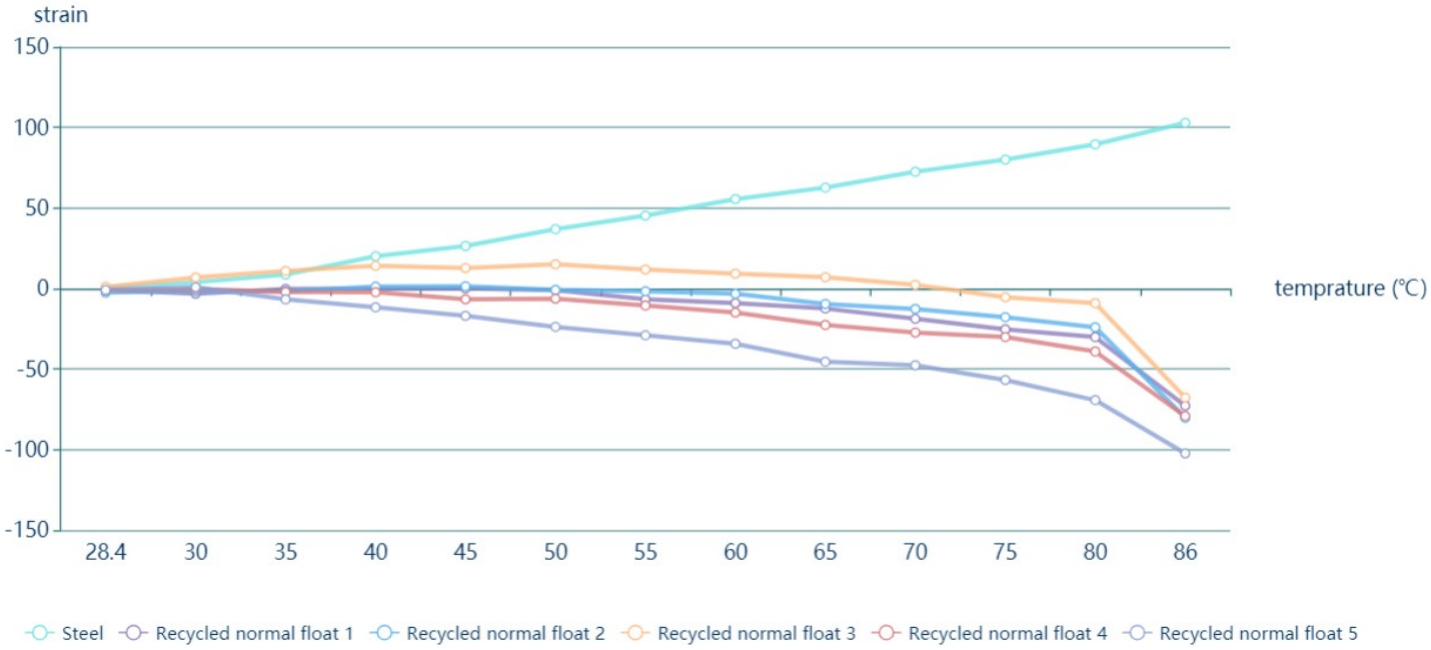

Chart 2.6: the strain-temperature curve for recycled normal float glass specimen and reference specimen over heating period.

To ensure the accuracy, the data of recycled normal float glass 3 and normal float glass 5 will be eliminated from the average value calculation. Therefore, the average value of test 1 and the value of recycled normal float glass 4 is used as "recycled normal float average" in chart 2.9. Similarly, the preliminary strain analysis for recycled hard coating specimen and original normal float glass in comparison with the stainless steel from the same test will be presented in chart 2.7 and chart 2.8.

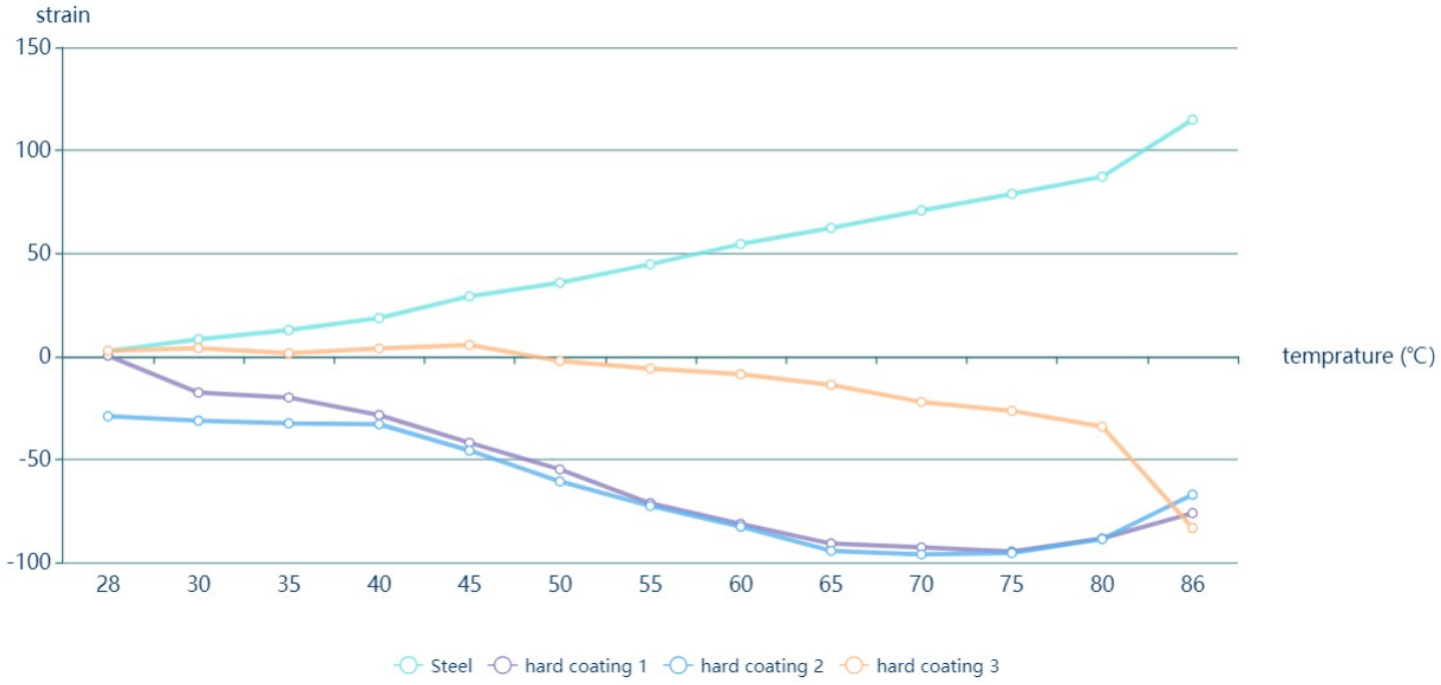

Chart 2.7: the strain-temperature curve for recycled hard coating specimens over heating period.

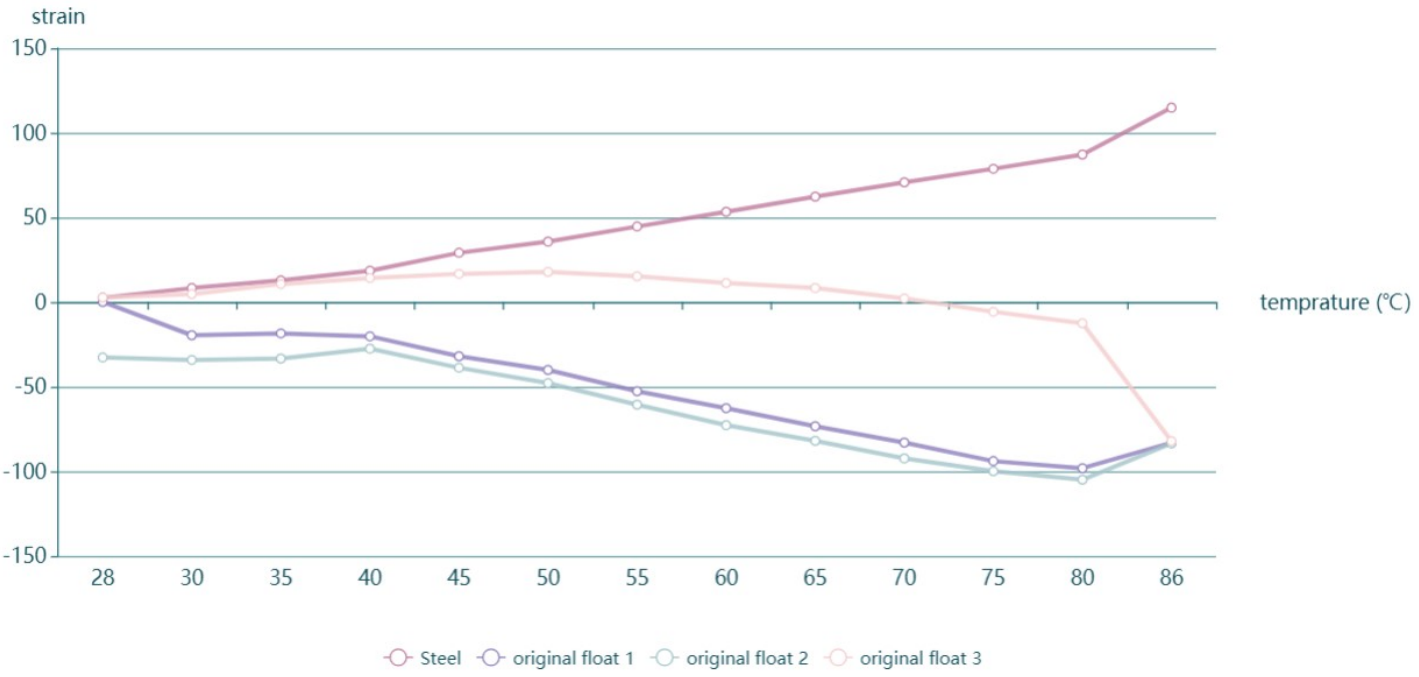

Chart 2.8: the strain-temperature curve for original float glass specimens over heating period.

From the charts above, it is obviously that the data for test 3 has apparent differences with the data from other two tests. One influence factor may resulting from the initial temperature, which is ambient temperature for test 1 and test 2 but higher for the specimen in test 3. The specimens in test 3 hasn't been completely chilling down after test 2, thus it requires more time to adapt to the

temperature change. However, in order to better illustrates the growth of strain, the data of test 3 will not taken into account in chart 2.9.

On the stacked trace plot, the amount of strain variation can be described for five categories. It is distinct that the original normal float glass and recycled hard coating glass are deform greatly than other types at the beginning period, whereas after a period of constant temperature at around 86 degrees, the strain of all specimen verging to a similar temperature. The reason of obvious differences in the beginning period can be explained by the instability of the wire connection or attachment between strain gauges and specimens for test 5, test 6 and test 7, which requires more time for adaptation in constant temperature. This phenomena also present in the fluctuation in the screenshot (shown in appendix). Considering the final strain at stable period, the strain of recycled glass are very close to the final strain for original normal float glass.

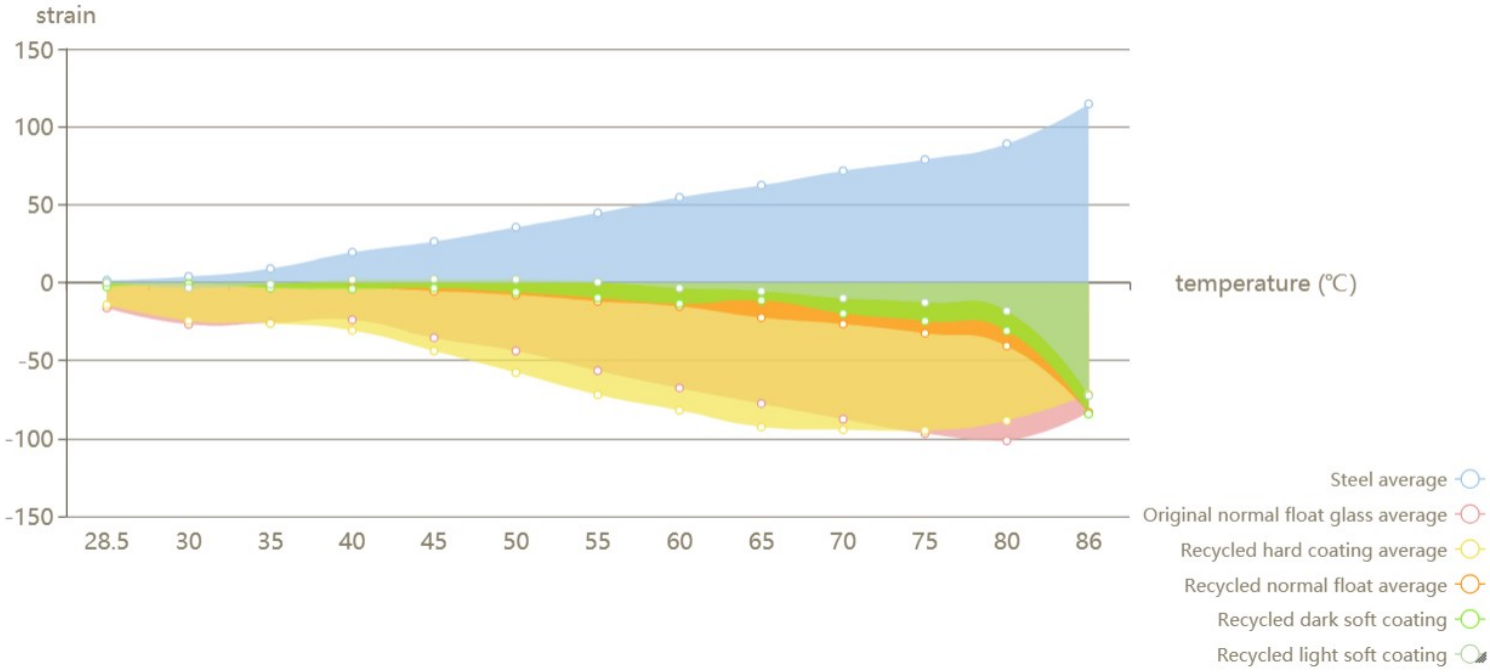

Chart 2.9: the strain-temperature curve for sample specimens and reference specimen over heating period.

CTE calculation

Aiming at CTE calculation, the strain value at initial temperature is taken as the initial strain value. Even though the program try to remain the temperature in a constant value, there are undulation existing in the constant temperature period. It is vague to distinguish the strain at highest temperature, thus the consideration of strain for stainless steel is taken. It has a distinct change along with the temperature variant. Therefore, for the highest strain of specimen is selected as the strain value corresponding to the highest strain of stainless steel, which indicates a stable period for all specimen

at highest temperature.

Based on the theory of Wheatstone bridge for strain gauges, J. Valentich [31] bring forward following equation to describe the value from strain gauge test of thermal expansion:

$$\varepsilon' = (\alpha - \alpha_c)\Delta T \qquad \text{(Equation 2.2)}$$

ε': Measured strain, micrometer per meter
α: CTE of sample specimen
α_c: CTE of reference specimen
ΔT: Temperature variation in degree

In order to gain the CTE of the sample specimen, the equation can be rewrote as below:

$$\alpha = \frac{\varepsilon'}{\Delta T} + \alpha_c$$
$$where: \quad \varepsilon' = \varepsilon - \varepsilon_c \qquad \text{(Equation 2.3)}$$

The ε is the measured strain of specimen, and the ε_c is the measured strain of reference material. Looking back to the data of measured strain for sample specimen, all the data for recycled glass are presented as negative value. One of the reason may comes from the different expansion rate between strain gauge and sample specimens. It is known that normal glass is much less sensitive to temperature than steel. Compared with faster expansion rate of strain gauges, the strain value of glass specimen may be shown as negative value in the plot. Moreover, the opposite circuit connection of the strain gauges is another possible reason. To enable the calculation, the negative information of glass specimen will be regarded as positive results in the following analysis. A detailed calculation sheet displayed below:

	Sample strain in highest temperature	Sample strain in lowest temperature	Reference strain in highest temperature	Reference strain in lowest temperature	Measured strain
Recycled hard coating glass	80.581349	1.041014	109.55766	2.636902	-27.380429
Recycled dark soft coating glass	60.369263	-1.457093	100.6772253	-0.208166	-39.054063
Recycled light soft coating glass	47.299155	0.901552	100.672253	-0.208166	-54.482816
Recycled	43.826396	3.88934	105.187406	-2.359356	-67.609706
normal float	40.231932	3.676222	105.187406	-2.359356	-70.991052
glass	45.911323	-1.527985	105.115108	0.00000	-57.675800

Table 2.13: Measured strain calculation.

	Highest temperature (℃)	Lowest temperature (℃)	Temperature variance (℃)
Recycled hard coating glass	86.730994	28.374457	58.356537
Recycled dark soft coating glass	87.329375	27.862433	59.466942
Recycled light soft coating glass	87.329375	27.862433	59.466942
Recycled normal float glass	86.081364	26.883334	59.19803
	86.081364	26.883334	59.19803
	86.687574	27.517864	59.16971

Table 2.14: Temperature variance calculation.

	CTE of reference material	Ɛ'/ ΔT	CTE of sample material	
Recycled hard coating glass	12	-0.469192149		11.53080785
Recycled dark soft coating glass	12	-0.656735687		11.34326431
Recycled light soft coating glass	12	-0.91618661		11.08381339
Recycled normal float glass	12	-1.14209385	10.85790615	
	12	-1.199213082	10.80078692	10.89464698
	12	-0.974752116	11.02524788	

Table 2.15: CTE value calculation.

Referring to the technical data from Pilkington, the CTE of soda lime silica float glass is 8.3 μm/ m℃, over the temperature range from 24℃ to 300℃. Theoretically speaking, the less temperature altered, the less expansion appears in the material, meaning the less CTE value will be. In the calculation above, the temperature variance is far less than the temperature range from reference literature, while the CTE value is higher than literature value, which indicates a indispensable correction. As the strain gauge and tested samples are produced from different material, the measured strain in CTE test might be influenced by the deformation of strain gauges. Besides, the other parts of the correction comes from the floating value of strain gauge electrical resistivity over temperature, it result from the strain gauge itself. To eliminate the influence, a definition called apparent strain is introduced, applying in correcting the result of CTE measurement. [32] It can be derived from the quadratic equation of thermal output as following:

$$\varepsilon_{app} = \text{-}2.27\times10 + 1.35\times T - 1.07\times10^{-2}\times T^2 + 8.57\times10^{-6}\times T^3 + 1.70\times10^{-8}\times T^4$$

(Equation 2.4)

The ε_{app} is the value of apparent strain, with a unit of micrometer per meter. And T is the on-time temperature with a unit of degrees. This equation can be obtained from the data sheet of strain gauge. Similarly, the strain gauge factor is also tested by the manufactures, such as from figure 2.22 in former sections, the strain gauge factor is regard as 2.01 by the producer. To full fill the correction, a equation using apparent strain and strain gauge factor together to amend strain:

$$\varepsilon_{compensated} = (\varepsilon - \varepsilon_{app}) \times \beta$$

(Equation 2.5)

Where β is the value of gauge factor, which equals to 2.01 in this test. The specific calculations shown in the appendix, here set the recycled dark soft coating glass as an example:

1) Electrical resistivity correction:

The apparent strain at highest temperature (86.41℃):

$$\varepsilon_{app\text{-}highest} = \text{-}2.27\times10 + 1.35\times86.41 - 1.07\times10^{-2}\times86.41^2 + 8.57\times10^{-6}\times86.41^3 + 1.70\times10^{-8}\times86.41^4$$
$$= 20.54$$

The apparent strain at lowest temperature (27.86℃):

$$\varepsilon_{app\text{-}lowest} = \text{-}2.27\times10 + 1.35\times27.86 - 1.07\times10^{-2}\times27.86^2 + 8.57\times10^{-6}\times27.86^3 + 1.70\times10^{-8}\times27.86^4$$
$$= 6.80$$

The gauge-corrected strain of recycled hard coating glass:

$$\varepsilon_{gaugecorrected-highest} = (84.38 - 20.54)\times2.01 = 128.32$$
$$\varepsilon_{gaugecorrected\text{-}lowest} = (\text{-}1.46 - 6.80)\times2.01 = -16.60$$

The uncompensated CTE for recycled hard coating glass:

$$\alpha' = [128.32 - (-16.60)]/(86.41 - 27.86) = 2.475$$

2) Thermal compensation correction:

The gauge-corrected CTE of reference stainless steel:

$$\varepsilon_{gaugecorrected\text{-}highest} = (110.52 - 20.54)\times2.01 = 180.86$$
$$\varepsilon_{gaugecorrectedd\text{-}lowest} = (\text{-}0.21 - 6.80)\times2.01 = \text{-}14.09$$
$$\alpha_c = [180.86 - (-14.09)]/(86.41 - 27.86) = 3.33$$

The final results of CTE value for recycled hard coating glass:

$$\alpha = \alpha' + \alpha_c = 2.475 + 3.330 = 5.805$$

On the basis of the calculation results, the recycled dark soft coating glass has the highest CTE value at 5.805, following by recycled normal float glass at 5.529. The recycled hard coating glass has a slightly higher CTE value than recycled light soft coating, which are 5.473 and 5.315 respectively. Meanwhile, the same test method is carried for original normal float glass as well, and the CTE results is 5.736.

	Original normal float glass	Recycled normal float glass	Recycled hard coating glass	Recycled dark soft coating glass	Recycled light soft coating glass
CTE value	5.736	5.529	5.473	5.805	5.315

Table 2.16: CTE value of different category.

As illustrated in chapter 2, the value of CTE are mainly influenced by the bond strength between metal cation and oxygen ion, indicating a important role for metal oxide. Especially to the soda lime glass, where the anion are oxygen ion, thus the bond strength in metal oxide is dominate by metal cation. There are two influence factor, for one thing the bigger ionic radius metal cation have, the weaker the bond will be. For another, the bond strength is proportional to the electrovalence of metal cation. Both a higher electrovalence and a smaller ionic radius means a higher chemical bond in metal oxide. [33]

Despite on the bond strength between metal cation and oxygen ion, among the metal oxide, the alkali and aluminum have special influence in glass thermal expansion. The alkali will increasing the basicity, which will damage the bond of silica dioxide structures, so that the expansion prevention from silica will be weaken. In contrast, the aluminum can perform as a modifier which stronger the silica-oxygen bond, leading to less expansion. Based on the Schott's table [28], the coefficient for sodium oxide and potassium oxide are 10 and 8.5 respectively, while a lower coefficient for aluminum is 5 in thermal expansion.

Apart from the influence illustrates above, a strong chemical bonding exists between cation and anion in silicon-oxygen tetrahedron, which prevent expansion when temperature increasing, so that the higher the silica contained the less the CTE value will be [34] [35]. However, the influence coefficient for silica is relatively low in Schott's table, which is 0.8. The silica will only be taken into consideration when it has a relatively high content in glass compositions.

Depending on the attached position of strain gauges is on the side face of the specimen, the XRF result of recycled light soft coating and dark soft coating can not be concluded into the analysis, since it only covers the surface composition. Therefore, for further investigation, the analysis goes deeper with the XRF results of the middle area of recycled normal float glass and recycled hard coating glass, as well as the bare side of original normal float glass. Identically, the bars below is the

description of chemical composition content, and the broken line shows the results of CTE test.

	Na_2O	K_2O	CaO	Al_2O_3	SiO_2	MgO
Coefficient	10	8.5	5	5	0.8	0.1

Table 2.17: Coefficient value of several chemical compositions for thermal expansion[28].

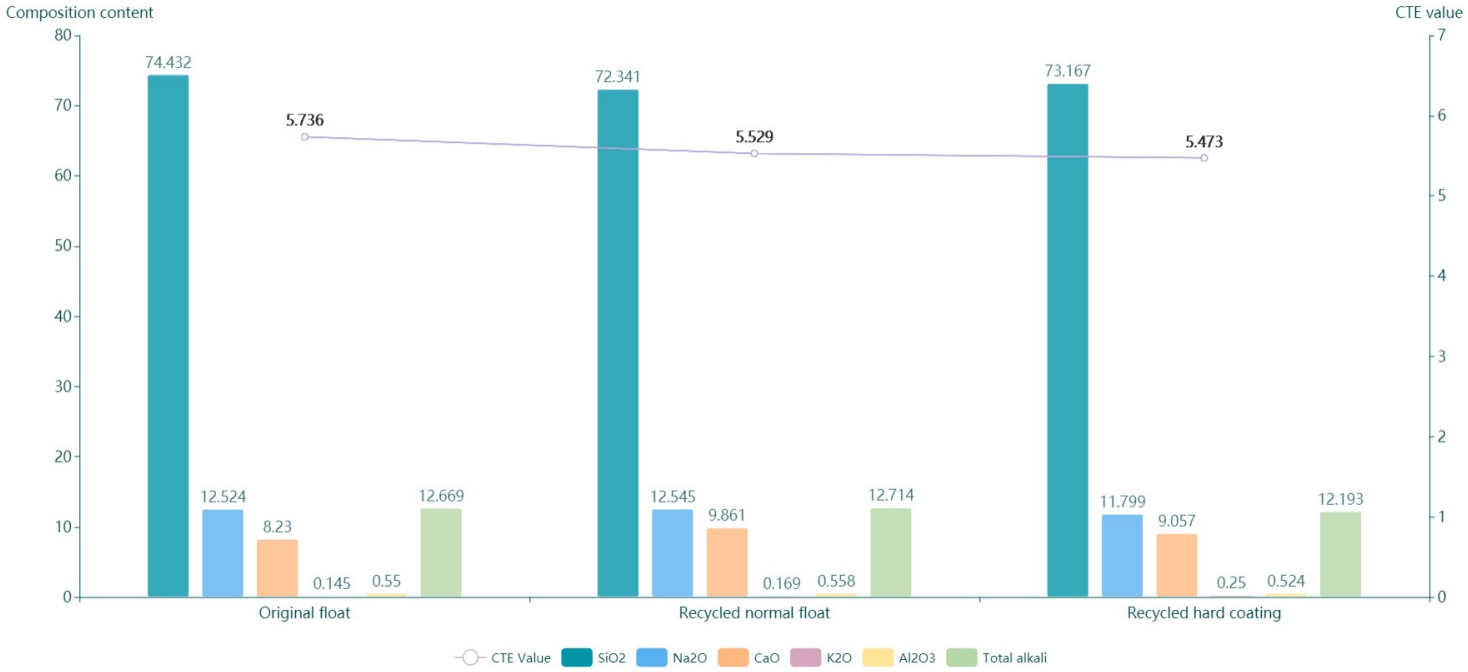

Chart 2.10: The comparison of chemical composition content and CTE value among different glass category.

Extracting from the chart above, the recycled normal float glass has a slightly higher CTE value than recycled hard coating glass, but lower than the CTE value of original float glass. Considering the comparison between recycled normal float glass and recycled hard coating glass, the alkali content for the former is higher than the later, as well as the content of calcium oxide which will increase the expansion as the same as the function of alkali oxide. In the chart, the total alkali value equals to the sum of sodium oxide and potassium oxide. According to Winkelmann additive model [28], the CTE of glass in not only relates to the component coefficient but also the weight percentage of the component. Thus, even though the influence of silica for thermal expansion is inappreciable compared with alkali, it takes the dominate composition in recycled float glass, which requires a sub consideration. Luckily, the recycled hard coating glass own higher amount of silica oxide, which indicates a lower CTE value and nicely matching the test results. In spite of the alkali and silicate, the calcium also helps expansion while the aluminum oxide prevent the expansion, both of them have the same degree of impact in thermal expansion [28]. Owing to the relatively low weight content of aluminum, the influence of the higher amount may be eliminated by other chemical compositions. In general, the reliability of the test result for recycled glass is believable, and it is rational to

demonstrate that the recycled hard coating glass has a lower CTE value than recycled normal float glass.

Nonetheless, through the comparison between original float glass and recycled normal float glass, the lower silicate content and higher alkali content for the recycled glass seems not able to growing the ability of expansion. Only the influence of aluminum is in consistence with the theory. This phenomena can be explained by the uniform distribution of silicate and alkali in recycled normal float glass, as mentioned in chapter three, the attaching area of strain gauge may have a higher silica and less alkali than original float glass. Hence, it is not completely trustworthy to predict the CTE only from the chemical composition without experiment.[47]

Chapter 6 Fracture strength test

As is know to all that glass is regarded as unsafe material due to its brittleness, illustrates by classical Griffith fracture theory. Although by years of estimation that glass has good performance in compressive capacity, and certainly the great advantage in appearance and translucency, the fracture strength is one of the most important properties of glass. The objective of this test is to obtain the fracture strength of the new material recycled from waste float glass with different coatings, so that the further computational research is executable. In this chapter, not only a laboratory experiment has been finished, a finite element analysis will be carried for further investigation.

6.1 Methodology

Owing to the beam structural, which is usually subject to tensile stresses, a fracture mechanism can be detected by bending test. Integrating with dimension of sample specimens and the stability during loading, a four point bending test has been selected. [36][37] A simplified diagram shown in figure 2.32, presenting the support and loading condition for the bending test, together with a shear and moment diagram on below.

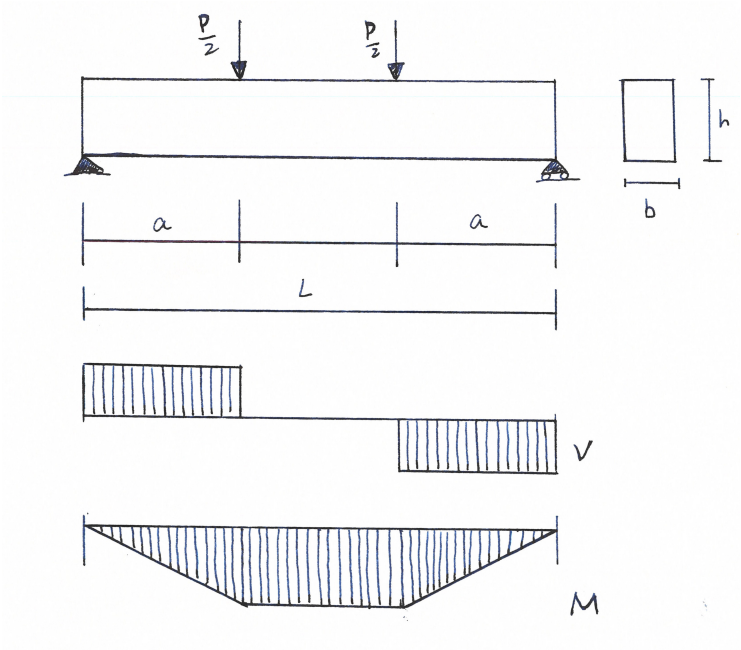

Figure 2.32: The diagram of four-point bending test and relative shear force and bending moment diagram.

Based on the fracture mechanics literature, there are mainly two failure modes for brittle material under bending load. Ideally, the beam will break between two loading points, and the cracks are most probabely produced in the tensile zone, following by quick propagation until passing through the height of beam. Once the beam break in the loading point, it is most likely that shear stresses is the dominate failure stress. The first mode failures in the maximum moment while the second mode failures at maximum shear stress, corresponding to equation 2.6 and equation 2.7 respectively. [36][37]

$$V_{\max} = \frac{P}{2} \qquad \text{(Equation 2.6)}$$

$$M_{\max} = \frac{P}{2} \cdot a \qquad \text{(Equation 2.7)}$$

V_{max}: The maximum shear stress of specimen;

M_{max}: The maximum moment of specimen;

P: The loading force;

a: The distance between loading point and supporting point.

On basis of beam theory, the break stress can be derived through the dimension property together with the testing results, through the equation 2.8.

$$\sigma_{\max} = \frac{M_c}{I} = \frac{3Pa}{bh^2} \qquad \text{(Equation 2.8)}$$

σ_{max}: The flexural stress in correspond to break force;

b: The width of the specimen;

h: The height of the specimen.

There are six specimens awaited for testing, all of them are made of the mixture of coated glass. A roughly dimension in 360mm in length, 36 mm in height and 12mm in thickness has been measured. Despite there is small initial cracks in the edge of glass beam, a elaborated polishing and grinding has been applied. Due to the lack of additional supporting system, as well as the thickness limits the beam ability to "stand up", the four point bending test will be proceeded in a horizontal direction, presented in figure 2.33.

Figure 2.33: The four-point bending test of recycled glass beam, photo by author.

The loading rate has been programmed as 1 milimeter per minute, and the software will record the force from loading point and the displacement from the same location. Depending on break force and maximum force, the corresponding stress can be derived, so that further analysis can continue marching.

6.2 Data collection

Before processing the bending test, a measurement of the geometry is mandatory. Table 2.18 give the geometry information for each test, incorporate with the explanation picture below:

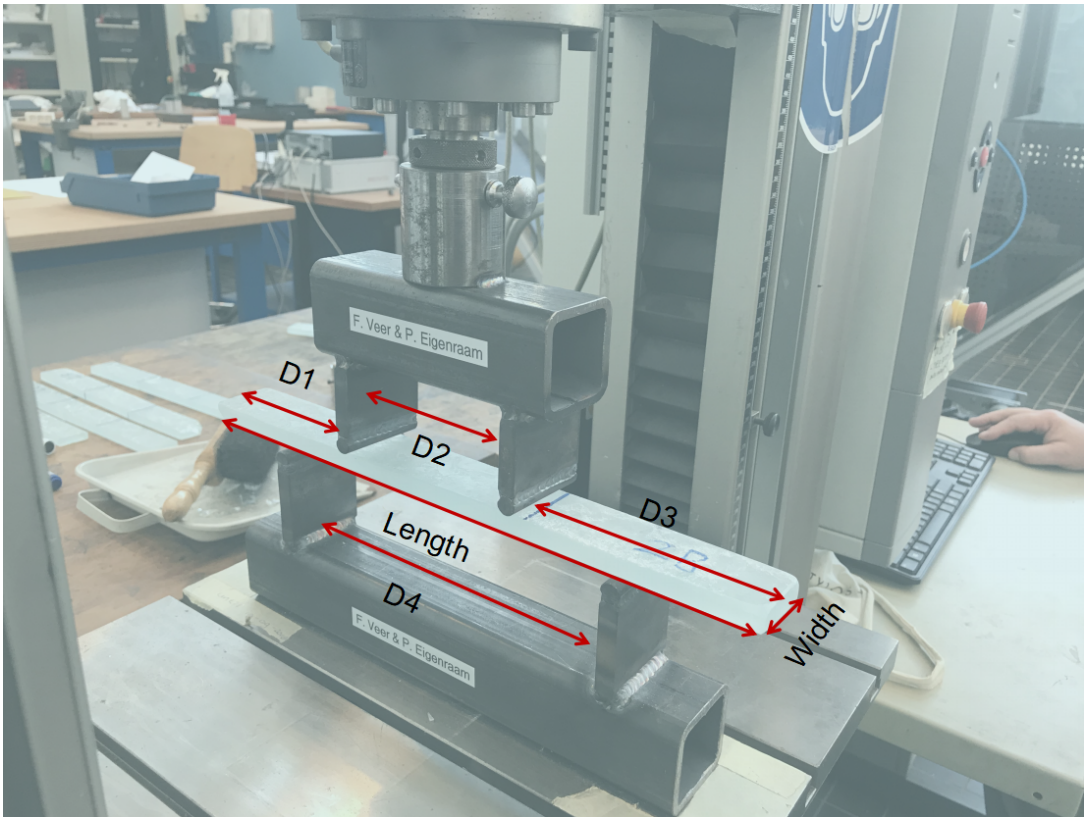

Figure 2.34: The corresponding geometry to measured information.

(mm)		L	b	D1	D2	D3	D4	a
Specimen 1	1 B	360	40	120	120	120	240	60
Specimen 2	1 A	358	40	118	120	120	240	60
Specimen 3	1 C	358	40	124	120	116	240	60
Specimen 4	2 A	360	39	118	120	122	240	60
Specimen 5	2 B	358	36	116	120	122	240	60
Specimen 6	2 C	357	37	115	120	122	240	60

Table 2.18: Geometry information for each bending test.

From the table above, L is the total length of the specimen, b is the width, which is the height when it placed in a vertical way, t is the thickness of the glass beam. D1, D2, D3 and D4 is the distance measured for each placement, except for the D2, which is the distance between two loading point, and D4, which is the distance between two supports, are fixed before bending test, D1 and D3 are slightly varies for different placement. Meanwhile, the a value is the distance between one support to

the nearest loading point, which is certainly fixed as well. The number of specimen origins from its production and quality, the same number in front means these specimen produced from one mould, while the alphabet behind elaborates the quality of the specimen, from A to C is the best property to the worst condition with visible cracks on the edge.

After loading, the corresponding force and displacement at the loading position has been recorded computationally, the results shows in table 2.19. To visualize the result, the data has been graphing in chart 2.11, with obvious similar trending for all glass samples. The small curve in the beginning period result from the adaption of the bending equipment, then the curve transfer into a linear phase, on where the Young's modulus is able to be gained, until the broken point.

	Maximum load (N)	**Displacement at maximum load (mm)**	**Break load (N)**	**Displacement at break load (mm)**
1 B	677.837	0.649	663.524	0.650
1 A	899.367	0.504	856.117	0.504
1 C	788.770	0.502	765.699	0.502
2 A	880.968	0.530	880.968	0.530
2 B	782.541	0.576	782.541	0.578
2 C	809.641	0.516	800.328	0.516

Table 2.19: The data collection from each bending test.

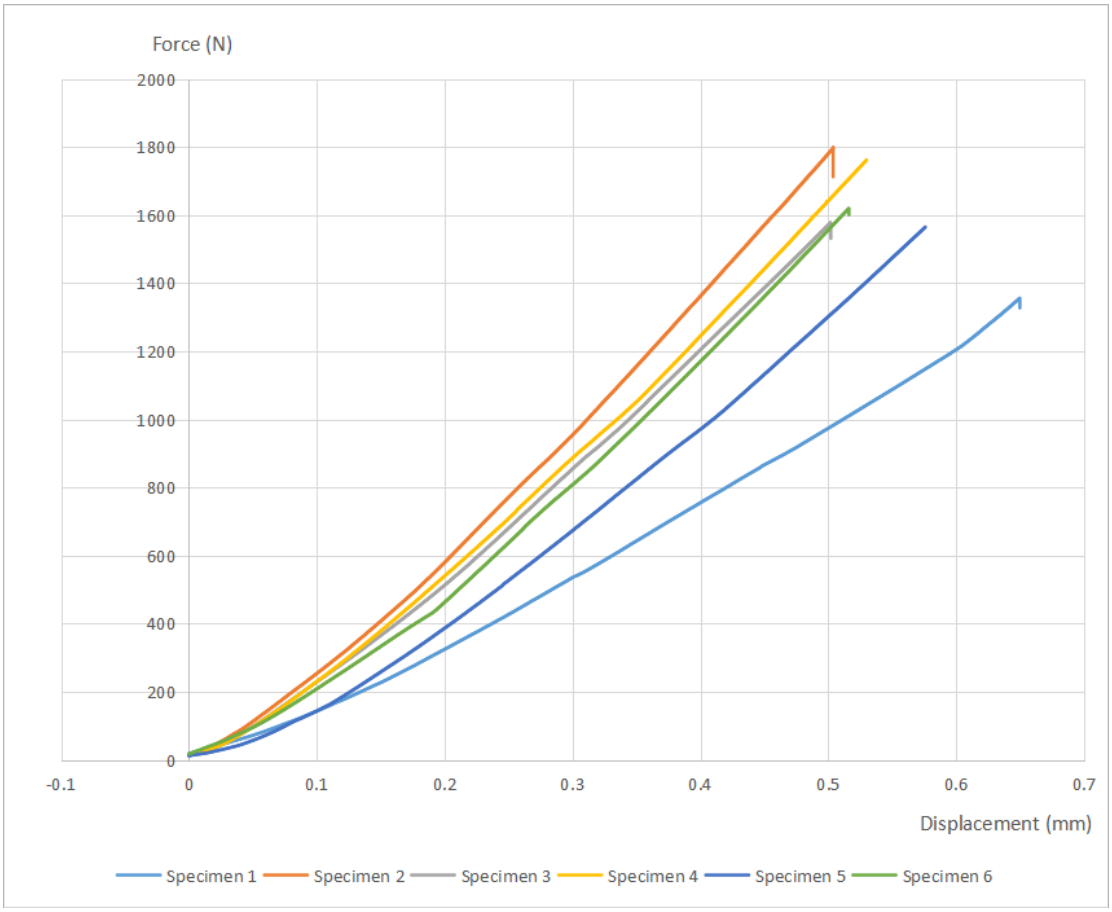

Chart 2.11: The Load-displacement curve for all specimens

Since the software only record the force in the one side, with two loading point, the results should be doubled before building the Load-displacement curve. Obtaining from the data, the maximum displacement is 0.65mm and the maximum break strength among this samples is 880.968 N.

6.3 Analysis and discussion

Build on the data above, the flexural stress under break load can be draw through equation 2.8. Since the width and length is variant for each specimen, the break stress is calculated individually for each specimen, the calculation form is presented in the appendix. The average value of flexural stress, which is 51.29 MPa, will be regarded as the final flexural stress of recycled float glass, also used as a known critical stress for the input in finite element analysis.

Besides, the magnitude of Young's modulus can be speculated from the load-displacement curve, since the curvature of load-displacement curve is the stiffness of recycled glass, which is in proportional of Young's modulus. Therefore, except for specimen 1 and specimen 5, the other specimen has similar Young's modulus.

Apart from the data analysis, the break position for each beam is also worthy of investigating. Figure 2.35 presenting the crack position for each specimen, only dominate crack has been marked, the unconsidered break in the corner result from the falling after breaking.

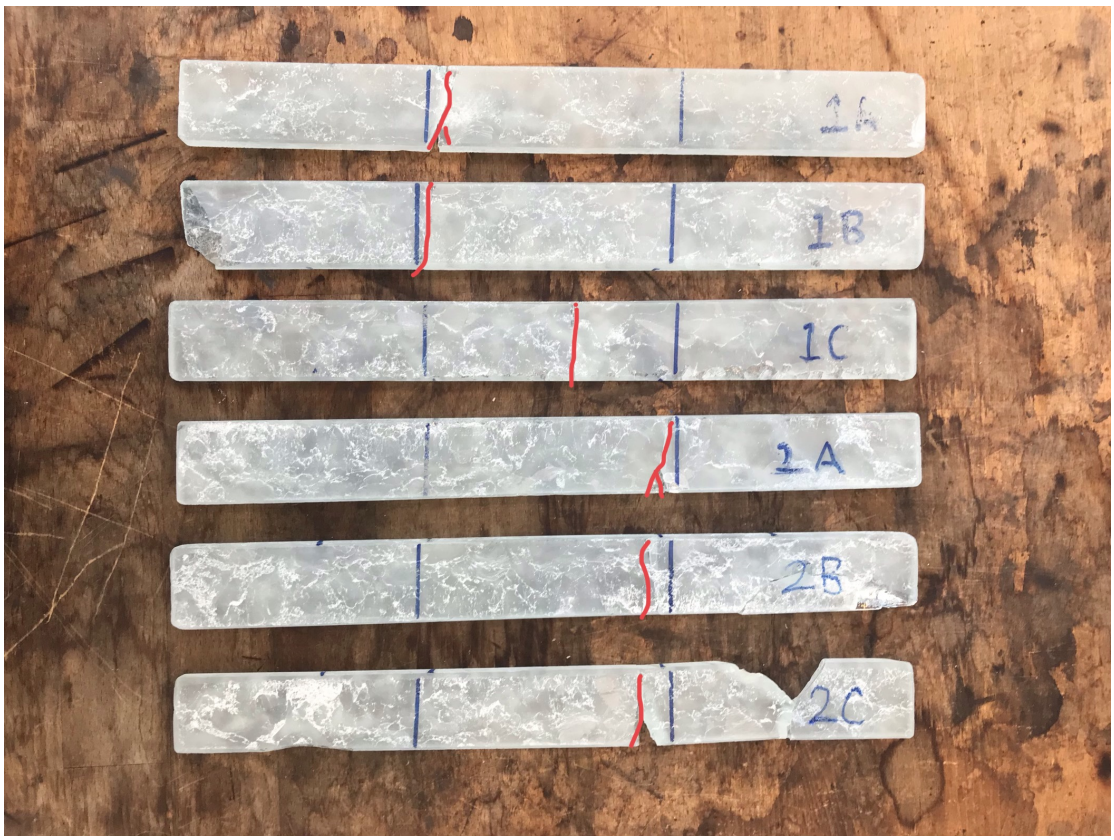

Figure 2.35: The dominate crack for each specimen.

Figure 2.36: The crack surface of specimen 1C.

Most of the specimen are break in the loading position, in addition to specimen 1C, it is not only break in the middle of two loading points but also crack in a tensile zone, which is observable in the fracture surface. However, due to the lack of inter layer between bending machine and recycled glass specimen, the beam is directly stressed by bending machine, which may introduce stress concentration in the loading position, where the break happens. Owing to the brittle property of glass, the fracture surface is regular and clean, a crack start point with rainbow trace can be found in tensile area.

Figure 2.37: The detailed flaws in the surface of specimen 1C, with normal light and camera.

To further analyze the cracks of the specimens, a detailed observation of the surface is carried. Through the microscope, the fractal patterns are found in the surface, which can provide the path of crack while loading. Besides, some of the patterns are found in the state of layers, more like in the condition of fusion rather than casting. These flaws in the side surface are all indicating possibilities for the reduction of fracture test results.

6.4 Finite element analysis

Limited by the time and condition, the four point bending test can only be carried for “laydown” recycled glass beam. In order to simulate the recycled glass beam performance under bending test in different geometry, the Finite Element Method (FEM) analysis has been introduced. Through detailed comparison, the Diana is selected as the FEM software, favouring in nice simulation in concrete structural, since the mechanical behavior of glass is analogy to concrete, and the proficiency of the author.

Experiment simulation

Based on the physical model from the experiment, a average dimension has been settled as 360mm in length (x direction), 12 mm in thickness (y direction) and 38mm in width (z direction). Then, a 2 dimensional finite element model has been established as figure 2.38, with one bottom support restrain the y direction movement and the other bottom support restrain the movement in both y and x directions. The support on top of the model is the loading position which will applying prescribed displacement in negative y direction during analyzing. The distance between bottom support is 240mm and the distance between loading points is 120mm.

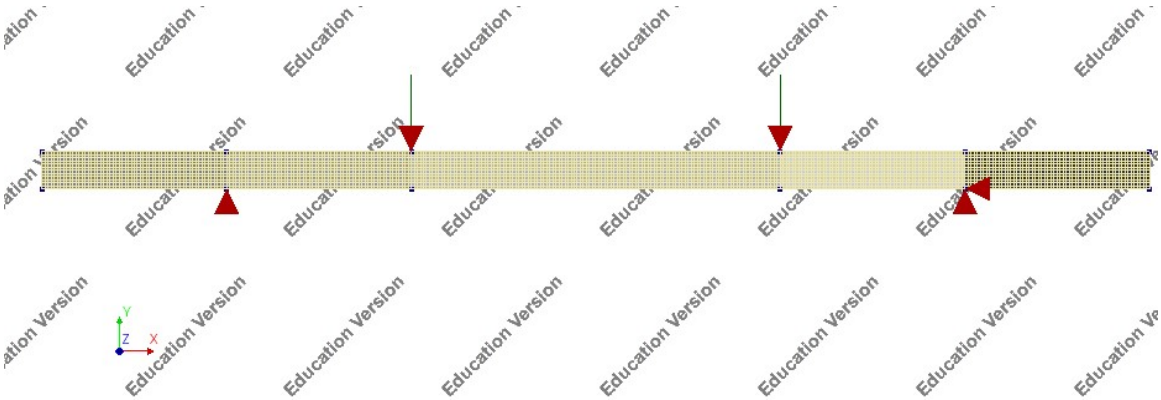

Figure 2.38: The geometry of FEM model by Diana.

The material property is assigned on basis of the test result from the experiments, shown in table below:

	Young’s modulus	Poisson’s ratio	Mass density	Tensile strength
Units	N/mm^2		T/mm^3	N/mm^2
Experiment simulation	66345.9	0.2	$2.739*10^{-9}$	51.94

Table 2.20: The material property of FEM model for experiment simulation.

The Young's modulus input equals to the average value of ultrasonic results from chapter 4 as well as the density value. Tensile strength is selected as the flexrual stress correspond to the fracture force from previous section. And for Poisson's ratio parameter is chosen as average value for common float glass. A Total Strain Based Crack model is selected with a rotating crack orientation, which means the crack direction will always perpendicular to the stress direction. To simulate the glass breaking behaviour, the brittle tensile curve has been chosen, indicating a linear elastic behaviour until failure. In addition to material assignment, the model has been applied a prescribed displacement for nonlinear analysis, with 0.01 milimeter per step, which means the model will converged based on the displacement.

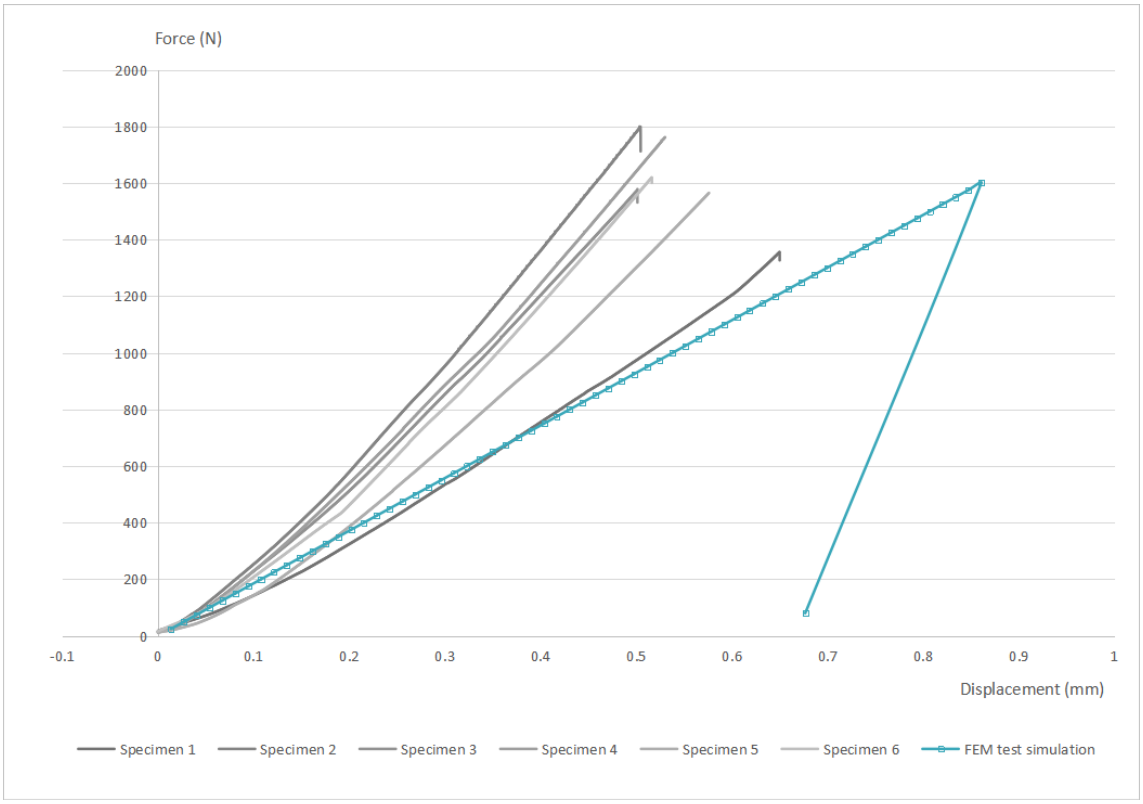

Chart 2.12: The load-displacement curve for FEM models, in comparison with experiment results.

Through graphing the relationship from the result of nonlinear analysis, a load-displacement curve for FEM test has shown in the figure above, in comparison with the experiment results. Obviously, the numerical curve is completely linear without any adaptation in the beginning period. Meanwhile, the FEM analysis is able to reach a higher displacement results at similar fracture strength. There are two reasons to explain the load-displacement curve distinction between test curve and FEM analysis curve. Firstly, due to the uneveness of the specimen surface, the loading equipment requires adaptation at the beginning, corresponding to the curve in the first phase of load-displacement curve. However, during the adaptation period, the force has already applied to the adaptation but the displacement is not able to be recorded completely. While for the FEM analysis, the adaptation period has been eliminated, resulting in a higher displacement record. Besides, the experiment specimens are made of

recycled mixture of three categories of float glass, whereas, for FEM analysis, the value of Young's modulus is derived from the average result of each recycled float glass, which are tested individually. The possibility of Young's modulus variant may affect the curve differences as well. By comparing the slope of the load-displacement curve, a smaller Young's modulus and stiffness appears in the FEM analysis. Theoretically, the ultrasonic test results are more trustworthy, but the higher Young's modulus indication from the test requires further discussion. Therefore, an additional model is established to simulate the bending test for original normal float glass. According to the information from NSG group, the Young's modulus of soda lime float glass is 72 GPa, and the typical mean tensile stress is 41 MPa of annealed glass, with the density of 2500 kg/m^3. The material properties is presented in table 2.21 with the same mesh element, loading and supporting conditions as well as the geometry dimensions.

	Young's modulus	Poisson's ratio	Mass density	Tensile strength
Units	N/mm^2		T/mm^3	N/mm^2
Experiment simulation	72000	0.2	2.756*10^{-9}	41

Table 2.21: The material property of FEM model for original float glass simulation.

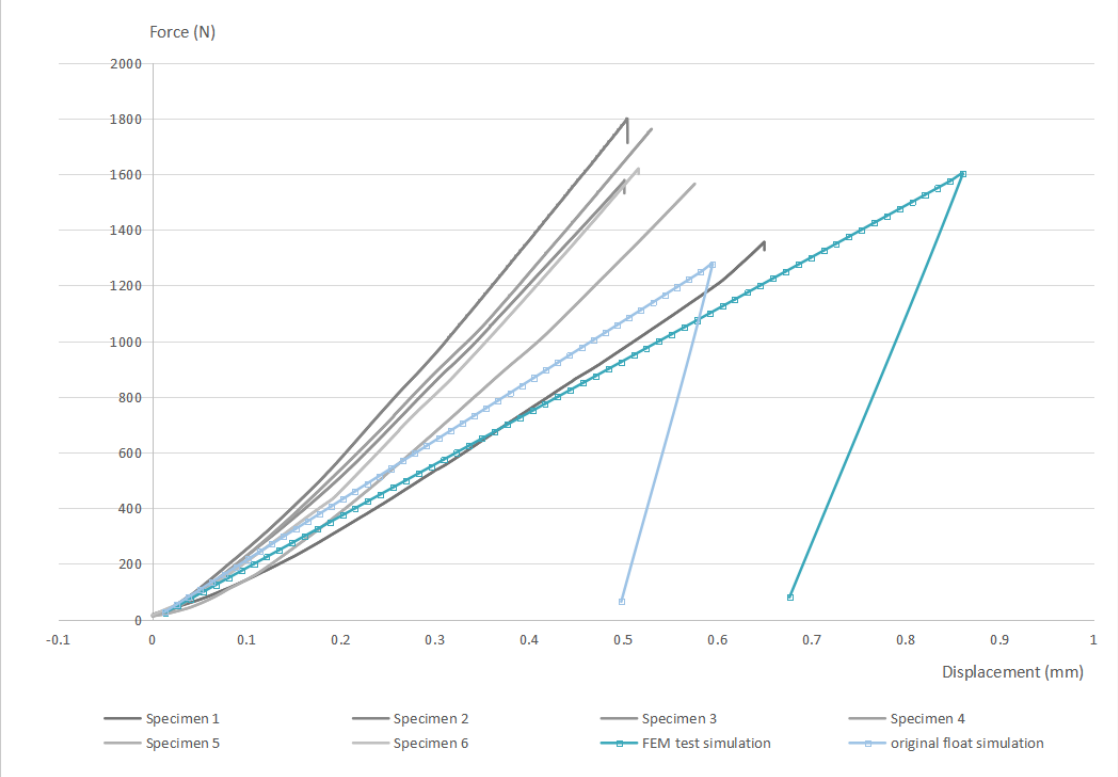

Chart 2.13: The load-displacement curve for original float glass FEM models, in comparison with other results.

The chart above presents the load-displacement curve for not only test simulation but also original float glass simulation, in comparison with the test results. The light blue curve for original float glass has a obvious higher slope than test simulation, which correspond to the higher Young's modulus input. However, comparing the light blue curve with the test results, the Young's modulus in the test results appears a modulus higher than 72 GPa. In consideration of the mixture material may have different composition with the individual recycled float glass, it is worthy to do XRF test has been carried out to illustrates the differences in the chemical view. The comparison of Young's modulus and chemical composition among the recycled hard coating glass, recycled normal float glass and recycled mixtures are shown in table below:

	Recycled hard coating	Recycled normal float	Recycled mixture
SiO2	73.167	72.341	71.843
Na2O	11.799	12.545	12.278
CaO	9.057	9.861	10.218
MgO	4.802	3.959	4.063
SnO2	0.054		
Al2O3	0.524	0.558	0.65
SO3		0.374	0.464
K2O	0.394	0.169	0.25
Fe2O3	0.142	0.1	0.09
P2O5	0.021	0.018	0.031
SrO	0.003	0.009	0.008
ZrO2	0.016		
Cl	0.007	0.048	0.067
ZnO		0.009	0.039
CuO		0.009	
Total alkali	12.193	12.714	12.528
Total metal oxide	26.649	27.219	27.596
Young's modulus(GPa)	67.22	71.54	≧66.34 (close to 72)
Total alkali = sum (Na2O + K2O)			
Total metal oxide= sum(Na2O+CaO+MgO+SnO2+Al2O3+K2O+Fe2O3+SrO+ZrO2+ZnO+CuO)			

Table 2.22: The comparison of chemical composition and Young's modulus among recycled glass.

As mentioned in chapter 4, the value of Young's modulus related to the content of aluminum, silica, alkali, metal oxide and the alkali earth element. Considering the highest influential coefficient of aluminum [28], the recycled mixture float glass has the highest content resulting in highest modulus. Analogously, it also has the highest content of metal oxide and dominate position of calcium in alkali earth element. The harm from alkali is less than recycled normal float glass but higher than recycled hard coating glass, which indicates less decrease in bond strength than recycled normal float glass.

Although the silica dioxide content of recycled mixture is smaller than other two categories, the influence can be regarded as smaller than aluminum based on the influential coefficient. Integrating all influence factor, it is possible that the recycled mixture float glass is able to reaching a similar or even higher Young's modulus than original float glass.

By looking into the crack width graph in figure 2.39, showing the crack correspond to principle stress born in the loading position, which is analogous to the experiment results. It is worth mentioning that the crack width can only be measured in the last loading step, corresponding to the brittle material property that once crack appears, it will propagate rapidly and go directly to failure mechanism. As presented in the simulation model, the maximum crack width is 0.12 millimeter, similar to the not measurable crack width after four points bending test.

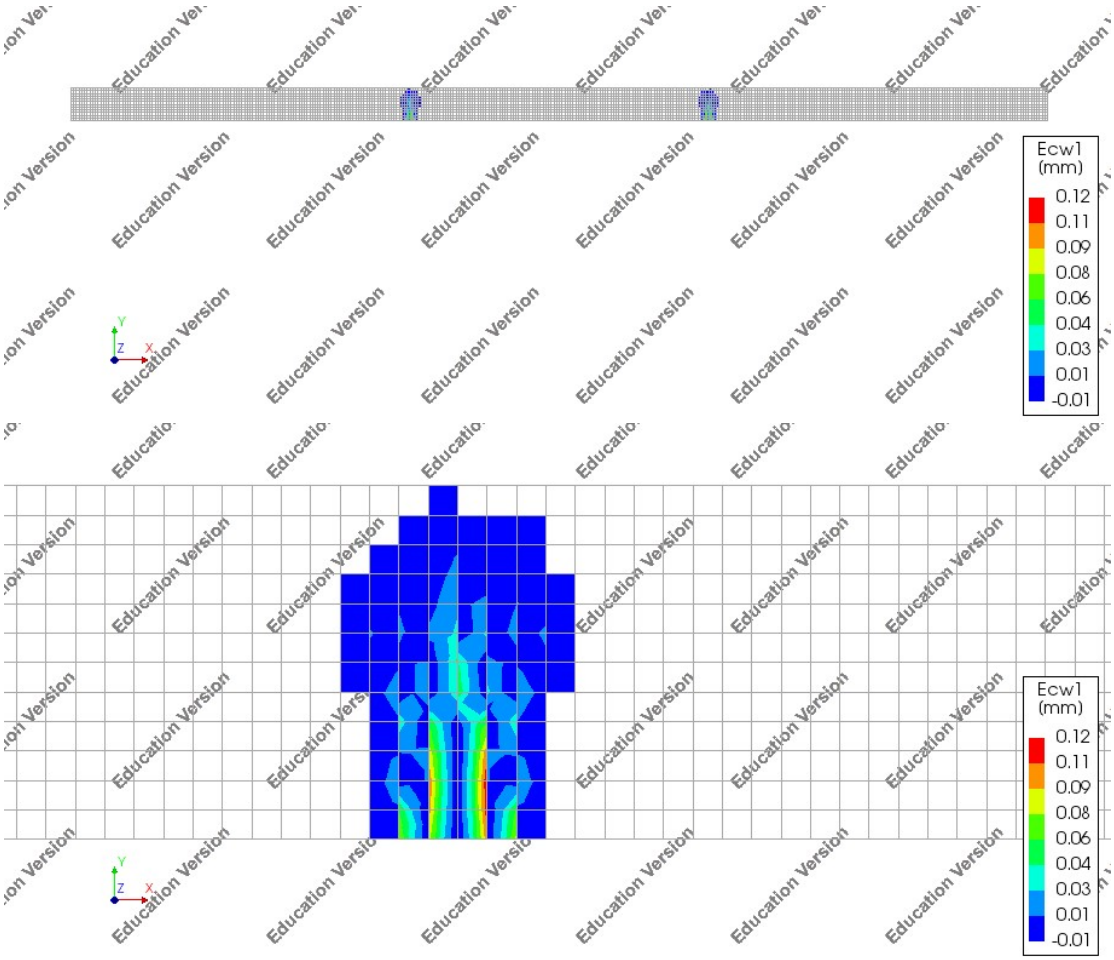

Figure 2.39: The crack width of FEM model for experiment simulation.

"Stand Up" simulation

Comparing with the common four points bending test, the beam is usually loaded and the supported in the direction of height. As illustrated before, the fracture strength test in this project is carried in the direction of thickness, limiting by the extra support system. The FEM analysis can be used to predict the break strength and corresponding deflection, as well as the crack width. Based on this objective, two "stand up" model is established including a model with recycled mixture material and another model with original float glass material. Through comparing the two models in original and recycled material, it is likely to predict the mechanical behavior of "stand up" beam made of recycled mixture float glass.

The geometry of the "stand up" model made of recycled mixture float glass, together with the mesh element, support condition and loading condition are shown in figure 2.40, following by the relative data of geometry in table 2.23. It has the identical material properties with test simulation model, presented in table 2.20. The same data will be settled for another model made of original float glass, except for the material properties, which derive from table 2.21.

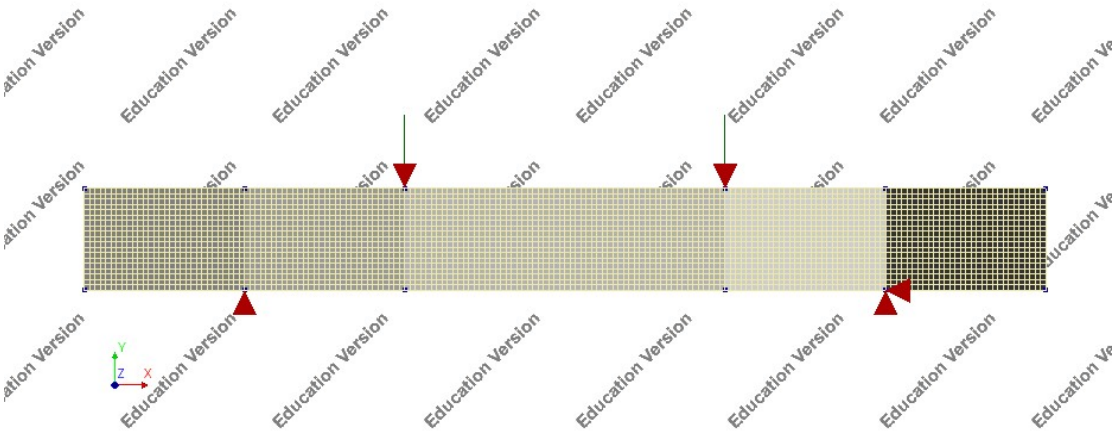

Figure 2.40: The geometry of FEM model for "stand up" simulation.

	Length	Height	Thickness	Length between support to nearest loading position
Units	mm	mm	mm	mm
"Stand up" simulation	360	36	12	60

Table 2.23: The geometry of "stand up" FEM model.

Identically, the loading steps are applied in 0.01 mm prescribed displacement per step as the former test simulation. Obtaining from the two "stand up" simulation, the load-displacement curves for original float glass and recycled mixture float glass are shown in the chart below,

comparing with the test results and former simulation results. Referring to the chart, the light yellow curve present the reaction force in correspond to the displacement of “stand up” model made of original float glass, which has lower reaction force at fracture point than “stand up” model made of recycled mixture float glass. In comparison with the “stand up” model with the test simulation, the reaction force for the former model is approximately three times than the test simulation. This results can be explained through the flexural stress equation (equation 2.8), due to the change of the cross section dimension, the value of height is three times higher than the test simulation, which leading to a higher reaction force. By comparing the original float glass model and recycled mixture model in “stand up” simulation, the higher reaction force for recycled mixture model may be a indication that when applying bending force, the beam made of recycled mixture float glass have a better performance than beam made of original float glass.

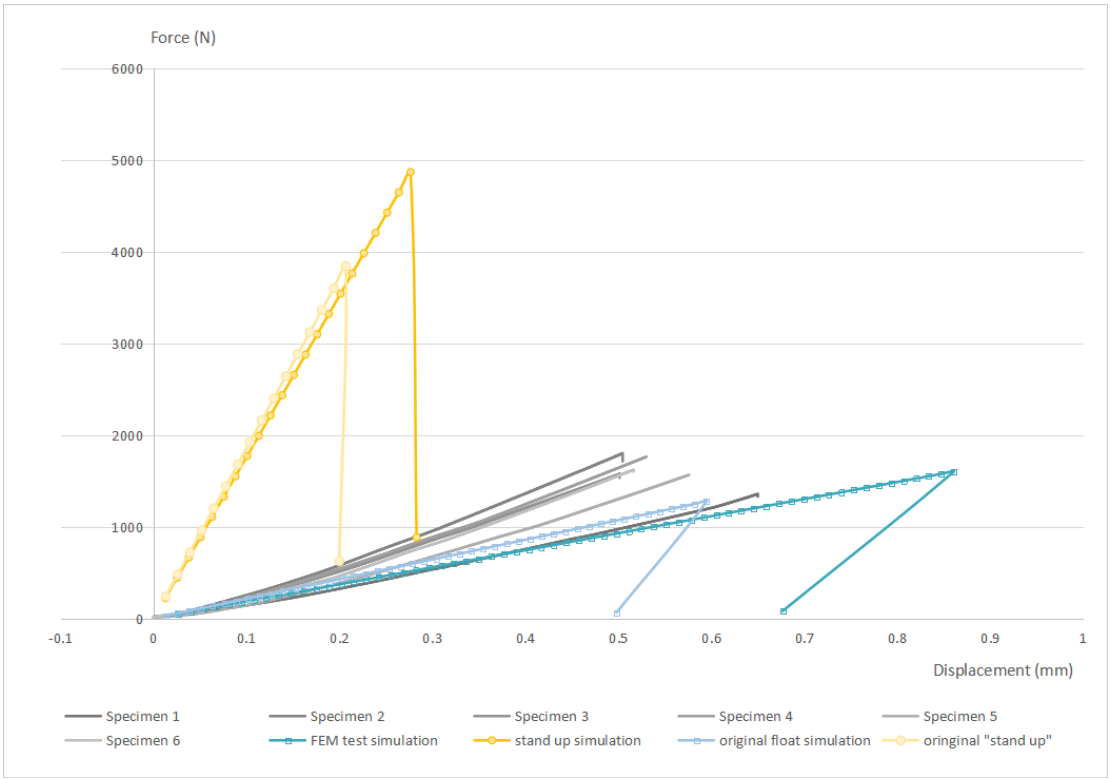

Chart 2.14: The load-displacement curve for “stand up” FEM models, in comparison with other results.

Similarly, the crack width of the “stand up” model with recycled mixture float glass is shown in the figure above. Unlikely with the former test simulation model, the cracks also appears in the tensile zone between two loading positions in addition to the cracks under loading position. Besides, the allowable crack width for “stand up” model is bigger than the test simulation model, but still appears in the last step just before cracking.

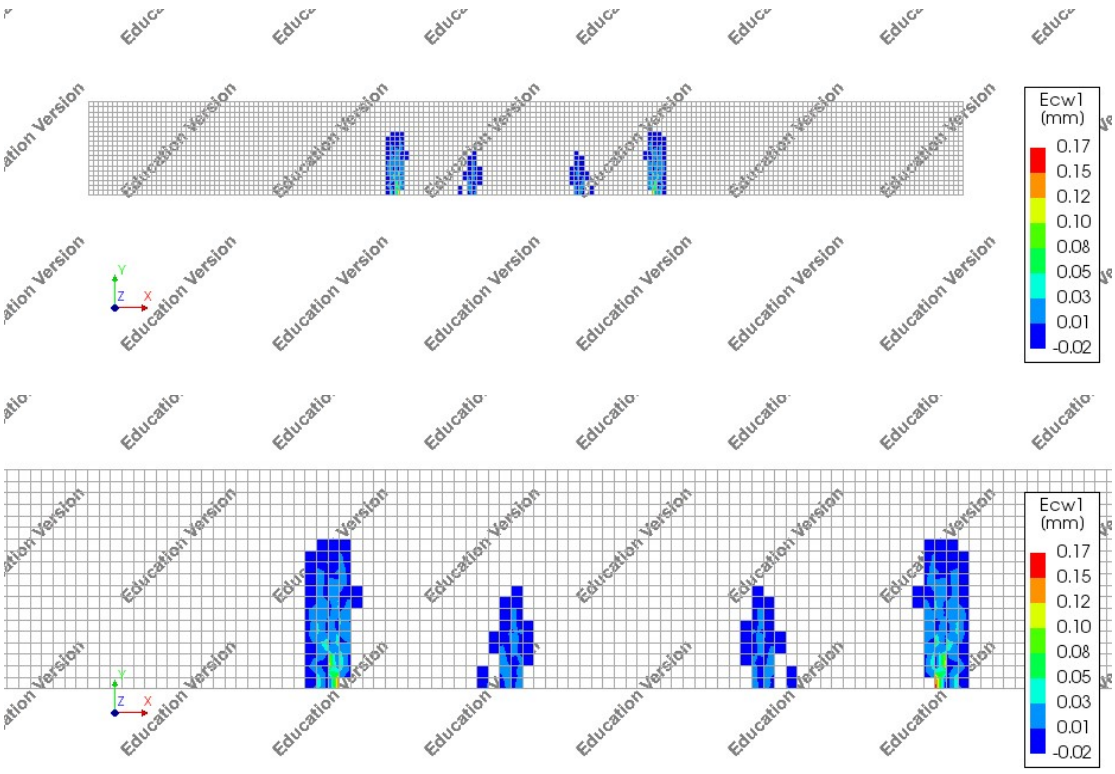

Figure 2.41: The crack width of FEM model for "stand up" recycled mixture float glass simulation.

Shear beam simulation

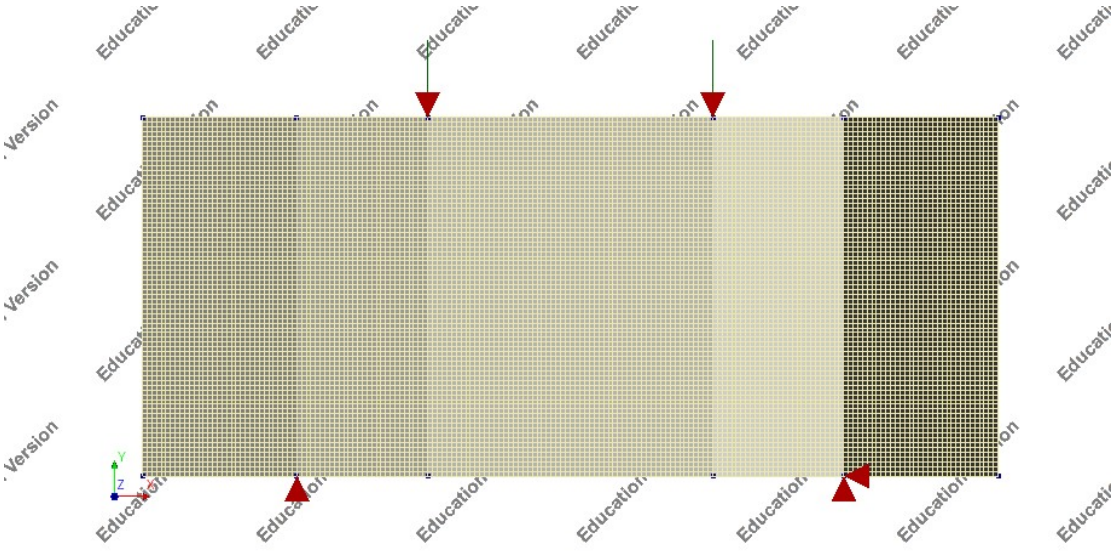

Figure 2.42: The geometry of FEM model for shear beam simulation.

The structural glass is usually applied in compression resistance components due to a relatively high Young's modulus. In analogy with the concrete shear beam behavior, the glass shear beam is likely to have cracks in the compression zone according to the similar material property with concrete. In order to simulate the shear beam behavior of the recycled mixture float glass

component, a two dimensional quadratic shear model is established with a geometry shown in figure 2.42. The shear model has the same length with test simulation, which is 36 centimeter, as well as the same distance between loading and supporting points, 12 centimeter and 24 centimeter respectively. While the dimension of cross section has been changed to 15 centimeter in height and 1.2 centimeter in thickness to form a shear beam. Due to the limitation of educational version for Diana, the mesh size has to be set two times as test simulation. The material properties, load process and supporting conditions are identical to the test simulation.

In shear beam model, the reaction force with corresponding displacement is shown as a green curve in chart 2.15. As shown in the chart, the maximum reaction force is more than 27 times than the maximum reaction force in test simulation, while the maximum displacement is less than 20% of the that in test simulation. The results are owing to the change of cross section dimension, also reflecting the possibility of a shear crack behavior.

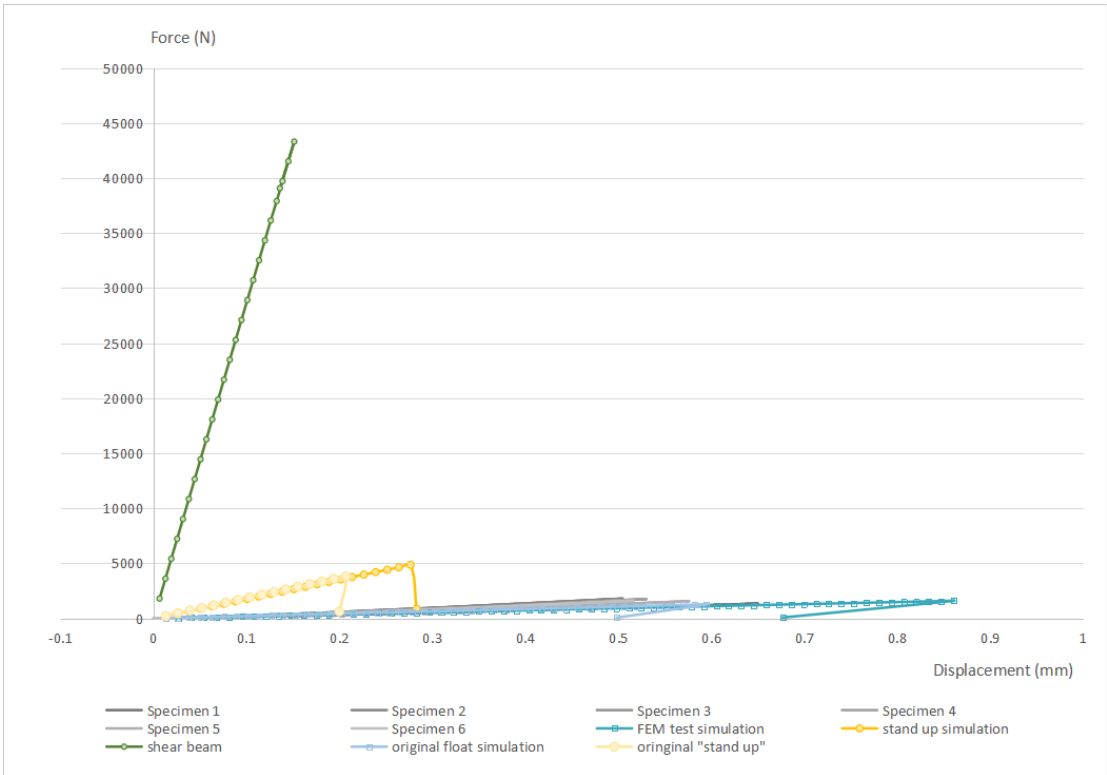

Chart 2.15: The load-displacement curve for shear beam FEM models, in comparison with other results.

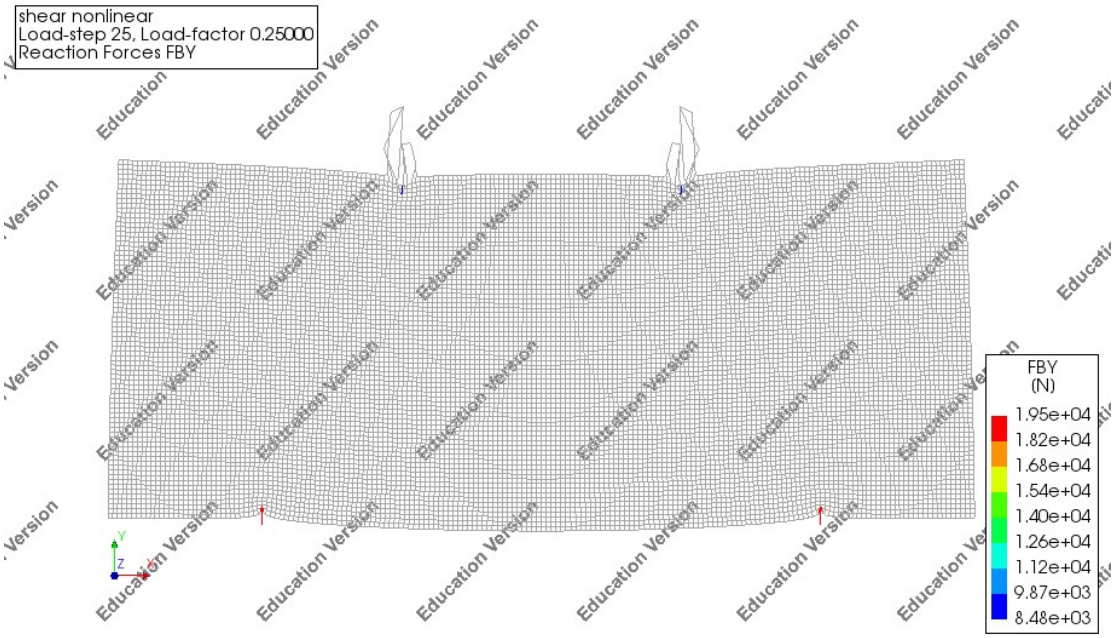

Figure 2.43: The reaction force of FEM model for shear beam simulation.

The failure behavior of the shear beam shown above with the reaction force presents analogical behavior with shear failure of concrete beam, from which the cracks forming in both the loading point and supporting point, following by cracks connecting and resulting in final shear failure. To further analysis the failure behavior, the crack position and maximum crack width are shown below.

Presenting in figure 2.43, the cracks are starting from the compression zone, which is the top area along the height direction, locating under the loading points. Except for the cracks with maximum crack width in the loading position, there are tiny cracks existing in the supporting point as well. Nonetheless, because of the brittle property, the cracks appears in the last step just before the beam failure. It is not possible to guarantee a crack path from the loading position directly to the nearest supporting point. The crack patterns in real test are affected by the supporting and loading conditions, as well as the surface status and treatment of attaching areas. In general, the shear failure behavior of recycled float glass beam is analogy to the shear failure behavior of concrete beam.

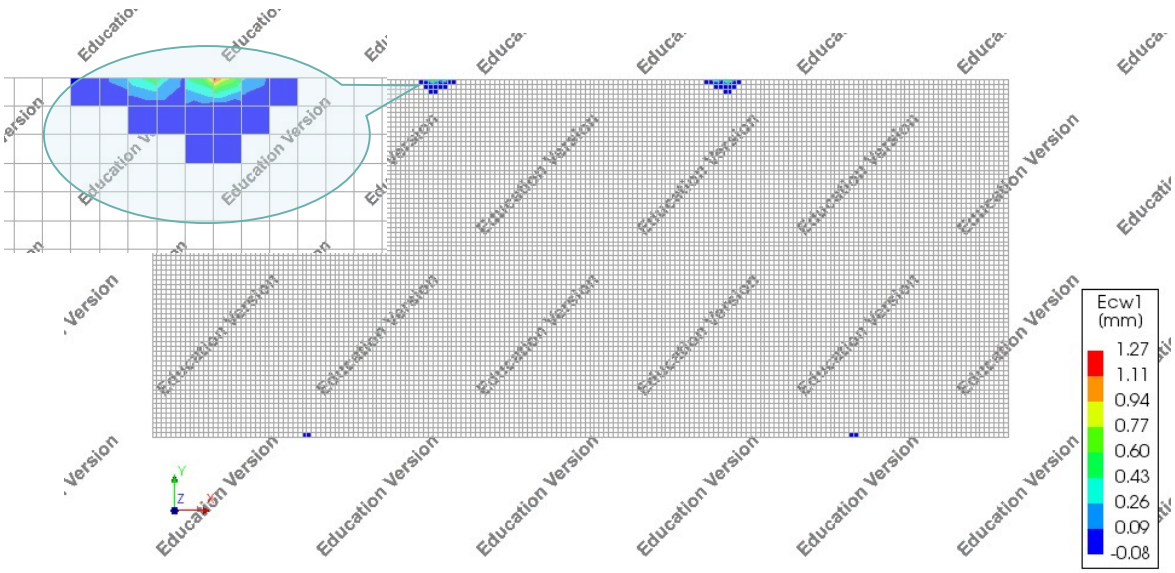

Figure 2.44: The crack width of FEM model for shear beam simulation.

Summary of FEM analysis

From the above, the FEM analysis are not only carried to make the comparison with existing test, but also simulation and predict the behavior of glass beams in different material properties or in various geometries. To digital the maximum reaction force and corresponding displacement for each model, the table 2.24 exhibits the relative data. Based on these simulation, the relative results are in consistence with the chemical composition analysis, and the test simulation certified that the simulation results is rational. It is reasonable to regard the structural behavior of recycled float glass is predictable.

	Test simulation	**Original float glass simulation**	**"Stand up" simulation**	**"Stand up" simulation with original float glass**	**Shear beam simulation**
Material	Recycled mixture float glass	Original float glass	Recycled mixture float glass	Original float glass	Recycled mixture float glass
Maximum reaction force (N)	1600.22	1248.18	4866.05	3840.54	43311.73
Corresponding displacement (mm)	0.86	0.59	0.28	0.21	0.15

Table 2.24: The conclusion of maximum reaction force and maximum displacement for all simulations.

Part 3 Finalization

From this part, the discussion and conclusion of this thesis will be illustrated in order to make a summary and develop the possibilities of this topic in further researches. In the discussion chapter, the feasible recycling and manufacture procedure will be proposed and two probable applications in structural view will be presented. Afterwards, the conclusion of this thesis will be made following by the suggestions in the further development. This part will describe the meaning of this topic and literally fulfil the objectives which were proposed at the beginning.

Chapter 7 Discussion

Based on the test and analysis from the former chapters, the recycled float glass has been proved of feasible application in structural component. Therefore, it is necessary to have forward-looking in the practical application of recycled float glass. This chapter will illustrates the applicability of recycled float glass in three aspects, including the application integrated with steel, the structural arrangement of glass beam as well as the industrial recycling and manufacturing procedure. All of the aspects will discussed based on the existing glass structural projects or industrial realities. The structural stability, the economy and the sustainability are three significant prerequisite of the discussion of future development in recycled float glass.

7.1 Industrial recycling and manufacturing process

Considering the application of recycled float glass element in industrial reality, the recycling process should be taken into account in the first position. As demonstrated in chapter 1, the dominant resource of float glass is window glass from building industry. In analogy with the mature recycling process of glass bottles, the recycling of waste float glass can share the same procedure. Through setting recycling stations, where the public can through their personal waste float glass to. Then the recycling company can collect and sort the float glass from other wastes, such as adhesives or paper labels, following by batching them and transfer them to the production factory. In spite of the recycling form individuals, a more intelligent recycling method can be realized by float glass manufacturer itself. For one reason, since the manufacturer knows the chemical constitution and material properties of the original glass, the recycling of waste float glass and the prediction of the mechanical properties of the final products will be easier for the manufacturer. For another reason, when a building requiring the change of facade or window glass, it is more convenient to contact the manufacture companies to recycle a large amount of waste float glass. It saves more time and money by skipping the link of the recycling company.

In this project, the manufacturing method of recycled float glass has been adopted as the kiln-casting method, by placing the waste glass cullets orderly in the crystalcast mould to form the shape. The casting process reaching the highest temperature at 1120 degrees. However, in the industry manufacture, it is not wise to use kiln casting and crystalcast mould for the shape creation. Since the dimension of the kiln limits the dimension of the structural components. Even though there is enough space for the kiln to cast structural component, the nonuniform temperature distribution inside the kiln is unavoidable, which will affect the homogeneity of recycled float glass. Meanwhile, in the economic consideration, the production process of the lost wax mould is too complicated and owing to the disposable character, the cost will significantly increase with this mould adoption.

Whereupon, the hot-forming method instead of kiln-casting is suggested by the author, integration with the permanent steel mould. There are several advantages based on the hot-forming method in industrial application, for instance, the environmental-friendly and economical for the employment of permanent mould, which can be consist of steel plates with different dimensions. It is also possible to combine the mould with different combinations of steel plates, to create an adjustable mould. Besides, as mentioned in the former chapters, there is nonuniform distribution of chemical composition along the height of the recycled float glass specimens, which might introduce the variant mechanical behavior of the components. While through the hot-forming method, the molten glass will be fluxible with intensively mixing so that the chemical compositions can be distributed more uniformly. Still, there are drawbacks derived from the higher casting temperature of hot-forming, at around 1200 degrees, which is less economical than the kiln-casting. But integrating with the waste of disposable

mould, the kiln-casting is less favour than the hot-forming method in the industrial application. What's more, in the advantage of the hot-forming casting method, the final products can be formed into different shapes or various dimensions.

According to the investigation of existing glass recycling industry, there are plenty of companies already started recycling waste float glass. But they are aiming at mixing the recycled end products, which produced by sorting, washing, crushing and examinations, with raw materials to make a new float glass. Not all float glass is recyclable such as hard coating glass, and the required temperature for new float glass is the same for the common manufacture temperature. It is not sustainable enough and the float glass is not recycled hundred percent as well. To realize the recycling of waste float glass, referencing the process of existing float glass recycling, the suggested recycling and manufacture process can be described as the following steps, together with flow diagram:

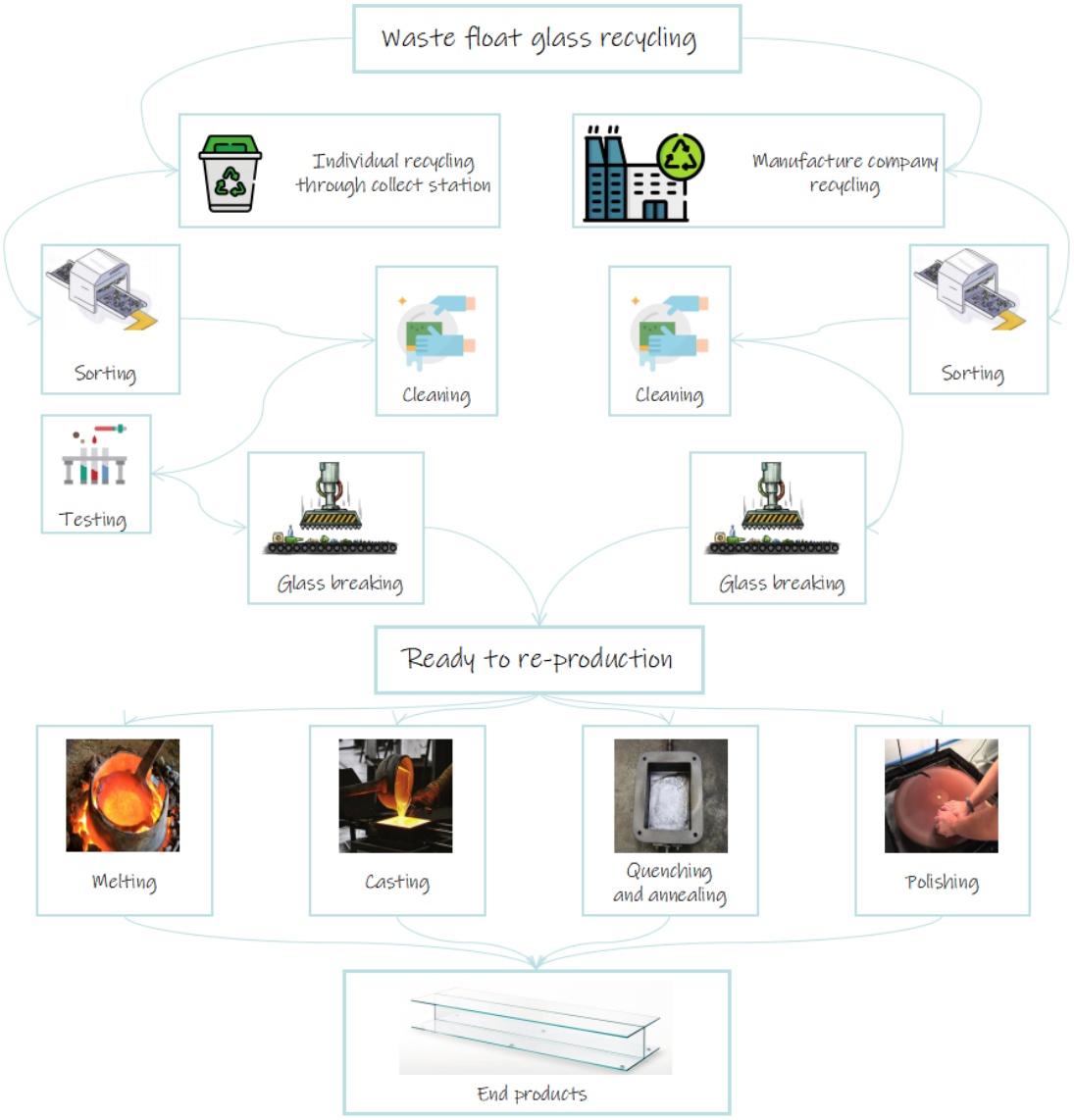

Chart 3.1: The suggested flowchart from recycling to reproducing of recycled float-glass beam.

7.2 The application integrated with steel

Owing to the brittle material property, the glass will break without curve of the element or initial cracks as an indicator. It nicely obeys the linear elastic behaviour until the crack appears, following by the sudden failure. However, in the view of the safety mechanism, the redundancy of the structure is unavoidable. There are many attempts for glass beam, such as the PVB laminated tempered glass beams in the Glass Museum in England, which was mentioned in the literature review. Besides, the glass beam in Apple store in New York is adopted as sentry glass, which is also a foil laminated glass panels together. However, in this project, under the premise of sustainability, the lamination or adhesives are abandoned, so that the glass can be easily recycled again. Deriving from the 10 to 15 times in compression than in tension of annealed float glass, the combination with steel, which has the advantage in tension, is taken into consideration. [38]

Figure 3.1: The PVB laminated tempered glass beams in Glass Museum in Kings Wingford (left), the sentry glass beam in Apple Store in New York (right).

Generally, there are two types of the combination by glass and steel referring to the existing literature. One of the integrations located in adding the reinforcement into glass beam, for example, the T-section beam in F.A. Veer's paper [39], which consists of glass sheets and prestressed stainless steel rob, presented in the figure below. The prestressed steel rob will help the glass beam in bending strength and load-bearing capacity through carrying the tensile forces after the glass has cracked.

Figure 3.2: The cross section (left) and the prototype (right) of T-section beam, from [40].

Apart from the T-section prestressed glass, more attempts are given by Louter [41], providing four alternative methods to transfer the post-tensioning force through steel end plate or aluminium wedges. Based on the tests, a safe failure mechanism can be obtained with the benefit from steel tendons, and the brittle behaviour of float glass can be avoided. As shown in the following figures, the glass beams are integrated together even though the cracks occurred.

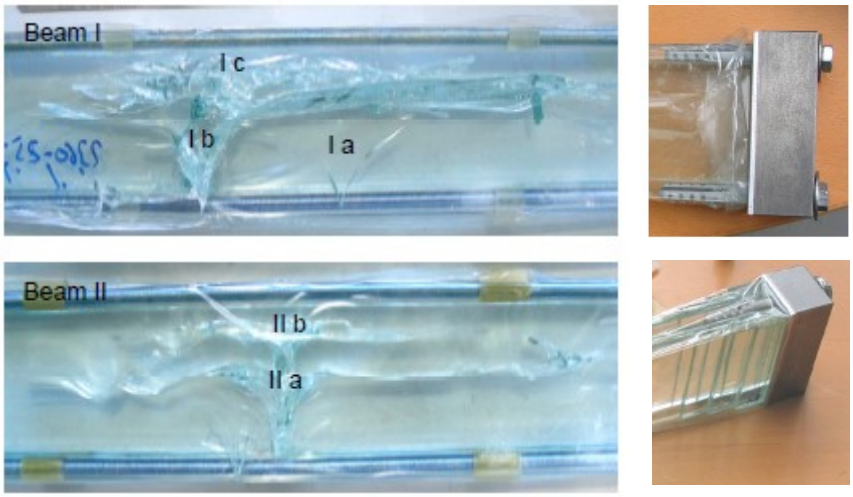

Figure 3.3: The fracture patterns in bending test (left), with corresponding prestressed method.

From all above, there are two concept created based on the references. The first idea is shown in figure 3.4, using the steel plate to fix the top area and bottom area of the recycled float glass. Once the recycled float glass reaching break strength, the broken glass can be blocked by the steel plate, meanwhile, the steel plate can carry the stress so that this structural component can withstand higher loads. Beyond that, by dividing the recycled float glass component into several sheets, this step can be realized in the casting period, secondary safety guarantee can be provided, as shown in figure 3.5.

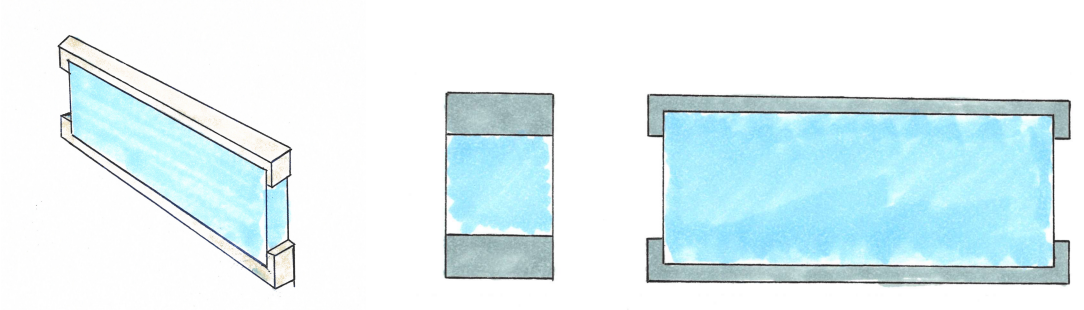

Figure 3.4: The first concept of integrating recycled float glass with steel plate.
From left to right: 3D view; cross section view; front view.

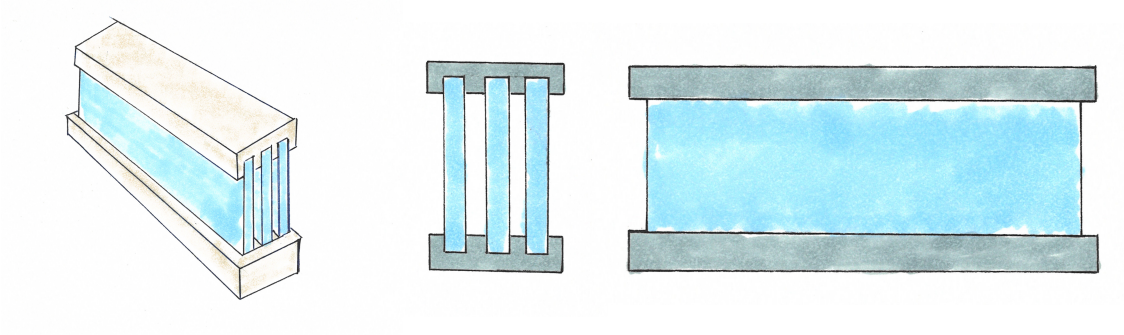

Figure 3.5: The first concept of integrating divided recycled float glass with steel plate.
From left to right: 3D view; cross section view; front view.

The other concept comes from the post tension glass beam. Profiting from the freedom in the dimension of recycled float glass component by the hot forming casting methodology, it is possible to produce a component with a reserved place for tendons. As presented in figure 3.6, the corresponding mould and end products with tendons are shown. Referring to the four-point bending test in the project, the cracks and flaws on the surface, which might be owing to the dimension and shapes of components, will affect the loading capacity of recycled glass beam. Therefore, it is wise to limit the dimension of single elements, instead, the tendons can not only working as a tensile resistance component but also connecting the recycled float glass elements to form a complete beam.

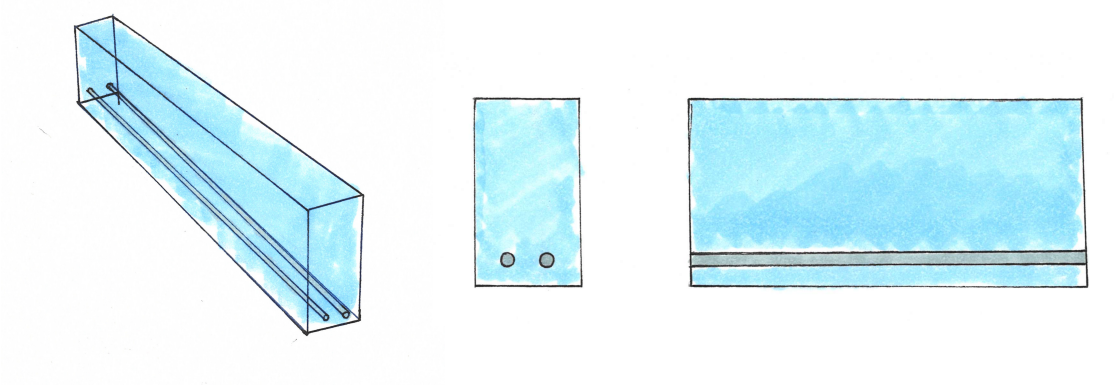

Figure 3.6: The second concept of integrating divided recycled float glass with steel plate.
From left to right: 3D view; cross section view; front view.

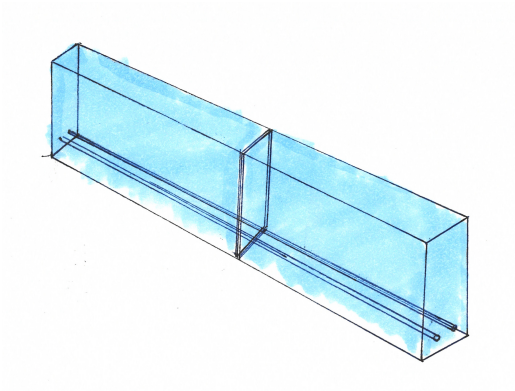

Figure 3.7: The concept of connecting recycled float glass components into complete beam, through tendons.

These two concepts are proposed based on the literature review and the manufacture of recycled glass samples in this project. The mechanical properties which derived from the test are also one of the references. The exact dimension of the components required further calculation and optimization, which can be done by computational optimization. The attaching area between glass and tendons requires special measurement to avoid concentrate force, which can be studied from Glass Bridge in Green Village. Besides, the connection between glass components should also be treated specially to avoid influential factors from surface defects. Even though the safety mechanism can be reached with the help of steel, an extra attention should be paid to the redundancy in the allowable loading strength of recycled float glass made by the casting method.

7.3 The structural arrangement of glass beam

In spite of the creation of glass beam itself, it is possible to apply different arrangement of the beam to provide secondary safety mechanism. Inspirations origins from the combination method of oriental wooden structure, which connected without adhesives or nails. In consideration of no lamination and adhesives, the mortise and tenon joint can be taken as references. Shown in the figure below are several ancient connection methods of timber structure in China. The left subfigure presents two methods for wooden beam connections while the right subfigure showing the beam and column connection.[42]

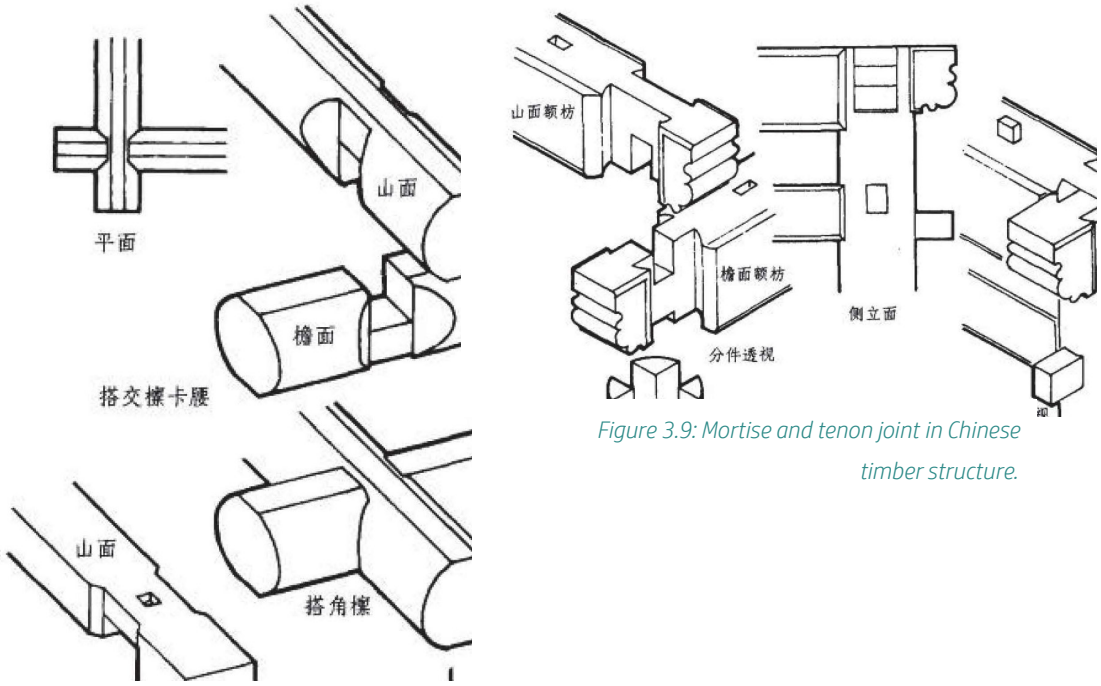

Figure 3.9: Mortise and tenon joint in Chinese timber structure.

Except for the ancient timber structure, there are modern attempts which express compact architecture concept in timber structure connections. Such as the timber structure for Yusuhara Wooden Bridge Museum, figure 3.10. In old days, the remarkable wooden structure is usually used for temples or towers which have slopes or curves. Instead, in modern expressions, the timber elements are connected in the horizontal and vertical layout. The Yusuhara Wooden Bridge Museum place the wooden beams in vertical and horizontal direction and stack them by layers. It is worth mentioning that on the upside of the bottom layer, there is small groove leave for the supporting of upper wooden beams laid in another direction. Comparing the material property of wood and glass, the wooden structural components perform better than glass in tensile behaviour. Thus, in the analogy with the wooden structure, the bending moment existing in the glass beam should be paid with special attention. Even so, integrating with the futuristic sense of the glass and the sustainable connection, it is still suitable to adopt this mortise and tenon joint for glass beam connection.

Figure 3.10: The timber structure of Yusuhara Wooden Bridge Museum, designed by Kengo Kuma, Japen.

Based on all the existing timber structures, combining with the connection within glass components, there is an idea, assisting by figure 3.11, in an arrangement of recycled glass beams. In order to compensate the brittle break failure of recycled float glass, is it essential to have enough guarantee in both load capacity and the secondary safety mechanism when one component failure occurred. In this beam system, there are regular upwards grooves in the beams which placed in x direction, meanwhile, for the beams places in z direction, there are corresponding downward grooves so that the two layers of beams can be steadily connecting together. By providing the two layer of glass beams, the safety mechanism can be satisfied and the loading capacity of the beam system can be strengthened. Moreover, with the grooves, the height of the beam system can be decreased in the premise of load capacity guarantee. However, there is still plenty of further investigation needs to be carried, such as the detailed dimension of this concept which requires precious calculation and optimization. The special treatment is also required in the right angle of the grooves, because of the influence by the defect of the edges in the glass material. [44][45]

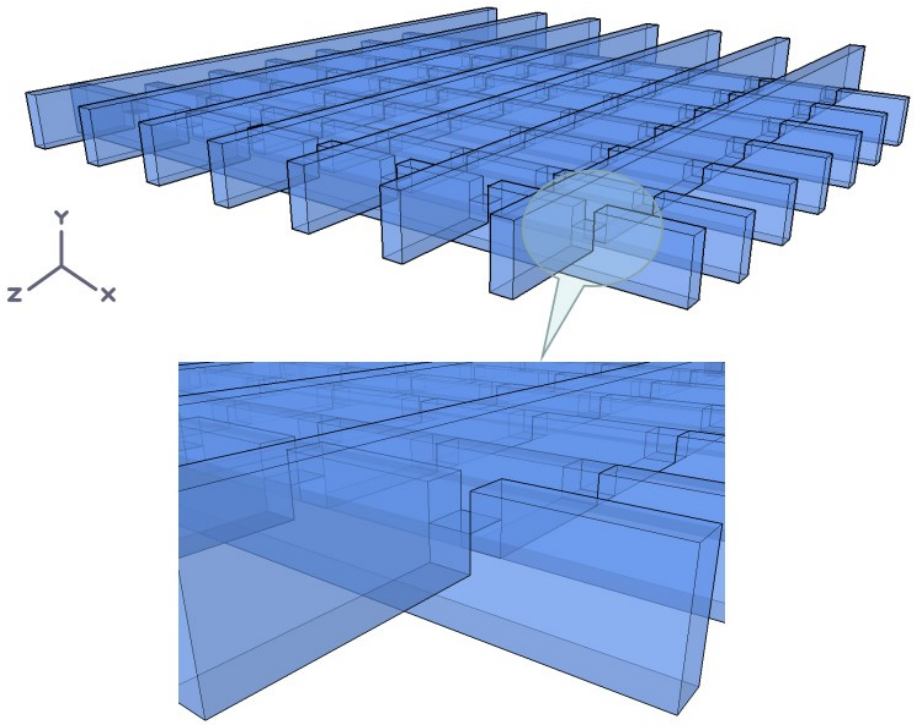

Figure 3.11: The concept on arrangement of recycled float glass beams.

Chapter 8 Conclusion

At the end of this project, the conclusion of this thesis will be summarized, along with the suggestions for further investigation. The conclusions will draw from each phase as the final result of this thesis, to accomplish the objectives raised in the beginning period. This research is not complete enough within the glass recycling field, even for float glass. There are possibilities, innovations and also difficulties exists in the glass recycling area, whereas, it is worthy to marching on.

8.1 Conclusion

Glass casting experiments

◎ Depending on the finished products, the float glass is recyclable as separate categories.

The final products are well-cast without any flaws on the surface, and the air bubbles are not likely to be captured during casting. Integrating with proper firing schedule, avoiding the crystallization danger zone, the crystallization will likely not to appear, although tin participates in the original material.

◎ Coated float glass is possible to be recycled without sorting from different coating types.

Referring to the recycled glass beams, even though there are flaws and tiny cracks in the mould-touching surface, the material is homogeneous inside the beam, which can be visualized through the clean break surface. The flaws and bubbles are mainly causing by the dimension of the products, which should be paid extra focus on.

◎ Glass tints will not influence the properties during kiln-casting recycling.

Through the comparison among recycled float glass origins from clean glass and tinted glass, the colour of recycled products is indistinguishable. With the help of the XRF test, the chemical composition who endow the glass with colour has just taken a small portion. Therefore, it is rational to conclude that the tints will not affect the mechanical properties of recycled float glass.

Young's modulus test

◎ The recycling process through casting will not decrease Young's modulus significantly.

By comparing the value of Young's modulus for original and recycled float glass, Young's modulus has a slight decrease after recycling, which will not make a considerable influence of the structural behaviour. The Young's modulus of recycled float glass is still able to be regarded as a great advantage in the structural application.

◎ The value of Young's modulus will not be decided by only one of chemical composition content.

Although the relationship between Young's modulus and the weight percentage of aluminium, as well as the metal oxide and alkali earth content of the recycled float glass, are consistent with the theoretical relations, the increase of silica dioxide and the decrease of alkali has not improved the Young's modulus of recycled hard coating glass. It is not persuasively to judge Young's modulus only by

one of the content, the weight percentage of chemical constitutions works together with coefficients to influence the Young's modulus.

CTE test

◎ Recycling through kiln-casting will not have a negative influence in CTE value of float glass.

Comparing the CTE value of original normal glass and recycled normal float glass, which is derived through the same test condition, the CTE value decreased after recycling. It is logical to have a deduction that recycling through casting may decrease the CTE value of float glass, basing on the experiment result.

◎ The CTE value of recycled float glass can not be decided just by chemical composition analysis.

According to the analysis in chapter five, the relation between chemical constitution and thermal expansion is not always in agreement. These results are connected with the coefficient of chemical composition, which analogy to the Young's modulus analysis. Besides, the nonuniform distribution of chemical element in the recycled float glass can be another correlation.

Fracture strength test

◎ The recycled mixture float glass may have a higher Young's modulus than original float glass.

Integrating with the four-point bending test and FEM analysis, the Young's modulus of the recycled mixture float glass has been discussed together with the XRF results. Comparing with the original glass, there is the possibility that the recycled mixture float glass has a higher Young's modulus than the resource material, based on the load-displacement curve.

◎ The recycled float glass is applicable as a structural beam.

Through the material properties, which are tested from the experiments, the main structural properties are obtained, shown in table 3.1. Comparing with original float glass, the structural property does not have substantial drawbacks. Therefore, part of the foundation of further study about recycled glass in the structural area has been established. More possibilities can be provided based on the result of this thesis.

Young's modulus	Density	Thermal	Fracture strength	Flexural stress
MPa	Kg/m^3	/℃ (25~80℃)	N	N/mm^2
66345.9	2485.1	5.53	791.53	51.94

Table 3.1: The main structural properties for recycled coated float glass.

8.2 Research expectation

◎ Considering the polarized result of volume recycled samples, and good performance in a structural perspective, the recycled float glass is able to be used as volumetric structural elements such as bricks in a relative volume. The polarized photos show good quality is residual stress, and the structural performance is close to the common glass. In a consideration of sustainability and economy, the recycled float glass is a good choice.

◎ Depending on the XRF test, the silica dioxide content for the surface of recycled float glass is extremely high, more than 90% per cent, which can be considered for the application in super high compression conditions or thermal resistance glass surface. However, the thickness of this high-silicate surface has to be defined beforehand.

◎ For the glass beam, the main question mark exists in the brittle mechanism, which breaks without any foretaste. The connection of recycled glass beam with steel plate or reinforcement without adhesive contamination is a promising field. As mentioned in chapter 7, a further investigation can be placed in the application of volumetric casting glass components in the structural beam, including the concept of combination with steel or the idea in imitative mortise and tenon joint in glass beam connections.

◎ Taken the industrial application into consideration, the exact temperature for melting point and softening point need to be clarified. In that case, the hot-forming casting process is possible to continue.

◎ Since in this thesis, the mixture of float glass is coming from the same company, which has similar dominant chemical composition. However, the waste float glass, in reality, is probably a mixture from different glass brand, when taken personal recycling into consideration. Therefore, it is interesting to check the final products which recycling from mixtures from different glass brand. There might be a range of the difference in the chemical composition of waste float glass.

Appendix

Appendix 1 Firing schedule

Step	Ramp	Temprature	Dwell	Total time consumption
	℃/hour	℃	hr	hr
1	50	25	2.7	2.7
		160	3	5.7
2	50	700	10.8	16.5
		700	4	20.5
3	50	1120	8.4	28.9
		1120	8	36.9
4	-160	623	3.1	40
		623	3.5	43.5
5	-20	571	2.6	46.1
		571	0	46.1
6	-20	560	0.55	46.65
		560	3.6	50.25
7	-20	555	0.25	50.5
		555	14	64.5
8	-1	525	30	94.5
		525	0	94.5
9	-2	505	10	104.5
		505	0	104.5
10	-3	455	16.67	121.17
		455	0	121.17
11	-6	370	14.16	135.33
		370	0	135.33
12	-25	25	13.8	149.13
		25	0	149.13

Table a.1: The firing schedule of hard coating glass recycling through kin-casting.

Step	ramp	Temperature	Dwell	Total time consumption
	℃/hour	℃	hr	hr
1	50	75	1.7	1.7
		160	3	4.7
2	50	700	10.8	15.5
		700	2	17.5
3	50	1120	8.4	25.9
		1120	10	35.9
4	-160	623	3.1	39
		623	4	43
5	-20	571	2.6	45.6
		571	0	45.6
6	-20	560	0.55	46.15
		560	10	56.15
7	-6	555	0.83	56.98
		555	14	70.98
8	-1	525	30	100.98
		525	0	100.98
9	-2	505	10	110.98
		505	0	110.98
10	-3	455	16.67	127.65
		455	0	127.65
11	-6	370	14.16	141.81
		370	0	141.81
12	-25	25	13.8	155.61
		25	0	155.61

Table a.2: The firing schedule of glass beam kiln-casting.

Appendix 2 Young's modulus calculation

	Sample 1 Recycled dark soft coating	Sample 2 Recycled light soft coating	Sample 3 Recycled normal float	Sample 4 Recycled hard coating
Length (m)	0.157	0.155	0.155	0.1535
Height (m)	0.045	0.045	0.044	0.0466
Width (m)	0.035	0.035	0.035	0.039
Calculated volume (m^3)	0.000247275	0.000244125	0.0002387	0.000278971
Volume (m^3)	0.00025	0.00025	0.00025	0.00026
Average volume (m^3)	0.000248638	0.000247063	0.00024435	0.000269485
Weight (kg)	0.60162	0.62539	0.61193	0.64657
Density (kg/m^3)	2419.667186	2531.302808	2504.317577	2399.276102
Time of sound travle through length (s)	0.0000295	0.000031	0.000029	0.000029
Sound speed travle through length (m/s)	5322.033898	5000	5344.827586	5293.103448
Young's modulus (N/m^2)	68534761818	63282570200	71541295830	67220384462
Young's modulus (GPa)	68.53	63.28	71.54	67.22
Average Young's modulus (GPa)	66.35			
Average density (Kg/m^3)	2485.1			

Table a.3: The table of Young's modulus calculation.

Appendix 3 Screenshot of CTE test

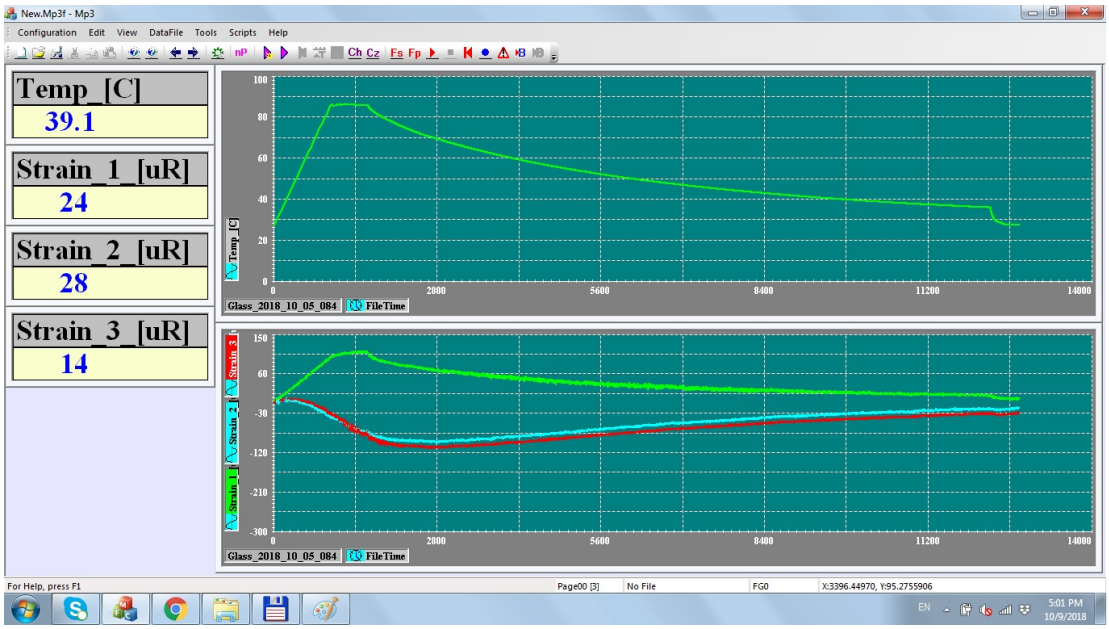

Figure a.1: The screenshot of CTE test 1, samples including two recycled normal float glass specimens.

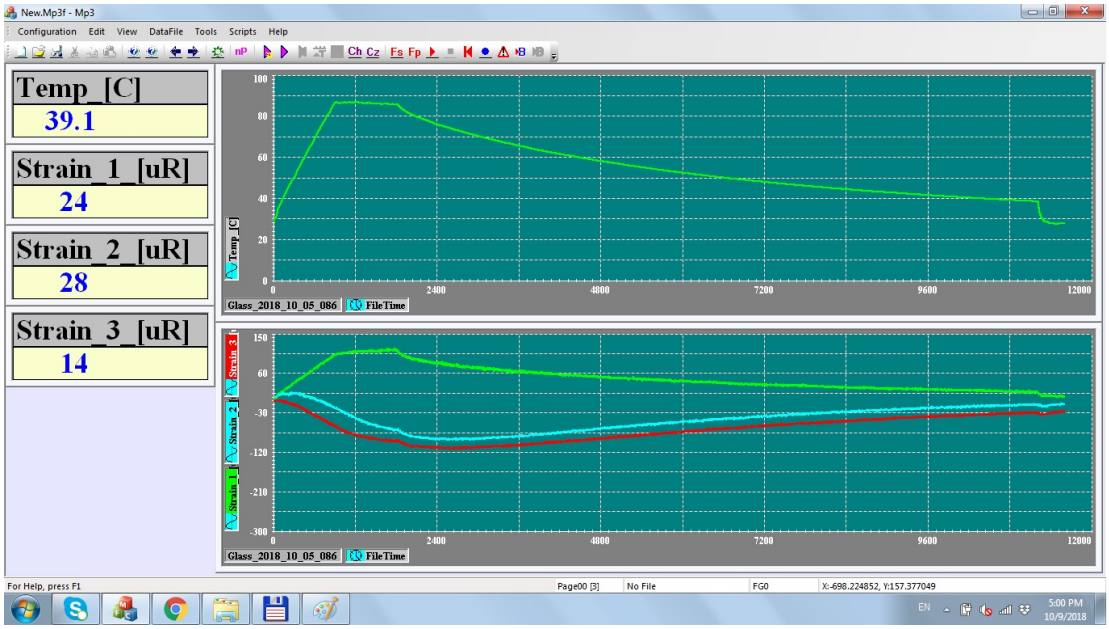

Figure a.2: The screenshot of CTE test 2, samples including recycled normal float glass specimen and recycled hard coating glass specimen.

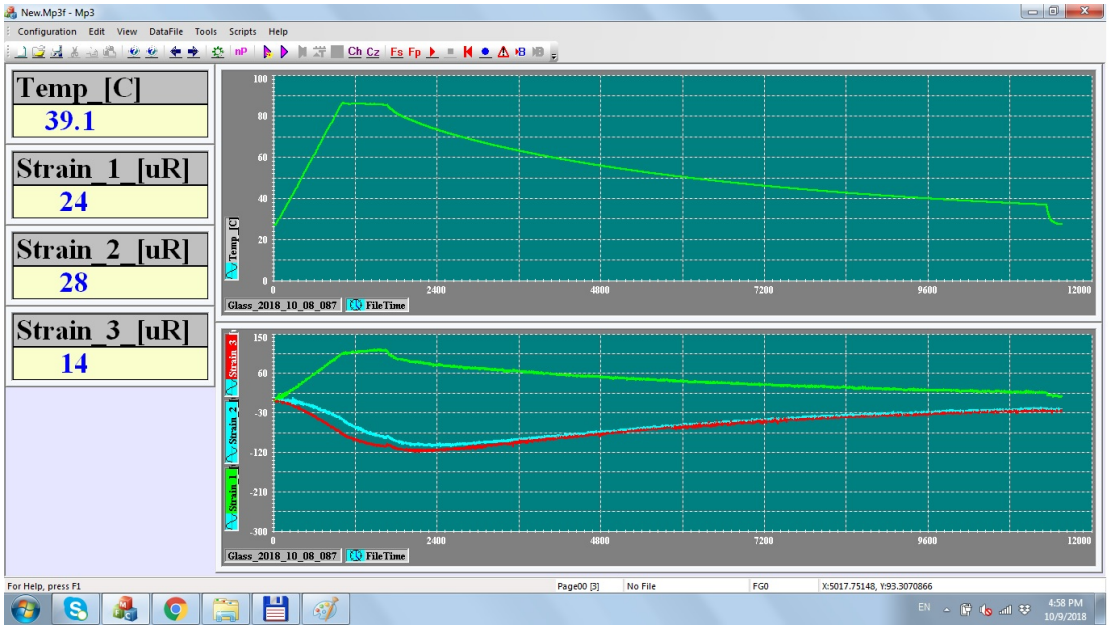

Figure a.3: The screenshot of CTE test 3, samples including two recycled normal float glass specimens.

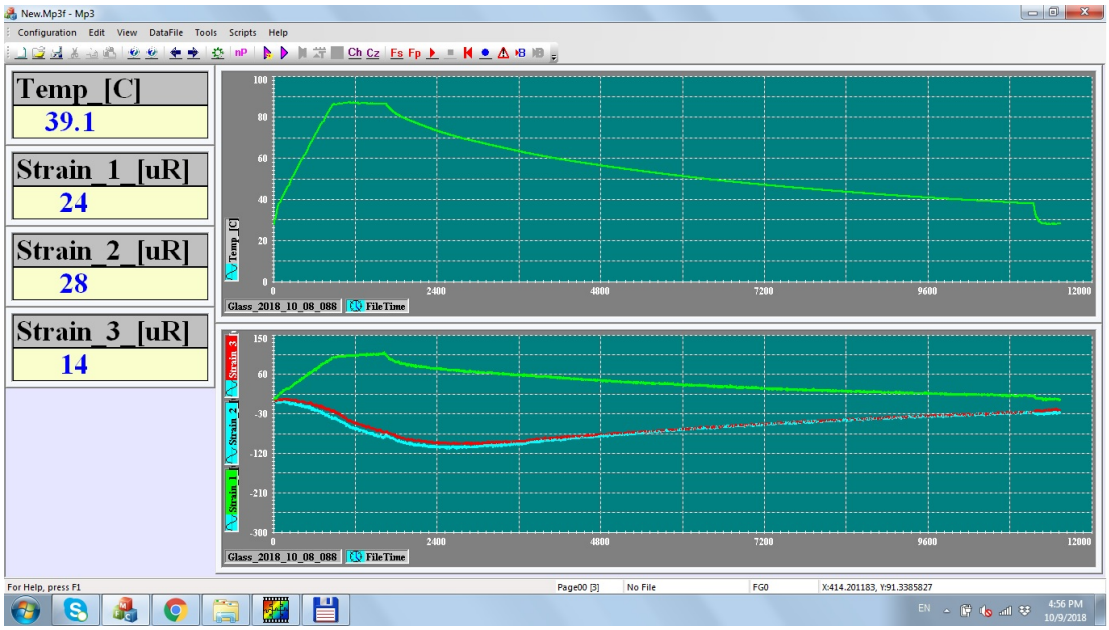

Figure a.4: The screenshot of CTE test 4, samples including recycled dark soft coating glass specimen and recycled light soft coating glass specimen.

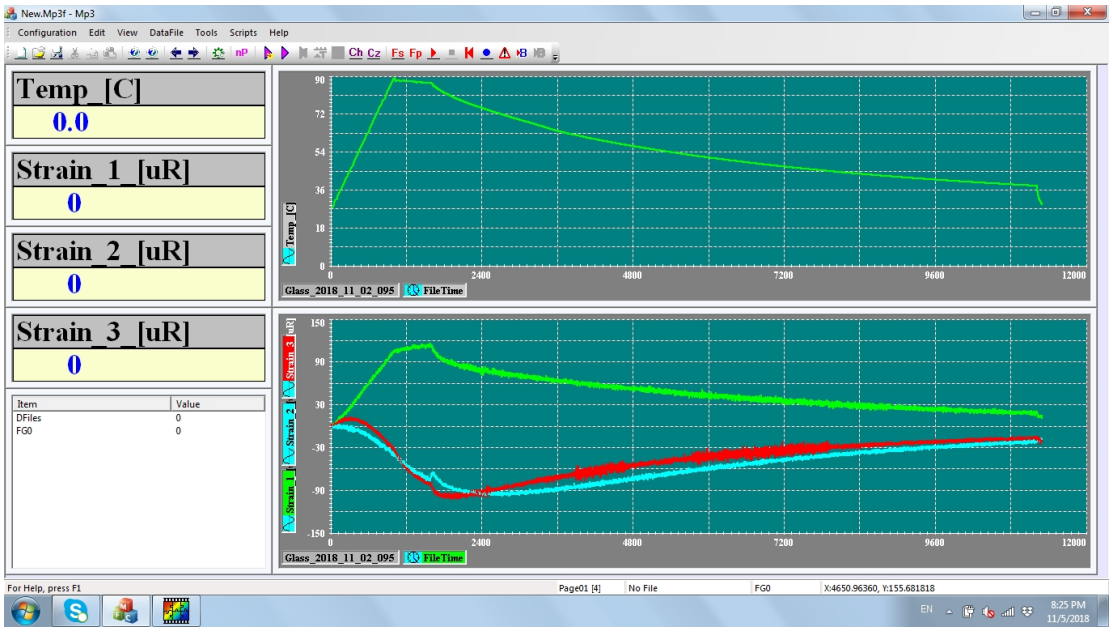

Figure a.5: The screenshot of CTE test 5, samples including recycled hard coating glass specimen and original normal float glass specimen.

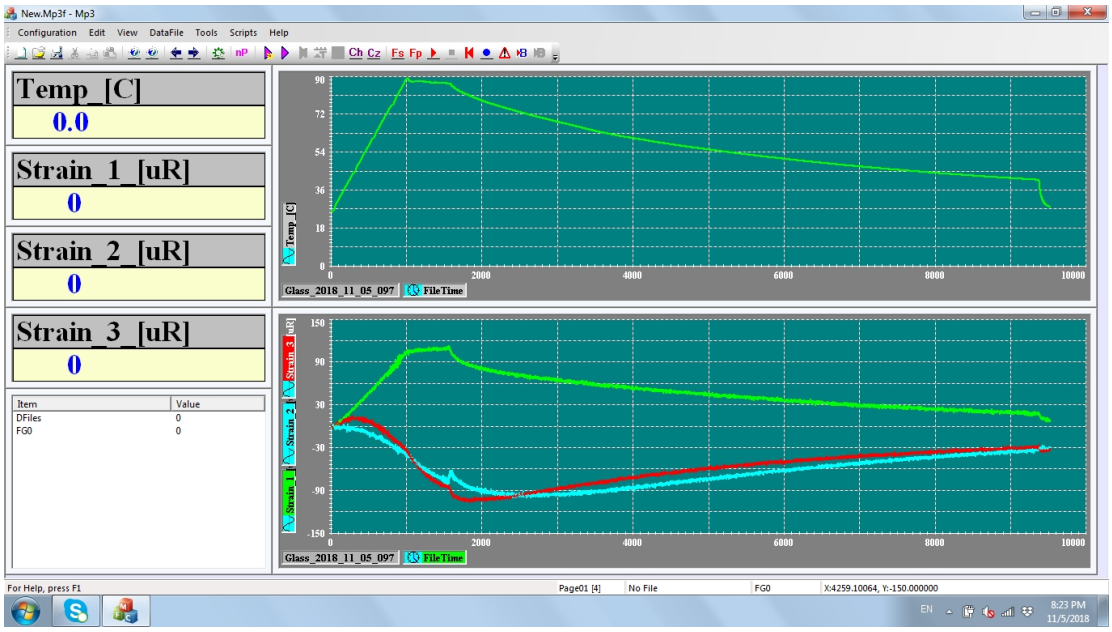

Figure a.6: The screenshot of CTE test 6, samples including recycled hard coating glass specimen and original normal float glass specimen.

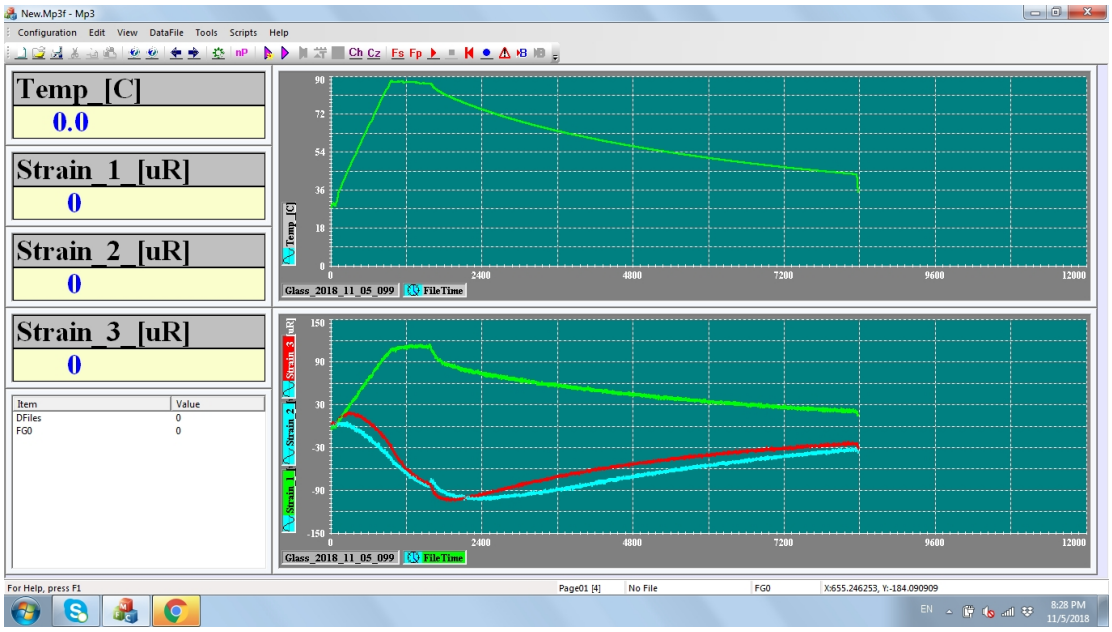

Figure a.7: The screenshot of CTE test 7, samples including recycled hard coating glass specimen and original normal float glass specimen.

Appendix 4 CTE calculation

	Highest temperature	Lowest temperature	Highest strain	Lowest strain	Delta temperature	Apparent strain highest temperature	Apparent strain lowest temperature	Corrected highest strain	Corrected lowest strain	$\alpha'(\alpha_c)$	α
steel 1	86.642158	27.579338	116.293144	0.624563	59.06282	20.4754954	6.58308501	192.593473	-11.976629	3.46360202	
steel 2	86.457427	25.637192	112.892268	-1.526696	60.820235	20.5245394	5.02921941	185.659134	-13.177390	3.26924952	
steel 3	86.455865	27.440727	115.38942	-2.983989	59.015138	20.5249518	6.47466925	190.677580	-19.011903	3.55314739	
specimen 1	86.642158	27.579338	83.135816	0.485726	59.06282	20.4754954	6.58308501	125.947244	-12.255691	2.33993121	5.80353323
specimen 2	86.457427	25.637192	83.41222	0.069388	60.820235	20.5245394	5.02921941	126.404238	-9.9692611	2.24223893	5.51148846
specimen 3	86.455865	27.440727	82.095158	-0.693896	59.015138	20.5249518	6.47466925	123.756114	-14.408816	2.34117779	5.89432519
Average CTE for original normal float glass											**5.7364**

Table a.4: The calculation table of CTE for original normal float glass.

	Highest temperature	Lowest temperature	Highest strain	Lowest strain	Delta temperature	Apparent strain highest temperature	Apparent strain lowest temperature	Corrected highest strain	Corrected lowest strain	α '(α_c)	α
steel 1	86.642158	27.579338	116.293144	0.624563	59.06282	20.4754954	6.58308501	192.593473	-11.976629	3.463602	
steel 2	86.457427	25.637192	112.892268	-1.526696	60.820235	20.5245394	5.02921941	185.659134	-13.177390	3.269249	
steel 3	86.455865	27.440727	115.38942	-2.983989	59.015138	20.5249518	6.47466925	190.677580	-19.011903	3.553147	
specimen 1	86.642158	27.579338	76.141789	2.567935	59.06282	20.4754954	6.58308501	111.889250	-8.0704515	2.031052	5.494654
specimen 2	86.457427	25.637192	67.187131	-0.416419	60.820235	20.5245394	5.02921941	93.7918090	-10.945733	1.722083	4.991333
specimen 3	86.455865	27.440727	83.361352	-0.55523	59.015138	20.5249518	6.47466925	126.301164	-14.130097	2.379580	5.932727
Average CTE for recycled hard coating glass											**5.4729**

Table a.5: The calculation table of CTE for recycled hard coating glass.

	Highest temperature	Lowest temperature	Highest strain	Lowest strain	Delta temperature	Apparent strain highest temperature	Apparent strain lowest temperature	Corrected highest strain	Corrected lowest strain	α '(α_c)	α
steel	86.414000	27.862433	110.523230	-0.208166	58.551567	20.5359923	6.80332686	180.874347	-14.093100	3.32984	
specimen light	86.414000	27.862433	72.476467	0.901552	58.551567	20.5359923	6.80332686	104.400354	-11.862567	1.98565	**5.3154**
specimen dark	86.414000	27.862433	84.380358	-1.457093	58.551567	20.53599237	6.803326864	128.3271749	-16.6034439	2.47526	**5.8051**

Table a.6: The calculation table of CTE for recycled light soft coating and recycled dark soft coating glass.

	Highest temperature	Lowest temperature	Highest strain	Lowest strain	Delta temperature	Apparent strain highest temperature	Apparent strain lowest temperature	Corrected highest strain	Corrected lowest strain	α '(α_c)	α
steel 1	85.650111	26.883334	112.610688	-2.359356	58.766777	20.7326867	6.03485035	184.674782	-16.872354	3.42961019	
steel 2	85.650111	26.883334	112.610688	-2.359356	58.766777	20.7326867	6.03485035	184.674782	-16.872354	3.42961019	
steel 3	85.785498	28.374457	117.119596	2.636902	57.411041	20.6984841	7.19763923	193.806434	-9.1670818	3.53544393	
steel 4	85.859692	27.517864	115.868125	0.000000	58.341828	20.6796202	6.53504962	191.328894	-13.135449	3.50459269	
steel 5	85.859692	27.517864	115.868125	0.000000	58.341828	20.6796202	6.53504962	191.328894	-13.135449	3.50459269	
Specimen 1	85.650111	26.883334	72.722117	3.88934	58.766777	20.7326867	6.03485035	104.498754	-4.3124758	1.85157730	5.28118749
Specimen 2	85.650111	26.883334	80.259208	3.676222	58.766777	20.7326867	6.03485035	119.648307	-4.7408429	2.11665769	5.54626788
Specimen 3	85.785498	28.374457	67.7228	-1.666899	57.411041	20.6984841	7.19763923	94.5188748	-17.817721	1.95670719	5.49215112
Specimen 4	85.859692	27.517864	79.184223	-1.527985	58.341828	20.6796202	6.53504962	117.594251	-16.206699	2.29339662	5.79798931
Specimen 5	85.859692	27.517864	102.329025	0.763049	58.341828	20.6796202	6.53504962	164.115303	-11.601721	3.01185326	6.51644595
Average CTE for recycled normal float glass											5.5294

Table a.7: The calculation table of CTE for recycled normal float glass.

Appendix 5 Break stress calculation

	F_{Break}	a	b	h	σ_{max}
	N	mm	mm	mm	N/mm^2
Specimen 1B	663.5240479	60	40	12	41.47025299
Specimen 1A	856.1168823	60	40	12	53.50730515
Specimen 1C	765.6992798	60	40	12	47.85620499
Specimen 2A	880.9678955	60	39	12	56.47230099
Specimen 2B	782.5407104	60	36	12	54.34310489
Specimen 2C	800.3280029	60	37	12	54.07621641
Average break stress					**51.29**

Table a.8: The calculation table of break stress for recycled glass beams.

List of table

List of chart

List of figure

References

[1] Rasmussen, Seth C. *Modern Materials in Antiquity: An Early History of the Art and Technology of Glass*. American Chemical Society, 2015.

[2] White, Rachel Lynn. "Glass as a structural material." (2007).

[3] Larson, Katherine Anne. "From Luxury Product to Mass Commodity: Glass Production and Consumption in the Hellenistic World." (2016).

[4] Powell, Ken, ed. *The Great Builders*. Thames & Hudson, 2011.

[5] Nascimento, Marcio Luis Ferreira. "Brief history of the flat glass patent–Sixty years of the float process." *World Patent Information* 38 (2014): 50-56.

[6] Kumar, R. V., and J. Buckett. "Float Glass." (2014).

[7] Oldenziel, Ruth, and Milena Veenis. "The glass recycling container in the Netherlands: symbol in times of scarcity and abundance, 1939–1978." *Contemporary European History*22.3 (2013): 453-476.

[8] Earthsfriends.com. https://www.earthsfriends.com/why-recycling-important/. Published 2018. Accessed November 16, 2018.

[9] Glass Recycling Facts. The Balance Small Business. https://www.thebalancesmb.com/facts-about-glass-recycling-2877982. Published 2018. Accessed November 16, 2018.

[10] 5.2. Recycling: open-loop versus closed-loop thinking | EME 807:. E-education.psu.edu. https://www.e-education.psu.edu/eme807/node/624. Published 2018. Accessed November 16, 2018..

[11] Bristogianni, T., et al. "Structural cast glass components manufactured from waste glass: Diverting everyday discarded glass from the landfill to the building industry." *Heron* 63.1/2 (2018).

[12] Wigginton, Michael, and Monica Pidgeon. "Glass in architecture." (1996).

[13] Xiaoxi Ma, Xian University of Architecture and Technology, The application of glass material in structural design, 2011 (in Chinese).

[14] Nijsse R. Glass in structures; promising developments. *IABSE Symposium Report*. 2013;101(1):1-7. doi:10.2749/222137813815776241

[15] Fu, Lei. *Glass beam design for architects: Brief introduction to the most critical factors of glass beams and easy computer tool*. University of Southern California, 2010.

[16] Oikonomopoulou, F., et al. "The potential of cast glass in structural applications. Lessons learned from large-scale castings and state-of-the art load-bearing cast glass in architecture." *Journal of Building Engineering* (2018).

[17] Ivo Sombroek, Structural Cast Glass, 2016

[18] Janis M. New Class! Introduction to Lost Wax Casting | Washington Glass Studio. Washingtonglassschool.com.http://washingtonglassschool.com/new-class-introduction-to-lost-wax-casting. Published 2018. Accessed November 16, 2018.

[19] Rees, J. S., P. H. Jacobsen, and J. Hickman. "The elastic modulus of dentine determined by static

and dynamic methods." *Clinical materials* 17.1 (1994): 11-15.

[20] Digilov, Rafael M. "Flexural vibration test of a cantilever beam with a force sensor: fast determination of Young's modulus." *European Journal of Physics* 29.3 (2008): 589.

[21] Achenbach, Jan. *Wave propagation in elastic solids*. Vol. 16. Elsevier, 2012.

[22] Ensminger, Dale. *Ultrasonics: Fundamentals, Technology, Applications, Revised and Expanded*. CRC Press, 1988.

[23] Guild, J. "A sensitive optical lever method for measuring the thermal expansion of small specimens." *Journal of Scientific Instruments* 1.7 (1924): 198.

[24] Mukhopadhyay, Anal K., and Dan G. Zollinger. "Development of dilatometer test method to measure coefficient of thermal expansion of aggregates." *Journal of materials in civil engineering* 21.12 (2009): 781-788.

[25] Micro-Measurements, Vishay. "Strain gage thermal output and gage factor variation with temperature." *1>< B+ LR> 1+] gbf] cY* 11054 (2010): 35-47.

[26] https://stewartengineers.com/docs/se-acuracoat-cvd.pdf. Published 2018. Accessed November 16, 2018.

[27] Zingoni, Alphose, ed. *Insights and Innovations in Structural Engineering, Mechanics and Computation: Proceedings of the Sixth International Conference on Structural Engineering, Mechanics and Computation, Cape Town, South Africa, 5-7 September 2016*. CRC Press, 2016.

[28] Zschimmer, Eberhard. *Chemical Technology of Glass: With 176 Figures and Sixteen Plates*. Society of Glass Technology, 2013.

[29] Varshneya, Arun K. *Fundamentals of inorganic glasses*. Elsevier, 2013.

[30] Kilinc, Erhan, and Russell J. Hand. "Mechanical properties of soda–lime–silica glasses with varying alkaline earth contents." *Journal of Non-Crystalline Solids* 429 (2015): 190-197.

[31] Valentich J. Thermal expansion of solids from −261°C to 173°C using strain gauges. *Cryogenics (Guildf)*. 1985;25(2):63-67. doi:10.1016/0011-2275(85)90105-5

[32] Gayevoy, A. V., and S. L. Lissel. "STRAIN READING CORRECTION FOR APPARENT STRAIN AND THERMAL EXPANSION COEFFICIENT OF MASONRY AND BRICK."

[33] White, G. K. "Thermal expansion at low temperatures of glass-ceramics and glasses." *Cryogenics* 16.8 (1976): 487-490.

[34] Karkhanavala, M. D., and F. A. Hummel. "Thermal expansion of some simple glasses." *Journal of the American Ceramic Society* 35.9 (1952): 215-219.

[35] Yuang Wang, The Coefficient of Thermal Expansion of Glass and the Relevance Chemical Composition, 1994 (in Chinese)

[36] Hertzberg, Richard W., Richard Paul Vinci, and Jason L. Hertzberg. *Deformation and fracture mechanics of engineering materials*. Vol. 89. New York: Wiley, 1996.

[37] Nyounguè, A., et al. "Fracture characterisation of float glass under static and dynamic loading." *Journal of Asian Ceramic Societies 4.4 (2016): 371-380.*

[38] Khorasani, Naimeh. Design principles for glass used structurally. Department of Building Science,

Univ., 2004.

[39] F A Veer, P.C.Louter, F.P.Bos, L.P.T. Schetters, Reinforced segmented float glass, a novel way to create safe transparent beams.

[40] Kozłowski, Marcin. "Hybrid glass beams. Review of research projects and applications." *ACEE Journal* 5.3 (2012).

[41] Louter, P. C., et al. "Post-tensioned glass beams." *Fracture of Nano and Engineering Materials and Structures nd* 597.8 (2006).

[42] Yao, Kan, H. T. Zhao, and H. P. Ge. "Experimental studies on the characteristic of mortise-tenon joint in historic timber buildings." *Engineering Mechanics* 23.10 (2006): 168-173.

[43] Bristogianni, Telesilla, et al. "Production and testing of Kiln-cast glass components for an interlocking, dry-assembled transparent bridge." *Glass Performance Days 2017 Conference Proceedings*. 2017.

[44] Brief, Architect. "GC Prostho Museum Research Center." *Introducing Architectural Tectonics: Exploring the Intersection of Design and Construction* (2016): 95.

[45] Oikonomopoulou, F., et al. "The potential of cast glass in structural applications. Lessons learned from large-scale castings and state-of-the art load-bearing cast glass in architecture." *Journal of Building Engineering* (2018).

[46] McKenzie, H. W., and R. J. Hand. *Basic optical stress measurement in glass*. Vol. 900682272. Sheffield, UK: Society of Glass Technology, 1999.

[47] Shelby, James E. *Introduction to glass science and technology*. Royal Society of Chemistry, 2007.